

Inversion-symmetric topological insulatorsTaylor L. Hughes,¹ Emil Prodan,² and B. Andrei Bernevig³¹*Department of Physics, University of Illinois, 1110 West Green Street, Urbana, Illinois 61801, USA*²*Department of Physics, Yeshiva University, New York, New York 10016, USA*³*Department of Physics, Princeton University, Princeton, New Jersey 08544, USA*

(Received 16 November 2010; revised manuscript received 30 March 2011; published 28 June 2011)

We analyze translationally invariant insulators with inversion symmetry that fall outside the current established classification of topological insulators. These insulators exhibit no edge or surface modes in the energy spectrum and hence they are not edge metals when the Fermi level is in the bulk gap. However, they do exhibit *protected* modes in the entanglement spectrum localized on the cut between two entangled regions. Their entanglement entropy *cannot* be made to vanish adiabatically, and hence the insulators can be called topological. There is a direct connection between the inversion eigenvalues of the Hamiltonian band structure and the midgap states in the entanglement spectrum. The classification of protected entanglement levels is given by an integer \mathcal{N} , which is the difference between the negative inversion eigenvalues at inversion symmetric points in the Brillouin zone, taken in sets of 2. When the Hamiltonian describes a Chern insulator or a nontrivial time-reversal invariant topological insulator, the entirety of the entanglement spectrum exhibits *spectral flow*. If the Chern number is zero for the former, or time reversal is broken in the latter, the entanglement spectrum does *not* have spectral flow, but, depending on the inversion eigenvalues, can still exhibit protected midgap bands similar to impurity bands in normal semiconductors. Although spectral flow is broken (implying the absence of real edge or surface modes in the original Hamiltonian), the midgap entanglement bands cannot be adiabatically removed, and the insulator is “topological.” We analyze the linear response of these insulators and provide proofs and examples of when the inversion eigenvalues determine a nontrivial charge polarization, a quantum Hall effect, an anisotropic three-dimensional (3D) quantum Hall effect, or a magnetoelectric polarization. In one dimension, we establish a link between the product of the inversion eigenvalues of all occupied bands at all inversion symmetric points and charge polarization. In two dimensions, we prove a link between the product of the inversion eigenvalues and the parity of the Chern number of the occupied bands. In three dimensions, we find a topological constraint on the product of the inversion eigenvalues thereby showing that some 3D materials are protected topological metals; we show the link between the inversion eigenvalues and the 3D Quantum Hall Effect, and analyze the magnetoelectric polarization (θ vacuum) in the absence of time-reversal symmetry.

DOI: [10.1103/PhysRevB.83.245132](https://doi.org/10.1103/PhysRevB.83.245132)

PACS number(s): 73.20.At, 73.43.—f

I. INTRODUCTION

One of the most active fields of research in recent years has been the study of nontrivial topological states of matter. The paradigm example of such a state is the quantum Hall effect, with its integer (IQHE) and fractional (FQHE) versions. More recently, examples of topological phases that do not require external magnetic fields have been proposed, the first being Haldane’s Chern insulator model.¹ Although this state has not been experimentally realized, a time-reversal invariant (TRI) version has been proposed and discovered.^{2–8}

Recent work in the theory of topological insulators^{2–4} showed that an important consideration is not only which symmetries the state breaks, but which symmetries must be preserved to ensure the stability of the state. A periodic table classifying the topological insulators and superconductors has been created. The table organizes the possible topological states according to their space-time dimension and the symmetries that must remain protected: time-reversal, charge conjugation, and/or chiral symmetries.^{9–11} The most interesting entries in this table, from a practical standpoint, are the two- and three-dimensional TRI topological insulators which have been already found in nature.^{5–8} These are insulating states classified by a Z_2 invariant that requires an unbroken time-reversal symmetry to be stable. There are several different methods to calculate the Z_2 invariant,^{3,7,9,12–16}

and a nontrivial value for this quantity implies the existence of an odd number of gapless Dirac fermion boundary states as well as a nonzero magnetoelectric polarizability in three dimensions.^{9,17}

The current classification of the topological insulators covers only the time-reversal, charge conjugation, or chiral symmetries and does not exhaust the number of all possible topological insulators. In principle, for every discrete symmetry, there must exist topological insulating phases with distinct physical properties, and a topological number that classifies these phases and distinguishes them from the “trivial” ones. So far, in our discussion we have used the term “topological” cavalierly so before proceeding we should ask what makes an insulator topological? We start by first defining a trivial insulator: This is the insulator that, upon slowly turning off the hopping elements and the hybridization between orbitals on different sites, flows adiabatically into the atomic limit. In most of the existent literature on noninteracting topological insulators, it is implicitly assumed that nontrivial topology implies the presence of gapless edge states in the energy spectrum of a system with boundaries. However, it is well known from the literature on topological phases that such systems can theoretically exist without exhibiting gapless edge modes.¹⁸ Hence the edge modes cannot be the only diagnostic of a topological phase and, consequently, the energy spectrum

alone, with or without boundaries, is insufficient to determine the full topological character of a state of matter. In the bulk of an insulator, it is a known fact that the topological structure is encoded in the eigenstates rather than in the energy spectrum. As such, one can expect that entanglement—which only depends on the eigenstates—can provide additional information about the topological nature of the system. However, we know that topological entanglement entropy (or the subleading part of the entanglement entropy),^{19–21} the preferred quantity used to characterize topologically ordered phases, does not provide a unique classification, and, moreover, vanishes for any non-interacting topological insulator, be it time-reversal breaking Chern insulators or TRI topological insulators. However, as we will see, careful studies of the full entanglement spectrum²² helps in characterizing these states.^{22–33}

The *total* entanglement entropy can be continuously deformed to zero for trivial insulators, since the atomic limit to which every trivial insulator can be adiabatically continued (by the above definition) is completely local and has flat, featureless bands. We could therefore suggest that a *nontrivial* topological state in a noninteracting translationally invariant insulator should be defined as having an entanglement entropy that cannot be adiabatically tuned to zero. However, even this definition cannot be entirely correct, as the entanglement entropy strongly depends on the nature of the cut made in the system. Let us briefly review this result. For a single-particle entanglement spectrum with eigenvalues $\{\xi_a\}$ the entanglement entropy is determined via

$$S_{\text{ent}} = - \sum_a [\xi_a \ln \xi_a + (1 - \xi_a) \ln(1 - \xi_a)]. \quad (1)$$

Taking IQH states on the sphere, the many-body wave function is a single Slater determinant of occupied Landau orbitals, and hence an orbital cut²² would result in zero entanglement entropy since all orbitals are fully occupied or unoccupied. This leads to a set of $\{\xi_a\}$ which are all 0's or 1's and do not contribute to S_{ent} . Similarly, for a translationally invariant Chern or TRI topological insulator on a lattice, a momentum space cut would always give zero entanglement entropy since the Hamiltonian is diagonal in this basis. A spatial cut, however, would show midgap bands in the entanglement spectrum of both the IQHE and the topological insulator case (i.e., a set of eigenvalues spanning the “gap” between 0 and 1) similar to the ones in the real energy spectrum.^{23,24,29,30,32,34} These midgap states give large contributions to the entanglement entropy. In fact, for such states, the entanglement entropy for the spatial cut cannot be made to vanish by any adiabatic changes in the Hamiltonian. We hence propose that a translationally invariant insulator can be classified as topological if it cannot be adiabatically connected to a state with zero entanglement entropy for *at least one kind of cut of the system*. Explicitly, an insulator should be characterized as topological if it has protected midgap states in the single-particle entanglement spectrum that cannot be pushed to eigenvalues 0 or 1 by any adiabatic changes of the Hamiltonian.

In the current paper we analyze the physics of insulators with inversion symmetry based on the above definition. Our purpose is twofold: (i) we use these insulators to illustrate interesting properties of the entanglement spectrum, and (ii) we discuss topological electromagnetic response properties

of these insulators which are controlled solely by the inversion eigenvalues of the occupied bands. While some of the inversion-symmetric insulators exhibit protected edge modes in the energy spectrum with boundaries (e.g., a Chern insulator with inversion symmetry), most do not. However, they can still be topological because their entanglement spectrum for a spatial cut exhibits protected midgap bands of states. This was first pointed out for three-dimensional (3D) strong topological insulators with inversion symmetry and soft time-reversal breaking in Ref. 29. Although it was indicated in Ref. 29 that the entanglement spectrum cannot distinguish between a TRI and inversion invariant topological insulator, and one with TRI slightly broken (compared to the bulk gap), we show that it can distinguish these states.

In Sec. III we explicitly show that inversion symmetric topological insulators have two types of entanglement spectra, both with protected midgap states. The characteristic which distinguishes the two types of entanglement spectra (and the two cases from Ref. 29) is the presence or absence of spectral flow. For nontrivial TRI or Chern insulators the entanglement spectrum exhibits spectral flow, very much like their energy spectra. Heuristically this means that the filled and empty bulk states are connected via an interpolating set of states which are localized in real space on the partition between the two entangled regions. Spectral flow in the energy spectrum implies spectral flow in the entanglement spectrum. However, if time reversal is broken for TRI topological insulators, or for T -breaking insulators with vanishing Chern number, we show that such spectral flow is interrupted in both the energy and entanglement spectra, and the occupied bands are disconnected from the unoccupied ones. One could then assume that, in systems without a continuous spectral connection between the bulk entanglement bands, one could push all the midgap entanglement bands to entanglement eigenvalues 0, 1, and hence to a trivial insulator with vanishing entropy on every cut. We find this not to be the case for special classes of inversion symmetric insulators distinguished by a set of inversion eigenvalues that change sign between two inversion symmetric points in the Brillouin zone. In this case, while most entanglement eigenvalues can continuously be deformed to 0 or 1, there is a set of protected midgap states/bands which give the insulator nonzero entanglement entropy (even when the spectral flow has been destroyed). For the case of time-reversal and inversion invariant topological insulators, these protected states were shown in Ref. 29 to exist even when time reversal is weakly broken, indicating that inversion symmetry is important. One of our main results is a formula relating the number of protected midgap bands in the entanglement spectrum to the inversion eigenvalues of the system at inversion symmetric points [Eq. (64)]. In fact, at inversion symmetric k , and for cuts which separate the system into two equal halves, the entanglement spectrum has protected entanglement edge or surface modes at *exactly* $\xi = 1/2$. This means that for this case there is no finite-size level repulsion (splitting) between these modes which is a common feature for the *energy* spectra of real boundary or interface states. Even if the original system has other topological invariants, such as the Chern number, or the TRI Z_2 invariant, which are all trivial, the number of protected entanglement edge modes can be nonzero. We illustrate many of these properties via examples in Sec. V. As

a guide to the reader, it may be better to skip Sec. III on a first reading. Sections II, IV, and V are more physically motivated and build on the conventional treatment of symmetry protected topological insulators. Section III only need be studied if one is interested in the entanglement spectra of such systems. The main results of our work on entanglement are written in Secs. III C 5, III C 6, and III D and are preceded by a review of the entanglement spectrum and some explicit proofs of our claims.

As for our second focus, in Sec. IV we analyze the physical response of a subset of these inversion symmetric insulators, and show important implications for charge polarization, the parity of the Chern number, the 3D quantum Hall effect, and the topological magnetoelectric polarizability. Namely, given the set of inversion eigenvalues for the occupied bands at all inversion symmetric points in the Brillouin zone, we provide explicit, compact formulas and complementary derivations for determining the physical responses which only depend on the inversion eigenvalues. In particular, we show the following: In one dimension, the product of inversion eigenvalues over all occupied bands and over all inversion symmetric points is related to the quantized charge polarization [Eq. (68)]. In two dimensions, the product over the inversion eigenvalues determines the parity of the Chern number of the occupied bands [Eq. (93)]. In three dimensions, we show several things: First, we prove a topological restriction for the product of inversion eigenvalues of any insulator: it must always equal +1. As such, some inversion symmetric systems are topologically protected metals, which cannot be made insulating with weak scattering. Second, we show that, depending on the product of inversion eigenvalues in different inversion symmetric planes, we will have 3D quantum Hall effects on different planes in the sample [Eq. (106)]. We then show that several inversion symmetric systems can exhibit a quantized magnetoelectric polarizability, even though the Hamiltonian may not be adiabatically continuable to a time-reversal invariant topological insulator [Eq. (110)]. In addition, we offer an alternative perspective by showing that some of the inversion topological invariants are equivalent to the wave-function monodromy, which in principle is an experimentally measurable quantity [Eq. (91)].

Finally in Sec. V we end the paper with several examples of interesting insulators and corresponding numerical results. While most of the examples we chose have a topological response connected with an inversion topological invariant, we stress that the presence of midgap states in the entanglement spectrum is not intrinsically related to the presence of a nontrivial topological response. For example, two identical copies of a strong-topological insulator with inversion and time-reversal symmetry has a trivial Z_2 invariant and thus a trivial response. However, this system will exhibit protected midgap entanglement states. So, while some inversion invariant insulators have protected topological responses, some do not. The situation is even more complicated: In several cases, we prove that inversion eigenvalues by themselves cannot uniquely determine the response. We can show that a nontrivial quantum spin Hall state and two copies of a Chern insulator each with Chern number unity have identical inversion eigenvalues but obviously represent very different states of matter. The question of relating *all* the inversion

eigenvalues to a response function remains, in the cases where possible, still unsolved.

II. PRELIMINARIES

Let us start our discussion with some observations for simple two- and four-band model Hamiltonians, which will be referenced throughout the paper and serve to illustrate the methods of analysis we propose for inversion symmetric insulators. The properties of the models that we discuss are only dependent on a generic inversion symmetry and not on other symmetries present “accidentally” in these simple models.

Two-band model. The two-band model is

$$H_2 = \sum_x \left[c_x^\dagger \frac{\alpha - \hat{\sigma}_3 - i\hat{\sigma}_1}{2} c_{x+1} + \text{H.c.} + c_x^\dagger (1+m) \hat{\sigma}_3 c_x \right],$$

where α , m are two parameters and $\hat{\sigma}_a$ are Pauli matrices. The model is symmetric under the inversion operation $c_x \rightarrow \hat{\sigma}_3 c_{-x}$. The Bloch representation of H_2 takes the simple form

$$\hat{H}_2(k) = \alpha \cos k + \sin(k) \hat{\sigma}_1 + (1+m - \cos k) \hat{\sigma}_3, \quad (2)$$

and the inversion is implemented by the operator $\mathcal{P} = \hat{\sigma}_3$:

$$\hat{\sigma}_3 \hat{H}(k) \hat{\sigma}_3 = \hat{H}(-k). \quad (3)$$

H_2 is gapped, except when $m = -2$ or 0 . The energy spectrum of the model with open boundary conditions is presented in Figs. 1(a) and 1(b), for $\alpha = 0$ and $m = \mp 1$, respectively. Throughout this paper, \hat{P}_k will denote the projector onto the occupied bands at momentum k , which is a $K \times K$ matrix ($K = \text{total number of bands}$), whose entries depend on k .

The two special points $k_{\text{inv}} = 0, \pi$ where $\hat{H}_2(k)$ is mapped onto itself by inversion will play a special role in the following discussion. We are going to examine the (nonzero) eigenvalues $\zeta(0)$ and $\zeta(\pi)$ of $\hat{P}_{k=0} \mathcal{P} \hat{P}_{k=0}$ and $\hat{P}_{k=\pi} \mathcal{P} \hat{P}_{k=\pi}$, respectively,

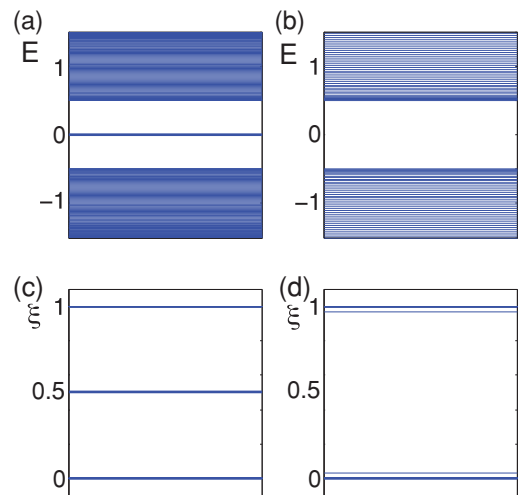


FIG. 1. (Color online) Energy spectra for the simple 1D two-band model with open boundary conditions for (a) $\alpha = 0$ $m = -1$ (nontrivial) (b) $\alpha = 0$ $m = 1$ (trivial). Entanglement spectra for the two cases are shown in (c) and (d), respectively, for a half filled Fermi sea ground state with periodic boundary conditions.

for the three different insulating phases of H_2 . What we find is the following:

- (1) $\zeta(0) = \zeta(\pi) = -1$, for $m > 0$.
- (2) $\zeta(0) = \zeta(\pi) = +1$, for $m < -2$.
- (3) $\zeta(0) = -\zeta(\pi) = +1$, $-2 < m < 0$.

We can form a Z_2 topological invariant:

$$\chi_{\mathcal{P}} = \prod_{k_{\text{inv}}, i \in \text{occ.}} \zeta_i(k_{\text{inv}}), \quad (4)$$

which is topologically stable since one cannot change its value without closing the gap of the Hamiltonian. The expression of $\chi_{\mathcal{P}}$ is similar to invariants formed for time-reversal and inversion invariant topological insulators in two and three dimensions.⁷

For the model of Eq. (2), $\chi_{\mathcal{P}}$ takes the values $\chi_{\mathcal{P}} = +1$ for the insulating phases with $m \notin [-2, 0]$, and $\chi_{\mathcal{P}} = -1$ for $m \in [-2, 0]$. A direct calculation indicates that the phase with $\chi_{\mathcal{P}} = -1$ displays a single end mode at each end of a system with open boundaries, while the phases with $\chi_{\mathcal{P}} = +1$ do not display any end modes. This simple model indicates that, indeed, systems with inversion symmetry do possess nontrivial topological phases that, for this simple case, can be classified by the $\chi_{\mathcal{P}}$ invariant. As we shall see in Sec. IV A, $\chi_{\mathcal{P}}$ can be linked to a physical response of the system, namely the electric charge polarization, but it cannot completely classify the topological phases of a system with inversion symmetry, even in one dimension.

Four-band model. It is instructive to repeat a similar analysis on a four-band inversion symmetric model. For this we use the following Hamiltonian, written directly in the Bloch representation:

$$\hat{H}_4(k) = \sin(k)\hat{\Gamma}_1 + b \sin(k)\hat{\Gamma}_2 + (1 - m - \cos k)\hat{\Gamma}_0 + \delta\hat{\Gamma}_{24} + \epsilon \cos(k)(1 + \hat{\Gamma}_0), \quad (5)$$

where $\hat{\Gamma}_1 = \sigma^z \otimes \tau^x$, $\hat{\Gamma}_2 = 1 \otimes \tau^y$, $\hat{\Gamma}_0 = 1 \otimes \tau^z$, and $\hat{\Gamma}_{24} = \sigma^x \otimes \tau^z$. The Pauli matrices τ^a, σ^a act in the orbital and spin spaces, respectively. $\hat{H}_4(k)$ is symmetric under inversion,

which is implemented by $\mathcal{P} = \hat{\Gamma}_0$, and is gapped except for a few values of the parameters b , δ , ϵ , and m . Note that this system also has an accidental time-reversal symmetry with $T = (i\sigma^y \otimes 1)K$ (where K is complex conjugation), but this can be broken without affecting the stability of the topological state or removing the midgap modes in the entanglement spectrum. The two lower energy bands are assumed occupied, and in this case $\hat{P}_0\mathcal{P}\hat{P}_0$ and $\hat{P}_\pi\mathcal{P}\hat{P}_\pi$ are 4×4 matrices, each displaying two nonzero eigenvalues $\zeta_i(0)$ and $\zeta_i(\pi)$, $i = 1, 2$.

We are going to present the inversion eigenvalues for the insulating phases of the model. There are six such phases (we discuss only five of them) and their energy spectra with open boundary conditions are shown in Figs. 2(a)–2(e). Choosing representative values for the parameters, we find the following:

Case 1. $b = \delta = \epsilon = 0$ and $m < 0$:

$$\zeta_1(0) = \zeta_2(0) = +1, \quad \zeta_1(\pi) = \zeta_2(\pi) = +1, \quad (6)$$

and consequently $\chi_{\mathcal{P}} = +1$.

Case 2. $b = \delta = \epsilon = 0$ and $m = 0.5$:

$$\zeta_1(0) = \zeta_2(0) = -1, \quad \zeta_1(\pi) = \zeta_2(\pi) = +1, \quad (7)$$

and consequently $\chi_{\mathcal{P}} = +1$.

Case 3. $b = 1$, $\delta = 0.7$, $\epsilon = 0$, and $m < 0$:

$$\zeta_1(0) = -1, \quad \zeta_2(0) = +1, \quad \zeta_1(\pi) = \zeta_2(\pi) = +1, \quad (8)$$

and consequently $\chi_{\mathcal{P}} = -1$.

Case 4. $b = 1$, $\delta = 1.7$, $\epsilon = 0$, and $m = 0.5$:

$$\zeta_1(0) = -1, \quad \zeta_2(0) = +1, \quad \zeta_1(\pi) = +1, \quad \zeta_2(\pi) = -1, \quad (9)$$

and consequently $\chi_{\mathcal{P}} = +1$.

Case 5. $b = 1$, $\delta = 1.7$, $\epsilon = 0.7$, and $m = 0.5$:

$$\zeta_1(0) = +1, \quad \zeta_2(0) = -1, \quad \zeta_1(\pi) = +1, \quad \zeta_2(\pi) = -1, \quad (10)$$

and consequently $\chi_{\mathcal{P}} = +1$.

The four-band model reveals a far richer internal structure. Case 1 can be identified with a trivial topological phase and, based on the value of $\chi_{\mathcal{P}}$ and on the presence of end modes seen

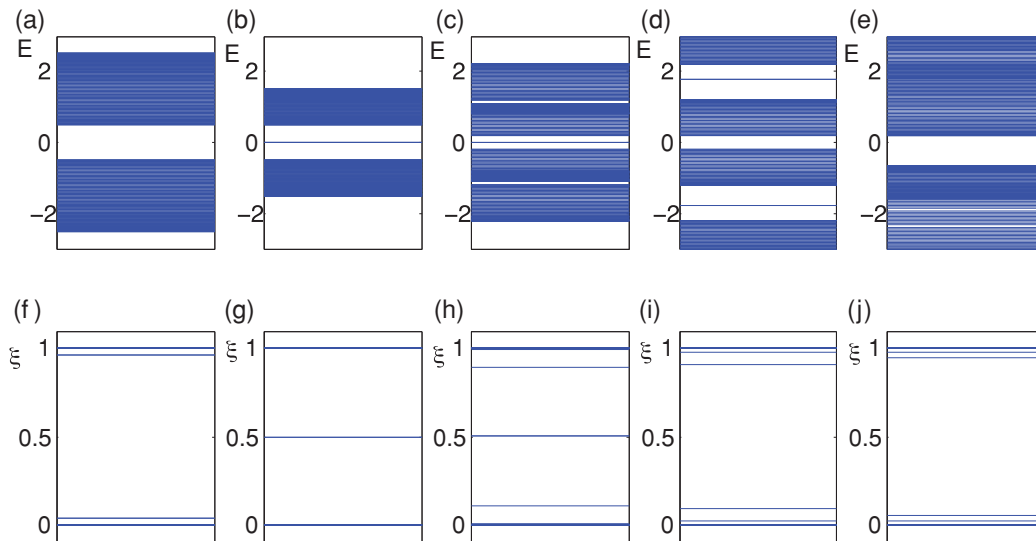


FIG. 2. (Color online) (a)–(e) Energy spectra for H_4 in cases 1–5, respectively, with open boundary conditions. (f)–(j) Entanglement spectra for H_4 in cases 1–5, respectively, with periodic boundary conditions.

in Fig. 2(c), one will be inclined to classify case 3 as a nontrivial topological insulator. But one will have clear difficulties with labeling cases 2, 4, and 5. This is a clear indicator that χ_P alone is not enough for a full classification of inversion symmetric insulators in one dimension and that additional topological invariants are needed for a complete picture.

To understand how we can classify cases 2, 4, and 5, it is instructive to consider the atomic limit of the model. By the atomic limit we mean the limit of the adiabatic process in which the hopping terms between *different* sites are tuned to zero. Since the bands are dispersionless and completely local (disentangled) in this limit, it makes sense to talk about the parity of an entire band (or orbital), since its inversion eigenvalues at $k = 0, \pi$ are identical. For a model with two occupied bands, the atomic limit can lead to the following cases, depending on how the occupied atomic orbitals behave under inversion: two occupied bands of parity + (labeled ++), two occupied bands of parity - (labeled --), and one band of parity + and one band of parity - (labeled +-). These three options give the complete classification of the trivial inversion symmetric insulators with two occupied bands in one dimension. Now, a direct calculation will show that cases 1, 4, and 5 can be connected to their atomic limits without closing the insulating gap and that case 1 can be identified with ++ trivial insulator, while both cases 4 and 5 can be identified with the +- trivial insulator. Note that cases 4 and 5 can be adiabatically connected to each other without closing the bulk insulating gap. The -- trivial insulator also appears as a phase in our four-band model if we take the large m limit and is the sixth insulating phase that we mentioned.

Based on the above discussion and on the absence/presence of the end modes in Fig. 2, we can consider cases 1, 4, and 5 as completely trivial and case 3 as nontrivial, but case 2 is still uncharacterized. It cannot be continued to the trivial atomic limit without closing the bulk gap; it displays end modes, yet $\chi_P = +1$. To distinguish this phase we must carefully consider the inversion eigenvalues. We see that when the k_{inv} points are considered separately, $\chi_P(k_{\text{inv}}) \equiv \prod_{i \in \text{occ.}} \zeta_i(k_{\text{inv}}) = 1$. Thus at each k_{inv} there are an even number of bands with negative inversion eigenvalues. In this situation, when for each k_{inv} the local product over the eigenvalues of the occupied bands is trivial (+1), we can define a second invariant

$$\chi_P^{(2)} \equiv \prod_{k_{\text{inv}}, i \in \text{occ.}/2} \zeta_i(k_{\text{inv}}), \quad (11)$$

where the product over bands is defined to be the product of *half* of the bands with negative inversion eigenvalues at each k_{inv} . Note that we do not require there to be an even number of filled bands, just an even number of negative inversion eigenvalues. Out of the five cases discussed above, the $\chi_P^{(2)}$ invariant can only be defined for cases 1 and 2 for which $\chi_P^{(2)}$ is trivial/nontrivial, respectively. As we shall see in Sec. IV C 4 the $\chi_P^{(2)}$ invariant is more relevant and important for inversion symmetric insulators in three dimensions and is not very useful for characterizing 1D insulators. However, we will see in Secs. III and IV [in Eqs. (64) and (91)] that a different invariant,

$$\mathcal{N} = |n_1 - n_2|, \quad (12)$$

where n_1 and n_2 are the number of negative inversion eigenvalues at $k = 0$ and π , respectively, is more useful for classifying the inversion symmetric insulators. This invariant generically indicates how many times the insulating gap must close when one takes the atomic limit. As we shall see, \mathcal{N} also gives the number of robust midgap modes in the entanglement spectrum localized on a single cut boundary. For our four-band model, $\mathcal{N} = 0$ for cases 1, 4, and 5; $\mathcal{N} = 1$ for case 3, and $\mathcal{N} = 2$ for case 2. This integer invariant, while not directly related to any physical response, will serve as a useful characterization of inversion symmetric insulators which cannot be adiabatically connected to an atomic limit. To conclude, the two- and four-band explicit models show that insulators with inversion symmetry can display topologically distinct phases, i.e., they cannot be continuously deformed into one another without closing the insulating gap.

We now wish to lay out the procedure for the classification for a generic insulator with inversion symmetry, the individual steps of which will be discussed in great detail in the remainder of the paper. The first step is to calculate the inversion eigenvalues of all the occupied bands of a given inversion symmetric model. We are implicitly assuming that (i) we have chosen a gauge such that the inversion operator takes the same form at each Bloch momentum, (ii) we have fixed a choice of an indivisible crystal unit cell. The first assumption is important for keeping the eigenvalue sign convention the same at each inversion invariant momentum point. The second assumption is important for the definition of the entanglement cut, as will be touched on in Sec. V A 3. The inversion eigenvalues alone determine whether or not the system is equivalent to an atomic insulator via a calculation of the invariant \mathcal{N} [cf. Eq. (12), and Sec. IV A]. If the system is in one dimension we can further characterize a possible nontrivial electromagnetic response by calculating χ_P , which determines the charge polarization (cf. Sec. IV A). If the insulator is in two or three dimensions we can calculate analogous invariants to test for topological responses including an IQHE (Sec. IV B), a 3D QHE (Sec. IV C 1), or a 3D magnetoelectric polarizability (Sec. IV C 4). It will turn out that the invariant \mathcal{N} also determines a set of protected modes in the entanglement spectrum, which clearly show the distinction between trivial and nontrivial insulators [Sec. III C 5, Eq. (64)]. This makes clear our scheme for characterizing inversion invariant insulators.

III. ENTANGLEMENT SPECTRUM OF TOPOLOGICAL INSULATORS WITH INVERSION SYMMETRY

In this section we discuss the bipartite single-particle entanglement spectra for inversion symmetric topological insulators. Previous work on entanglement spectra in translationally invariant topological insulators was carried out in Refs. 23, 29, 30, and 34, where it was shown that the primary contributions to entanglement arise from states localized near the spatial cut between regions A and B. Additionally the entanglement spectrum of disordered Chern insulators has been investigated in Ref. 32. The first indication that the presence of inversion symmetry is important for the structure of the entanglement spectrum was presented in Ref. 29. Here it was shown that, while the physical edge spectrum of a time-reversal and inversion invariant topological insulator is gapped

in the presence of an added Zeeman field (which does not close the bulk gap), the entanglement spectrum still contains a gapless mode. The authors of that work link the existence of midgap states for each cut in the entanglement spectrum with the existence of a $\theta = \pi$ vacuum characteristic of a TRI nontrivial topological insulator.⁹ Although, as we mentioned before (and will discuss more in Sec. IV), there is not always a direct and unique connection between the physical response and protected states in the entanglement spectrum, this was an essential indication that inversion symmetry could support topological states and that the properties of the entanglement spectra were closely connected with inversion symmetry.

We start this section by detailing how to obtain the entanglement spectrum for noninteracting insulators. We then look at the entanglement spectrum of topological insulators and show that there are two fundamental properties which may be present: (i) protected midgap states at entanglement eigenvalue $\xi = 1/2$, and (ii) spectral flow in the entanglement spectrum. In the presence of inversion symmetry, there can be midgap states in the entanglement spectrum, and these may or may not be connected to the entanglement bulk band edges via a spectral flow pattern. Hence there are two distinct types of nontrivial entanglement spectra. One example that we will see is TRI topological insulator parent states, which are inversion symmetric but which may have time reversal slightly broken. The time-reversal invariant case has both protected midgap modes and spectral flow, while the T -broken case only has protected midgap modes.

For now we focus solely on insulators with a generic inversion symmetry and show its consequences on the entanglement spectrum. First, we show that if the system is cut exactly in half, then there can be midgap states in the entanglement spectrum located exactly at a value of $1/2$. This is equivalent to the statement that the midgap eigenvalues of the flat band Hamiltonian, for cuts exactly in half, exhibit no finite-size level repulsion. We then give an expression for the number of $1/2$ eigenvalues in the entanglement spectrum as a function of the numbers of negative inversion eigenvalues at inversion symmetric points. Reference 29 also points out the existence of multiple exact midgap states in the entanglement spectrum but does not relate them to the difference of the inversion eigenvalues *between* inversion symmetric points.

In everything presented below, it is very important to clarify that by a spatial cut in a translationally invariant system we mean a cut *between* primitive unit cells. This point is important when we consider systems with partially broken translation symmetry, e.g., the dimerized models in Sec. V. The physics is independent of the choice of the unit cell. For example, in a multiorbital system with a one-site unit cell, the cut should *not* be made through the orbitals on the same site.

A. Obtaining the entanglement spectrum of an insulator

All of the models we study are free fermion Hamiltonians. To find the single-particle entanglement spectrum we use Peschel's method.³⁵ We begin by assuming a quadratic Hamiltonian of an insulator with $\alpha = 1 \dots K$ quantum states per site, which is translationally invariant:

$$H = \sum_k c_{\alpha,k}^\dagger H_{\alpha\beta}(k) c_{\beta,k}, \quad (13)$$

and the canonical transformation U that diagonalizes it:

$$U^\dagger H U = \text{diag}(E_n). \quad (14)$$

U is the matrix of eigenvectors $u^n(k)$ of energy $E_n(k)$:

$$U(k) = (u^1(k), u^2(k) \dots u^K(k)), \quad (15)$$

where each $u^n(k)$ is a K -component vector. In general, we will use k to denote the wave vector of components k_x, k_y , etc.

The relationship between the normal-mode operators $\gamma_{\beta k}$ and the electron creation operators is

$$c_{\alpha k} = U_{\alpha\beta}(k) \gamma_{\beta k} = u_\alpha^n(k) \gamma_{nk}. \quad (16)$$

To calculate the single-particle entanglement spectrum we simply need the correlation function:

$$C_{ij}^{\alpha\beta} = \langle c_{i\alpha}^\dagger c_{j\beta} \rangle, \quad (17)$$

where $c_{i\alpha}^\dagger$ creates an electron in state α at site i . The expectation value is taken in the ground state. We can view this correlator as a matrix \hat{C}_{ij} , with entries that depend on i and j . We have

$$\begin{aligned} C_{ij}^{\alpha\beta} &= \sum_{k_1, k_2} e^{ik_1 i - ik_2 j} \langle c_{\alpha k_1}^\dagger c_{\beta k_2} \rangle = \sum_k e^{ik(i-j)} \sum_{n \in \text{occ.}} u_\alpha^n(k)^* u_\beta^n(k) \\ &= \sum_k e^{ik(i-j)} P_k^{*\alpha\beta}, \end{aligned} \quad (18)$$

or more compactly

$$\hat{C}_{ij} = \sum_k e^{ik(i-j)} \hat{P}_k^*. \quad (19)$$

We want to make a translationally invariant cut along the y direction so that k_y is still a good quantum number (k_y is a shorthand notation for all the momenta parallel to the cut, so we are implicitly also treating systems in two and three dimensions). Thus we have

$$\hat{C}_{ij}(k_y) = \frac{1}{L} \sum_{k_x} e^{ik_x(i-j)} \hat{P}_{k_x, k_y}^*, \quad (20)$$

where L is the total number of sites along the cut. Following Peschel, for the entanglement spectrum, we restrict i, j to be in region A, which is an explicit cut in position space. There are several physical choices for cuts, but for topological insulators we will show that a spatial cut can distinguish between topological and trivial insulators.

As an aside, note that for an insulator the spectrally flattened Hamiltonian matrix where the states above/below the gap are flattened to energies $+1/2$ and $-1/2$, respectively, is given by

$$\hat{H}_{\text{flat}}(k_x, k_y) = \frac{1}{2} - \hat{P}_{k_x, k_y}^*. \quad (21)$$

The two above expressions of the correlation function and of the flat band Hamiltonian explicitly show that the entanglement spectrum, i.e., the eigenvalues of the restricted $C_{ij}^{\alpha\beta}$, are identical to the energy levels of the flat band Hamiltonian with open boundaries in region A shifted by a constant (since the eigenvalues of \hat{P}_k are the same as \hat{P}_k^*). As such, if the flat band Hamiltonian is topological (i.e., has protected edge states), then immediately we know the entanglement spectrum will have states localized on the cut. This agrees with the results of Ref. 30. The interesting thing is that the flattened Hamiltonian

can have midgap states even when the unflattened one does not.

B. Properties of the entanglement spectrum

We would like to first get an intuitive idea of how the entanglement spectrum of an insulator should look. The one-body correlation function over the *full system* (not only over region A) is a projector. It is the real-space representation of the projector onto the occupied bands, and as such only has the eigenvalues 0 and 1. This is shown explicitly in Appendix A. When we make a cut, the eigenvalues of the one-body correlator deviate from 0,1 but most of them only deviate slightly. However, in the topologically nontrivial case, we must get entanglement “edge” modes similar to the edge states, but localized on the entanglement cut, because we are really diagonalizing the spectrum of the open boundary flat band Hamiltonian of a topological insulator.

From now on we choose to cut the system *exactly* in half. A cut exactly in half will enable us to show the existence of exact degeneracies rather than levels that are split by finite-size effects with degeneracies only arising in the thermodynamic limit. Our choice of cut does not matter in the thermodynamic limit, where it *cannot* physically matter whether we make a cut exactly in the middle or away from the middle. It is, however, the case that if we cut the system in two identical halves, we can prove things exactly, otherwise we can just give arguments.

The one-body matrix, computed in the basis $c_{i,\alpha}^\dagger|0\rangle$, takes the block form

$$C = \begin{pmatrix} C_L & C_{LR} \\ C_{RL} & C_R \end{pmatrix}, \quad (22)$$

where C_L is the matrix of the left half (the one we diagonalize for the entanglement spectrum) $(C_L)_{ij} = C_{ij}^{\alpha\beta}$, $i, j \in A$; C_R is the matrix of the right half $(C_R)_{ij} = C_{ij}^{\alpha\beta}$, $i, j \in B$; C_{LR} is the left-right coupling, $(C_{LR})_{ij} = C_{ij}^{\alpha\beta}$, $i \in A$, $j \in B$; with $C_{RL} = C_{LR}^\dagger$. Since $\hat{C}_{i,j} = \hat{C}_{i+n,j+n}$, the following extra property is true if the cut is exactly symmetric (in which case a proper translation of A gives B):

$$C_R = C_L. \quad (23)$$

Moreover, the projector property $C^2 = C$,

$$\begin{pmatrix} C_L & C_{LR} \\ C_{LR}^\dagger & C_L \end{pmatrix} \begin{pmatrix} C_L & C_{LR} \\ C_{RL} & C_L \end{pmatrix} = \begin{pmatrix} C_L & C_{LR} \\ C_{LR}^\dagger & C_L \end{pmatrix}, \quad (24)$$

gives the following additional identities:

$$\begin{aligned} C_L(1 - C_L) &= C_{LR}^\dagger C_{LR} C_{LR} C_{LR}^\dagger \\ &= C_{LR}^\dagger C_{LR} C_L C_{LR} + C_{LR} C_L = C_{LR}. \end{aligned} \quad (25)$$

Using the last equation, if ψ is an eigenstate of the entanglement spectrum matrix C_L with eigenvalue (probability) p ,

$$C_L \psi = p \psi, \quad (26)$$

then $C_{LR} \psi$ is also an eigenstate with eigenvalue $1 - p$:

$$\begin{aligned} C_L C_{LR} \psi &= C_{LR} \psi - C_{LR} C_L \psi \\ &= C_{LR} \psi - p C_{LR} \psi = (1 - p) C_{LR} \psi. \end{aligned} \quad (27)$$

If $p = 1/2$, ψ and $C_{LR} \psi$ have the same 1/2 entanglement probability, but as we shall see, this does not automatically mean that the $p = 1/2$ entanglement probability is doubly degenerate because ψ and $C_{LR} \psi$ are not linearly independent, in general.

1. Properties of entanglement spectrum with time-reversal symmetry

The entanglement spectrum maintains the symmetries of the original Hamiltonian. For example, for time-reversal symmetry of the original Hamiltonian $T \hat{H}(k) T^{-1} = \hat{H}(-k)$ (equivalently, $T \hat{P}_k T^{-1} = \hat{P}_{-k}$):

$$\begin{aligned} T \hat{C}_{ij}(k_y) T^{-1} &= \sum_{k_x} T e^{ik_x(i-j)} \hat{P}_{k_x, k_y}^* T^{-1} \\ &= \sum_{k_x} e^{-ik_x(i-j)} T \hat{P}_{k_x, k_y}^* T^{-1} \\ &= \sum_{k_x} e^{-ik_x(i-j)} \hat{P}_{-k_x, -k_y}^* \\ &= \sum_{k_x} e^{ik_x(i-j)} \hat{P}_{k_x, -k_y}^* = \hat{C}_{ij}(-k_y), \end{aligned} \quad (28)$$

so we see that the correlator also has time-reversal symmetry, and for spin-1/2 particles for which $T^2 = -1$, the entanglement levels come in pairs at k and $-k$. Thus there are entanglement Kramers' doublets at time-reversal invariant points where $k \equiv -k \pmod{G}$ where G is a reciprocal-lattice vector.

C. Inversion symmetric topological insulators

In this section we give explicit arguments that the entanglement spectrum of an insulator with inversion symmetry (and without any other symmetry) can have midgap states pinned at *exactly* 1/2, *without level repulsion* when cut exactly in half. An integer number of such modes is robust without splitting, so the classification of the entanglement spectra of insulators with inversion symmetry is given by an integer Z (compare with the Z_2 case where an even number of modes would be unstable). As an example, in one dimension, if a bulk insulator has a number n_1 of filled bands with negative inversion eigenvalues at $k = 0$ and a number n_2 at $k = \pi$, we give explicit arguments that the entanglement spectrum for a system with periodic boundary conditions (when the system is cut exactly in half) will have $2|n_1 - n_2|$ protected midgap modes at exactly 1/2. In more than one dimension, there will be conserved momenta parallel to the cut (say k_y), for an insulator cut in the x direction. When cut exactly in half, there will be $2|n_1 - n_2|$ zero modes situated at the $K_y^1 = -K_y^1 \pmod{G_y}$ for which, in the periodic bulk (before the cut), there were n_1 negative inversion eigenvalues at $(k_x, k_y) = (0, K_y^1)$ and n_2 negative inversion eigenvalues at $(k_x, k_y) = (\pi, K_y^1)$. We illustrate this explicitly with several examples in Sec. V.

1. Properties of entanglement spectrum with inversion symmetry

With inversion symmetry,

$$\mathcal{P} \hat{H}(k) \mathcal{P}^{-1} = \hat{H}(-k), \quad \mathcal{P}^2 = 1; \quad \mathcal{P} = \mathcal{P}^{-1}, \quad (29)$$

we can define a unitary matrix $B_{ij}(k)$, which connects the bands at k and $-k$:

$$|u_i(-k)\rangle = B_{ij}^*(k)\mathcal{P}|u_j(k)\rangle, \quad (30)$$

where the indices i, j run over the occupied bands $1, \dots, N$. In fact, by performing simple band crossings between the N bands below the gap (which does not influence the physics in the gap which depends only on the ground state), we can make the bands nondegenerate, in which case we can use $B_{ij}^*(k) = e^{i\phi(k)}\delta_{ij}$, but we do not need to choose this gauge here. Since $\hat{P}_k = \eta[E_F - \hat{H}(k)]$, where $\eta(x)$ is the Heaviside function, we have

$$\mathcal{P}\hat{P}_k\mathcal{P} = \hat{P}_{-k}, \quad (31)$$

which can be used to show

$$\mathcal{P}\hat{C}_{ij}\mathcal{P} = \sum_k e^{ik(i-j)}\hat{P}_{-k}^* = \hat{C}_{ji} = \hat{C}_{ij}^\dagger. \quad (32)$$

We now want to relate the appearance of these $1/2$ eigenvalues with the inversion eigenvalues of the occupied bands. We first consider the one-dimensional case where we will be able to infer the behavior of the insulator just from $k_x = 0, \pi$. In principle only two sites in the x direction should be enough to reveal the physics. Of course, with just two sites, our cut has to be made right in the middle of the two-site problem, i.e., we are computing the entanglement spectrum of one site vs the other site. This seems a bit problematic at first because if we are looking for the properties of the *energy* spectrum in a topological insulator phase the wave functions of the states localized on each end will overlap and the degeneracy of these low-energy end states will be lifted because of the small size. Crucially, we show that the flat-band Hamiltonian does not have such finite-size eigenvalue repulsion between the edge modes even when these modes rest on top of each other on the same site. That is, even if we bring the ends close to each other, e.g., on the same site (which is the meaning of the one-site entanglement spectrum), it is still true that the end modes do not exhibit level repulsion and are degenerate. This statement is true in higher dimensions where the end states become propagating edge and surface states. We prove this statement for several particular cases, which indicate that it is true in the thermodynamic limit. We first show that for one occupied band (we do not particularize to a specific model), there are two midgap modes at exactly $1/2$ if the inversion eigenvalue at $k = 0, \pi$ is opposite. Then we repeat this procedure for a chain of four sites cut in half. We then show that for two occupied bands (we do not particularize to a specific model), there are two midgap modes at exactly $1/2$ if there is one inversion eigenvalues at $k = 0, \pi$ opposite (while the other two are the same), whereas there are four midgap modes at exactly $1/2$ if both inversion eigenvalues at $k = 0$ are opposite from the ones at $k = \pi$ (i.e., at one momentum both are negative and at the other momentum both are positive). We again do this for a chain of two sites cut in half, then for a chain of four sites cut in half. The main conclusion to be drawn from this is that in the flat-band Hamiltonian (entanglement spectrum), these midgap modes *do not* experience eigenvalue repulsion. It is physically clear that, although our proofs are only for two- and four-site flat

band Hamiltonians (cut in half for the entanglement spectrum), level repulsion will *not* set in for larger systems: level repulsion between edge modes gets *weaker* as the distance between them is increased. Finally, at the end, we look at the general case of N occupied bands for the two-site problem and prove that the number of $1/2$ modes in the entanglement spectrum is $2|n_1 - n_2|$ where n_1, n_2 are the number of negative eigenvalues at $k = 0, \pi$. As there is no level repulsion when all modes are spatially on top of each other, we do not expect level repulsion when the number of sites is increased to the thermodynamic limit. We check this numerically for several examples with larger system sizes (e.g., 100 sites). Our exercise shows that time-reversal invariant insulators with inversion symmetry (or even the case with T slightly broken) are not the only inversion symmetric topological insulators with protected entanglement midgap states. These are but one of a whole series of inversion symmetric insulators with midgap entanglement modes.

2. One occupied band, two-site problem

First we look at a generic case with one occupied band, two sites, and periodic boundary conditions. In this case, k space contains only the points $k = 0, \pi$. The wave function of the occupied band is $|\psi_1(k)\rangle$,

$$\hat{H}(k)\psi_1(k) = \varepsilon(k)\psi_1(k), \quad (33)$$

with inversion eigenvalues

$$\mathcal{P}|\psi_1(0)\rangle = \zeta(0)|\psi_1(0)\rangle, \quad \mathcal{P}|\psi_1(\pi)\rangle = \zeta(\pi)|\psi_1(\pi)\rangle. \quad (34)$$

Since \mathcal{P} is a unitary operator which squares to unity, we have $\mathcal{P}^\dagger = \mathcal{P} (= \mathcal{P}^{-1})$ and by taking scalar products in the above we have

$$[\zeta(0) - \zeta(\pi)]\langle\psi_1(0)|\psi_1(\pi)\rangle = 0. \quad (35)$$

Hence if $\zeta(0) = -\zeta(\pi)$ (the eigenvalues can never be zero due to $\det \mathcal{P} = 1$) we have $\langle\psi_1(0)|\psi_1(\pi)\rangle = 0$. Notice that the Hamiltonian $\hat{H}(k)$ does not impose any restrictions on the wave functions at different momenta k , i.e., at $k = 0$ and $k = \pi$ we are effectively diagonalizing independent Hamiltonians. What allows us to relate wave functions at $k = 0, \pi$ is that they are both eigenstates of the same matrix \mathcal{P} (it is important to recall that \mathcal{P} is k independent).

For the two-site problem ($i = 1, 2$),

$$\hat{C}_L = \hat{C}_{11} = \frac{1}{L} \sum_k \hat{P}_k^* = \frac{1}{2}(\hat{P}_0^* + \hat{P}_\pi^*). \quad (36)$$

The eigenstates of the original Hamiltonian have opposite inversion eigenvalues then per the above:

$$\hat{P}_0^*|\psi_1(\pi)\rangle = \hat{P}_\pi^*|\psi_1(0)\rangle = 0, \quad (37)$$

which means that $\psi_1(0)$ and $\psi_1(\pi)$, the original Hamiltonian eigenstates, are also the eigenstates of the entanglement spectrum, with two eigenvalues at $1/2$:

$$C_L|\psi_1(0)\rangle = \frac{1}{2}|\psi_1(0)\rangle; \quad C_L|\psi_1(\pi)\rangle = \frac{1}{2}|\psi_1(\pi)\rangle. \quad (38)$$

We see that the original Hamiltonian can change, leading to a change of $\psi_1(k)$, but as long as the inversion eigenvalues remain fixed and opposite to each other, and as long as we can

take the flat band limit (both of which mean no gap closing), the eigenvalues of the entanglement spectrum will be fixed at $1/2$. It does not matter what the actual explicit model for $\hat{H}(k)$ is. If the inversion eigenvalues at $k = 0, \pi$ are not opposite, there is no reason why $\langle \psi_1(0) | \psi_1(\pi) \rangle = 0$, and the $1/2$ modes might not exist or will not be protected.

3. One Occupied Band, Four-Site Problem

With one occupied band with opposite inversion eigenvalues, the two-site Hamiltonian has exact $1/2$ modes in the entanglement spectrum. This is the first indication that the modes are stable and experience zero level repulsion. We now show that the generic four-site Hamiltonian with one occupied band also has exact $1/2$ modes without level repulsion. This strongly suggests that these modes are stable in the thermodynamic limit, as long as the entanglement spectrum is computed for a system cut exactly in half. But, in the thermodynamic limit we know there can be no physical difference between a cut in half and any other cut except for exponentially suppressed finite-size level splittings. Thus there will be asymptotic zero modes in the thermodynamic limit regardless of the cut.

For the four-site problem, k space contains four momenta, $k_j = \frac{j\pi}{2}$, $j = 0, 1, 2, 3$. Call the occupied eigenstate of the Hamiltonian, as above $|\psi_1(k)\rangle$, $\hat{H}(k)\psi_1(k) = \varepsilon(k)\psi_1(k)$. For a system cut in half, the entanglement spectrum is given by diagonalizing the matrix $C_{ij} = C_{i-j}$ with $i, j = 1, 2$:

$$C_L = \begin{pmatrix} \hat{C}_{11} & \hat{C}_{12} \\ \hat{C}_{12}^\dagger & \hat{C}_{22} \end{pmatrix}. \quad (39)$$

We have

$$\hat{C}_{11} = \hat{C}_{22} = \frac{1}{4}(\hat{P}_0^* + \hat{P}_\pi^* + \hat{P}_{\pi/2}^* + \hat{P}_{3\pi/2}^*) \equiv \hat{C}_0, \quad (40)$$

$$\hat{C}_{12} = \frac{1}{4}(\hat{P}_0^* - \hat{P}_\pi^* + i\hat{P}_{\pi/2}^* - i\hat{P}_{3\pi/2}^*) \equiv \hat{C}_1. \quad (41)$$

The eigenstate of C_L corresponding to the eigenvalue ξ takes the form (ψ_A, ψ_B) , which satisfies the equation

$$\hat{C}_0\psi_A + \hat{C}_1\psi_B = \xi\psi_A, \quad \hat{C}_1^\dagger\psi_A + \hat{C}_0\psi_B = \xi\psi_B. \quad (42)$$

Due to the presence of inversion symmetry, irrespective of the inversion eigenvalues, we showed before that $\mathcal{P}\hat{C}_{ij}\mathcal{P} = \hat{C}_{ji} = \hat{C}_{ij}^\dagger$, which renders the second equation of Eq. (42):

$$\hat{C}_1\mathcal{P}\psi_A + \hat{C}_0\mathcal{P}\psi_B = \xi\mathcal{P}\psi_B. \quad (43)$$

We see that this is consistent with the first equation of Eq. (42) if $\psi_B = m\mathcal{P}\psi_A$, with $m^2 = 1$. The eigenvalue equation to solve is then

$$(\hat{C}_0 + m\hat{C}_1\mathcal{P})\psi_A = \xi\psi_A. \quad (44)$$

Also because of inversion symmetry, we have that

$$\hat{P}_{3\pi/2}^* = \mathcal{P}\hat{P}_{\pi/2}^*\mathcal{P}. \quad (45)$$

For the one-band problem, we know that

$$\hat{P}_0^*\mathcal{P} = \zeta(0)\hat{P}_0^*; \quad \hat{P}_\pi^*\mathcal{P} = \zeta(\pi)\hat{P}_\pi^*, \quad (46)$$

where $\zeta(0), \zeta(\pi)$ are the inversion eigenvalues at $k = 0, \pi$ of the occupied band $\psi_1(k)$. Hence to find the entanglement spectrum we need to diagonalize the following operator:

$$\hat{F} = \frac{1}{4}\{[1 + m\zeta(0)]\hat{P}_0^* + [1 - m\zeta(\pi)]\hat{P}_\pi^* + \hat{P}_{\pi/2}^*\mathcal{P}(\mathcal{P} + im) + \mathcal{P}\hat{P}_{\pi/2}^*(\mathcal{P} - im)\}. \quad (47)$$

For the half mode, we pick an ansatz,

$$\psi_A = a\psi_1(0) + b\psi_1(\pi), \quad (48)$$

which we show can diagonalize \hat{F} for an appropriate choice of a, b :

$$a = -[1 + im\zeta(\pi)] \left\langle \psi_1\left(\frac{\pi}{2}\right) \middle| \psi_1(\pi) \right\rangle, \quad (49)$$

$$b = [1 + im\zeta(0)] \left\langle \psi_1\left(\frac{\pi}{2}\right) \middle| \psi_1(0) \right\rangle.$$

This choice of a and b makes $(\hat{C}_0 + m\hat{C}_1\mathcal{P})\psi_A$ independent of both $\psi_1(\frac{\pi}{2})$, and $\mathcal{P}\psi_1(\frac{\pi}{2})$ in general (i.e., $[\hat{P}_{\pi/2}^*\mathcal{P}(\mathcal{P} + im) + \mathcal{P}\hat{P}_{\pi/2}^*(\mathcal{P} - im)]\psi_A = 0$), as it should in order for our ansatz to be an eigenstate. With this choice of a, b we find (by taking $\frac{1}{4}\{[1 + m\zeta(0)]\hat{P}_0^* + [1 - m\zeta(\pi)]\hat{P}_\pi^*\}\psi_A$) that in general the entanglement spectrum eigenvalue is dependent on $\langle \psi_1(0) | \psi_1(\pi) \rangle$, and hence the mode is not fixed at $1/2$. However, if the inversion eigenvalues at $k = 0, \pi$ are opposite $\zeta(\pi) = -\zeta(0)$ then $\langle \psi_1(0) | \psi_1(\pi) \rangle = 0$ and we find the eigenvalue of the entanglement spectrum of our ansatz to be

$$\xi = \frac{1}{4}[1 + m\zeta(0)]. \quad (50)$$

Recall that we have the liberty to choose the values of $m = \pm 1$, which is equivalent to saying $m = \pm\zeta(0)$. If we pick $m = \zeta(0)$, then our ansatz gives an eigenstate with entanglement eigenvalue equal to exactly $1/2$. The other choice leads to $\xi = 0$, so it is of no interest to us. The eigenstate at $1/2$ is $(\psi_A, \epsilon_0\mathcal{P}\psi_A)$, where

$$\psi_A = i \left\langle \psi_1\left(\frac{\pi}{2}\right) \middle| \psi_1(\pi) \right\rangle \psi_1(0) + \left\langle \psi_1\left(\frac{\pi}{2}\right) \middle| \psi_1(0) \right\rangle \psi_1(\pi). \quad (51)$$

In the pathological case when $\langle \psi_1(\frac{\pi}{2}) | \psi_1(\pi) \rangle = \langle \psi_1(\frac{\pi}{2}) | \psi_1(0) \rangle = 0$, both $\psi_1(0), \psi_1(\pi)$ are $1/2$ modes, but in general only their combination ψ_A gives a robust $1/2$ mode.

A second stable $1/2$ eigenvalue can be found by picking $m = \zeta(\pi) = -\zeta(0)$, but using a different ansatz:

$$\psi'_A = a'\psi_1\left(\frac{\pi}{2}\right) + b'\mathcal{P}\psi_1\left(\frac{\pi}{2}\right). \quad (52)$$

With this choice for m , the \hat{F} matrix to be diagonalized is

$$\frac{1}{4}\{\hat{P}_{\pi/2}^*\mathcal{P}[\mathcal{P} - i\zeta(0)] + \mathcal{P}\hat{P}_{\pi/2}^*[\mathcal{P} + i\zeta(0)]\}. \quad (53)$$

After straightforward calculations, we find the exact $1/2$ mode to be

$$\psi'_A = \psi_1\left(\frac{\pi}{2}\right) + i\zeta(0)\mathcal{P}\psi_1\left(\frac{\pi}{2}\right). \quad (54)$$

Thus for a completely generic Hamiltonian and its eigenstates we have shown that for one occupied band, if the inversion eigenvalues at $0, \pi$ in the bulk are the opposite of each other, there are two exact midgap states at $1/2$ in the entanglement spectrum. These midgap states have linearly independent eigenstates: $[\psi_A, \zeta(0)\mathcal{P}\psi_A]$, $[\psi'_A, -\zeta(0)\mathcal{P}\psi'_A]$ and ψ_A, ψ'_A as above. The standard intuition about interface or boundary states is that the eigenvalues repel less as the length of the system is increased, and the entanglement spectrum for the case analyzed here will have two exact $1/2$ modes in the thermodynamic limit, when cut exactly in half. Numerical simulations on specific models agree. In the thermodynamic limit, there can be no physical difference between a half cut and a cut away from half, and the levels will asymptote to $1/2$ in the infinite size limit if the cut is not exactly in half.

4. Two Occupied bands, Two-Site Problem

On our way to the most general case we now analyze the two-site, two occupied band problem. This follows in the same fashion as the previous example, except that we now have an extra complication. Namely, there are more options for the sets of occupied-band inversion eigenvalues.

We have the two occupied bands of the original Hamiltonian:

$$\hat{H}(k)\psi_1(k) = \epsilon_1(k)\psi_1(k); \quad \hat{H}(k)\psi_2(k) = \epsilon_2(k)\psi_2(k). \quad (55)$$

For $k = 0, \pi$ we generically have

$$\langle \psi_1(0) | \psi_2(0) \rangle = \langle \psi_1(\pi) | \psi_2(\pi) \rangle = 0. \quad (56)$$

We denote the inversion eigenvalues for $\psi_1(0), \psi_2(0), \psi_1(\pi), \psi_2(\pi)$ by $\zeta_1(0), \zeta_2(0), \zeta_1(\pi), \zeta_2(\pi)$, respectively. The order of the occupied inversion eigenvalues at each inversion symmetric momentum can be changed without affecting the topological structure so we assume that all negative inversion eigenvalues are listed first. We now calculate the number of midgap $1/2$ eigenvalues in the entanglement spectrum. If the number of negative inversion eigenvalues at $k = 0$ is the same as the number of negative inversion eigenvalues at π (which means the number of positive inversion eigenvalues is also the same), it is easy to prove that in general there are no protected $1/2$ modes because the entanglement eigenvalues depend on the overlap of bands at the two inversion symmetric momenta [cf. Eq. (62)]. If the number of negative eigenvalues at the inversion symmetric points is different, then we distinguish two cases:

Case 1. The number of negative eigenvalues at $k = 0$ differs from the number of negative eigenvalues at $k = \pi$ by ± 2 (i.e., they are both different):

$$\zeta_1(0)\zeta_1(\pi) = \zeta_1(0)\zeta_2(\pi) = \zeta_2(0)\zeta_1(\pi) = \zeta_2(0)\zeta_2(\pi) = -1 \quad (57)$$

implies

$$\begin{aligned} \langle \psi_1(0) | \psi_1(\pi) \rangle &= \langle \psi_1(0) | \psi_2(\pi) \rangle = 0, \\ \langle \psi_2(0) | \psi_1(\pi) \rangle &= \langle \psi_2(0) | \psi_2(\pi) \rangle = 0. \end{aligned} \quad (58)$$

The one-site entanglement spectrum obtained by cutting the system in half is obtained by diagonalizing the operator $C_L = (\hat{P}_0^* + \hat{P}_\pi^*)/2$ where $\hat{P}_0^* = \sum_{i=1}^2 |\psi_i(0)\rangle \langle \psi_i(0)|$, $\hat{P}_\pi^* = \sum_{i=1}^2 |\psi_i(\pi)\rangle \langle \psi_i(\pi)|$. Due to their inversion eigenvalues,

eigenstates at π have zero eigenvalue under the projector at 0 (and vice versa) but unit eigenvalue under the projector at π . We see that the modes at $1/2$ in the entanglement spectrum are given by exactly the occupied eigenstates of the original Hamiltonian $\psi_1(0), \psi_2(0), \psi_1(\pi), \psi_2(\pi)$. There are exactly four of them, twice the difference between negative and positive eigenvalues at the two inversion symmetric points.

Case 2. The number of negative eigenvalues at $k = 0$ differs from the number of negative eigenvalues at $k = \pi$ by ± 1 : this implies that at one k point, both inversion eigenvalues are identical. Without loss of generality, let this point be $k = \pi$ and let the eigenvalue products be

$$\begin{aligned} \zeta_1(0)\zeta_1(\pi) &= \zeta_1(0)\zeta_2(\pi) = -1, \\ \zeta_2(0)\zeta_1(\pi) &= \zeta_2(0)\zeta_2(\pi) = 1, \end{aligned} \quad (59)$$

which renders the following inner products to be zero:

$$\langle \psi_1(0) | \psi_2(0) \rangle = \langle \psi_1(0) | \psi_1(\pi) \rangle = \langle \psi_1(0) | \psi_2(\pi) \rangle = 0.$$

Consider the eigenvalue problem:

$$\frac{1}{2}(\hat{P}_0^* + \hat{P}_\pi^*)\psi_A = \alpha\psi_A. \quad (60)$$

We expand the state ψ_A into the (nonorthogonal) set of eigenstates $\psi_1(0), \psi_2(0), \psi_1(\pi), \psi_2(\pi)$:

$$|\psi_A\rangle = a_1|\psi_1(0)\rangle + a_2|\psi_2(0)\rangle + b_1|\psi_1(\pi)\rangle + b_2|\psi_2(\pi)\rangle. \quad (61)$$

As $\psi_1(0)$ is orthogonal with all the other eigenstates at both $k = 0, \pi$ since it has a different inversion eigenvalue, it is then obvious to see that the first $1/2$ mode solution is $(a_1, a_2, b_1, b_2) = (1, 0, 0, 0)$. To find another $1/2$ mode, we must expand in the three remaining eigenstates: $|\psi_A\rangle = a_2|\psi_2(0)\rangle + b_1|\psi_1(\pi)\rangle + b_2|\psi_2(\pi)\rangle$. There is a slight complication with this expansion since nothing guarantees that the states $|\psi_2(0)\rangle, |\psi_1(\pi)\rangle, |\psi_2(\pi)\rangle$ are orthogonal: in fact, in the generic case, they are not. Moreover, it is not clear that they are even linearly independent. We will assume that the states are linearly independent. This is a perfectly valid procedure since if the $|\psi_2(0)\rangle, |\psi_1(\pi)\rangle, |\psi_2(\pi)\rangle$ are not independent, we will simply get a nontrivial null space. However, the nonzero eigenvalues are still good eigenvalues of the entanglement matrix. The matrix to diagonalize is

$$\begin{pmatrix} \frac{1}{2} & \langle \psi_2(0) | \psi_1(\pi) \rangle & \langle \psi_2(0) | \psi_2(\pi) \rangle \\ \langle \psi_2(0) | \psi_1(\pi) \rangle^* & \frac{1}{2} & 0 \\ \langle \psi_2(0) | \psi_2(\pi) \rangle^* & 0 & \frac{1}{2} \end{pmatrix} \quad (62)$$

with an obvious $1/2$ eigenvalue for the state $(a_2, b_1, b_2) = (0, -\langle \psi_2(0) | \psi_2(\pi) \rangle, \langle \psi_2(0) | \psi_1(\pi) \rangle)$ ($a_1 = 0$). In the nongeneric case when $\langle \psi_2(0) | \psi_2(\pi) \rangle = \langle \psi_2(0) | \psi_1(\pi) \rangle = 0$, $\psi_2(0)$ is the other $1/2$ eigenvalue. We have hence proved the existence of two exact $1/2$ eigenvalues for the two-site problem, cut in half, when the difference between the number of negative inversion eigenvalues at $0, \pi$ is ± 1 .

As in the one-band case, this argument can be extended analytically to a system with four sites as shown in Appendix F, indicating that the conclusions hold for chains longer than two sites.

5. N occupied bands, two-site problem

We now show that the two-site problem with n_1 negative inversion eigenvalues at $k = 0$ and n_2 negative inversion eigenvalues at $k = \pi$ with a total number N of occupied bands contains $2|n_1 - n_2|$ zero modes in the entanglement spectrum when a real-space cut is made on a system with periodic boundary conditions (i.e., there are two cuts). The simplest case, which should be obvious from our previous examples, is that all the N inversion eigenvalues at $k = 0$ are identical and are the opposite of the N eigenvalues at $k = \pi$. In this case, the projector at one of the inversion symmetric k 's annihilates all the eigenstates at the other inversion symmetric k , and the $2N$ occupied eigenstates of the original two-site Hamiltonian are also the eigenstates of the entanglement spectrum at fixed eigenvalue $1/2$. Due to their orthogonality, they are linearly independent. From here it is clear that our formula is correct for this case.

Now we will prove the more general formula. Let n_1 and n_2 be the number of eigenvectors for the -1 eigenvalue of $\hat{P}_0^* \mathcal{P} \hat{P}_0^*$ and $\hat{P}_\pi^* \mathcal{P} \hat{P}_\pi^*$, respectively, and assume $n_1 > n_2$. Recall that K is the number of orbitals per site, so \mathcal{P} is a $K \times K$ matrix acting on \mathbf{C}^K where \mathbf{C}^K is a K -dimensional complex vector space, i.e., a set of K -dimensional complex column vectors. \mathcal{P} has ± 1 eigenvalues and we denote the invariant subspaces corresponding to the positive/negative eigenvalue by \mathcal{H}_\pm ($\mathcal{H}_- + \mathcal{H}_+ = \mathbf{C}^K$).

Now the subspaces $\hat{P}_0^* \mathbf{C}^K$ and $\hat{P}_\pi^* \mathbf{C}^K$ are invariant under the inversion operation \mathcal{P} , and $\hat{P}_0^* \mathbf{C}^K \cap \mathcal{H}_-$ is precisely the subspace spanned by the n_1 eigenvectors of $\hat{P}_0^* \mathcal{P} \hat{P}_0^*$ corresponding to its negative eigenvalue. Similarly, $\hat{P}_\pi^* \mathbf{C}^K \cap \mathcal{H}_-$ is precisely the subspace spanned by the n_2 eigenvectors of $\hat{P}_\pi^* \mathcal{P} \hat{P}_\pi^*$ corresponding to its negative eigenvalue. Since $\dim[\hat{P}_0^* \mathbf{C}^K \cap \mathcal{H}_-] = n_1$ and $\dim[\hat{P}_\pi^* \mathbf{C}^K \cap \mathcal{H}_-] = n_2$, with $n_1 > n_2$, we can always find $n_1 - n_2$ vectors Ψ_n in $\hat{P}_0^* \mathbf{C}^K \cap \mathcal{H}_-$ that are orthogonal to any vector in $\hat{P}_\pi^* \mathbf{C}^K \cap \mathcal{H}_-$. Since these vectors are in \mathcal{H}_- , they are also orthogonal to any vector in $\hat{P}_\pi^* \mathbf{C}^K \cap \mathcal{H}_+$. In other words, Ψ_n 's are $n_1 - n_2$ vectors in $\hat{P}_0^* \mathbf{C}^K$ perpendicular to all the vectors in $\hat{P}_\pi^* \mathbf{C}^K$. Consequently,

$$C_L \Psi_n = \frac{1}{2}(\hat{P}_0^* + \hat{P}_\pi^*)\Psi_n = \frac{1}{2}\Psi_n, \quad (63)$$

for all $n_1 - n_2$ vectors Ψ_n . Following the same arguments, we can find $n_1 - n_2$ vectors in $\hat{P}_\pi^* \mathbf{C}^K \cap \mathcal{H}_+$ that are orthogonal to $\hat{P}_0^* \mathbf{C}^K$, and consequently another set of $n_1 - n_2$ eigenvectors with eigenvalue $\frac{1}{2}$. In total, there are $2(n_1 - n_2)$ robust modes of C_L at $1/2$. We remind the reader that the factor of 2 is simply coming from the fact that we are cutting a periodic system and thus there exist *two* separate cuts. For a more explicit proof see Appendix B. As mentioned at the end of Sec. II the number of exact $1/2$ modes is equal to $2\mathcal{N}$ [cf. Eq. (12)]. This connection between the invariant \mathcal{N} and the protected modes in the entanglement spectrum is one of the main results of the paper, namely

$$\text{number of protected } 1/2 \text{ modes per cut} = \mathcal{N}. \quad (64)$$

6. Extension to higher dimensions

The extension to higher dimensions is just a matter of reinserting the extra momenta which are conserved in the

presence of the cut. As an example let us consider two dimensions with an entanglement cut parallel to the y axis so that k_y is a conserved quantum number. The exact midgap modes in the entanglement spectrum will exist only at inversion symmetric points in the momentum parallel to the cut, i.e., $k_y = 0, \pi$. However, since bands become continuous when k_y is finely discretized, in the thermodynamic limit the existence of $1/2$ modes at these two discrete k points implies the existence of midgap bands. The number of bands will be equal to the number of $1/2$ modes. These bands typically disperse away from $1/2$ but do not have to connect with the ‘‘bulk’’ entanglement bands at entanglement eigenvalues close to 0,1 (in the special cases of Chern insulators and time-reversal symmetric nontrivial insulators, they do connect and have spectral flow, as pointed out previously). However, since the modes at $1/2$ are robust upon changes in the original Hamiltonian that do not close the band gap, the midgap bands cannot be entirely pushed to the entanglement bulk band edges at 0 or 1. This means the system is a nontrivial insulator (i.e., S_{ent} cannot be made to vanish) if the number of negative (or positive) inversion eigenvalues is different between inversion symmetric points. We would like to know at which inversion symmetric k_y the exact $1/2$ modes will occur. The answer is simple: there will be exactly $2|n_1 - n_2|$ $1/2$ modes at $k_y = 0$ when the number of negative inversion eigenvalues at $(k_x, k_y) = (0, 0)$ differs by $|n_1 - n_2|$ from the number of negative inversion eigenvalues at $(k_x, k_y) = (\pi, 0)$. Additionally there will be exactly $2|n'_1 - n'_2|$ $1/2$ modes at $k_y = \pi$ when the number of negative inversion eigenvalues at $(k_x, k_y) = (0, \pi)$ differs by $|n'_1 - n'_2|$ from the number of negative inversion eigenvalues at $(k_x, k_y) = (\pi, \pi)$. The generalization to higher dimensions is the trivial extension of this. We can think of this procedure in terms of a set of \mathcal{N} invariants, one for each inversion invariant momentum. This procedure is straightforward and we will not detail it here.

D. Spectral flow in the entanglement spectrum

As mentioned earlier in this section, the two important features of the entanglement spectra of inversion symmetric insulators are protected midgap modes, and spectral flow. What we mean by spectral flow is a continuous connection between the valence and conduction bulk entanglement bands through the entanglement edge states [an example is seen in Figs. 8(h) and 8(i)]. For a TRI topological insulator in two and three dimensions, or for a Chern insulator in two dimensions, the entanglement spectrum mirrors the energy spectrum of the open-boundary Hamiltonian. In fact, we have already shown an explicit map between the entanglement spectrum and the energy spectrum of the open boundary spectrally flattened Hamiltonian.³⁰ This implies that if there is spectral flow between the conduction and valence bands in the energy spectrum then such a flow exists in the entanglement spectrum. In fact, this is the only case where there is true spectral flow in the entanglement spectrum. Out of the entire set of inversion invariant topological insulators only a small subset have spectral flow. Instead most nontrivial systems simply exhibit protected midgap states (or bands) but these do not continuously interpolate between the bulk entanglement bands.

There is a nice example that illustrates this dichotomy. Let us consider the 3D strong topological insulator with both inversion and time-reversal symmetries. If we preserve \mathcal{P} but break T , spectral flow generically disappears from the energy spectrum because gaps are opened in the surface-state spectrum. The degeneracies that existed in the entanglement spectrum at the time-reversal invariant momenta when T is preserved are almost all broken, with the exception of the protected degeneracy for states at $\xi = 1/2$. This degeneracy splitting breaks the spectral flow in the entanglement spectrum, and opens gaps at the TRI momenta as shown for a specific model in Figs. 9(h) and 9(i). As such, the entanglement spectrum is capable of distinguishing the subtle difference between topological insulators with T and \mathcal{P} symmetry from topological insulators with only \mathcal{P} symmetry.

IV. LINEAR RESPONSE

To date, some of the most spectacular features of topological insulators are their responses to external fields. The Chern insulators exhibit a quantized Hall effect and the 3D TRI topological insulators exhibit a topological magnetoelectric effect. The topological invariants which distinguish these states from trivial insulators are directly connected with the corresponding response coefficient. In fact, a whole ladder of topological responses was uncovered in Ref. 9. With this precedent one would hope that the inversion invariant topological insulators would also exhibit some type of defining physical response. However, this turns out to be true in only a limited set of the inversion invariant topological insulators. The situation is quite varied (remember that we only have generic access to the information held in the inversion eigenvalues): Some insulators have unique well defined topological responses, some systems can exhibit one of several allowed topological responses, and for others it is unclear if there is any topological response at all. We will see examples of all three cases in Sec. V. In this section though we focus on the first case where insulators do exhibit a unique response which is the most interesting physical case. We discuss responses in one, two, and three dimensions and then we briefly mention how the general pattern might be extended to higher dimensions to make contact with Refs. 9 and 11 in Appendix J.

A. 1D inversion symmetric insulators

The following discussion applies to a generic one-dimensional K -band insulator with N occupied bands, and with a generic inversion symmetry, i.e.,

$$\mathcal{P}\hat{H}(k)\mathcal{P}^{-1} = \hat{H}(-k), \quad (65)$$

where the inversion matrix \mathcal{P} is unitary and squares to the identity

$$\mathcal{P}^\dagger\mathcal{P} = 1, \quad \mathcal{P}\mathcal{P} = 1. \quad (66)$$

As explicitly shown in Appendix D, the charge polarization P_1 of a 1D insulator behaves as

$$P_1 \rightarrow -P_1 + je \quad (67)$$

under inversion, where j is a gauge-dependent integer. This shows that the polarization of 1D systems with inversion

symmetry can take only two values, 0 and $e/2$, modulo a gauge-dependent integer multiple of e .³⁶ We will prove that if the $\chi_{\mathcal{P}}$ invariant, defined as the product of all inversion eigenvalues of the occupied bands, takes the value 1, then $P_1 = 0$, and if $\chi_{\mathcal{P}} = -1$, then $P_1 = e/2$. More precisely, we will establish that

$$P_1 = \frac{e}{2\pi i} \ln \left[\prod_{i=1}^N \zeta_i(0)\zeta_i(\pi) \right]. \quad (68)$$

The integer ambiguity of the logarithm is identical to the integer ambiguity of the polarization.

For this, we define the k -dependent $N \times N$ unitary matrix $\hat{B}(k)$,

$$B_{ij}(k) = \langle u_{i,-k} | \mathcal{P} | u_{j,k} \rangle, \quad (69)$$

where the indices i and j run only over the occupied bands. The inversion eigenvalues $\zeta_i(0)$ and $\zeta_i(\pi)$ coincide with the eigenvalues of the matrix $\hat{B}(k)$, when evaluated at the special inversion k points $k = 0$ and π . It is then obvious that the determinant of $\hat{B}(k)$ at these k_{inv} points is the product of the inversion eigenvalues at that inversion invariant point:

$$\det[\hat{B}(k_{\text{inv}})] = \prod_{i=1}^N \zeta_i(k_{\text{inv}}). \quad (70)$$

We now turn to the calculation of the polarization,

$$P_1 = \frac{e}{2\pi} \int_{-\pi}^{\pi} dk A(k), \quad (71)$$

where $A(k)$ is the adiabatic connection:

$$A(k) = -i \sum_{i \in \text{occ}} \langle u_{i,k} | \nabla_k | u_{i,k} \rangle. \quad (72)$$

We will use the following important relation, which is proven in Appendix E:

$$A(-k) = -A(k) + i \text{Tr}[\hat{B}(k) \nabla_k \hat{B}^\dagger(k)]. \quad (73)$$

The last term can be written in the equivalent form:

$$\text{Tr}[\hat{B}(k) \nabla_k \hat{B}^\dagger(k)] = -\nabla_k \ln(\det[\hat{B}(k)]). \quad (74)$$

We can now proceed as follows:

$$\begin{aligned} P_1 &= \frac{e}{2\pi} \int_0^\pi dk [A(k) + A(-k)] \\ &= \frac{e}{2\pi i} \int_0^\pi dk \nabla_k \ln(\det[\hat{B}(k)]), \end{aligned} \quad (75)$$

with the final answer:

$$P_1 = \frac{e}{2\pi i} [\ln(\det[\hat{B}(\pi)]) - \ln(\det[\hat{B}(0)])]. \quad (76)$$

This, together with Eq. (70) and the fact that the determinants can take only the values ± 1 , so that $\det[\hat{B}] = 1/\det[\hat{B}^\dagger]$, prove the statement of Eq. (68).

We mention that similar arguments were used in Ref. 9 to classify 1D particle-hole symmetric insulators via a Z_2 invariant. In fact, the Z_2 invariant found there is exactly the value of the charge polarization modulo an integer. For a 1D model with both inversion and particle-hole symmetry, such as the 1D lattice Dirac model, the invariants coincide.

In the nontrivial phase, the 1D Dirac model exhibits midgap energy modes bound to the ends of an open chain. The requirement of particle-hole symmetry restricts these modes to lie at zero energy if there are an odd number of them. An even number on each end is not stable and the degeneracy can be lifted, which is another manifestation of the Z_2 nature. The minimal case is one mode on each end and with particle-hole symmetry at half filling one mode is filled and one is empty. This leads to an excess charge of $+e/2$ on the side with the filled state and $-e/2$ on the empty side. If we break particle-hole symmetry but keep inversion symmetry then both modes can be empty or filled, but they are empty or filled together because inversion symmetry connects the two modes. This means that the excess charge is either $+e/2$ on *both* ends or $-e/2$ on *both* ends. However, because of the gauge variance of the polarization this is equivalent to the polarization in the particle-hole symmetric case. Thus both insulators have the same topological electric response. One can form a complimentary argument by using the effective response action for particle-hole symmetric insulators given in Refs. 9 and 37:

$$S_{\text{eff}} = \frac{1}{2} \int dx dt P_1 \epsilon^{\mu\nu} F_{\mu\nu}, \quad (77)$$

where $F_{\mu\nu}$ is the field-strength tensor of the externally applied electromagnetic field. The argument for the quantization of P_1 is as follows. In the partition function the phase due to this term is $e^{iS_{\text{eff}}}$ and under particle-hole symmetry $P_1 \rightarrow -P_1$. Thus if our system is to be particle-hole symmetric we must have $e^{2iS_{\text{eff}}} = 1$. For constant P_1 the integral gives $2\pi n$ for integer n and we have $e^{4\pi i n P_1} = 1$ and thus $P_1 = 0, 1/2 \pmod{Z}$ in dimensionless units. Since $P_1 \rightarrow -P_1$ under inversion symmetry the *same* argument holds and P_1 is quantized there as well. A similar argument for magnetoelectric polarizability of 3D insulators with inversion symmetry was given in Ref. 29. As an aside, we recall that in one dimension we also had an invariant $\chi_{\mathcal{P}}^{(2)}$ which helped classify the four-band insulator example. We do not know of any response related to this invariant in 1D inversion invariant insulators.

Additionally, Eq. (68) can be derived using an alternative approach based on a monodromy argument. The effect of a magnetic flux Φ through a large one-dimensional ring can always be gauged away by a transformation $\Psi \rightarrow e^{-i\Phi} \Psi$, which is equivalent to a translation in k space by Φ . The evolution of the states in response to an adiabatically slowly varying magnetic flux can be understood from the evolution of the Bloch states in response to an adiabatic translation of k space.³⁸ The monodromy $\hat{U}(k, k_0)$ describes the evolution of the occupied Bloch states when the k of the Bloch Hamiltonian $\hat{H}(k)$ is adiabatically varied, and it is the unique solution of the equation

$$i \frac{d}{dk} \hat{U}(k, k_0) = i [\hat{P}_k, \partial_k \hat{P}_k] \hat{U}(k, k_0), \quad (78)$$

with the initial condition $\hat{U}(k_0, k_0) = \hat{P}_{k_0}$, assuming that we start the evolution from k_0 .

The monodromy $\hat{U}(k_0, k_0)$ maps the space of occupied Bloch states $\hat{P}_{k_0} \mathcal{C}^K$ at k_0 into the space of occupied Bloch states $\hat{P}_k \mathcal{C}^K$ at k . Since $k = \pm\pi$ are the same, $\hat{U}(\pi, -\pi)$ takes the space $\hat{P}_{-\pi} \mathcal{C}^K$ into itself, and is a unitary operator

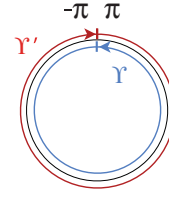


FIG. 3. (Color online) The adiabatic transport is carried over γ, γ' .

that we call \hat{U}_γ , where γ is one of the paths shown in Fig. 3. U_γ gives the change occurring after a full quantum of magnetic flux has been pumped through the system. If bases $\{\psi_i(k)\}$ were prechosen for all $\hat{P}_k \mathcal{C}^K$ spaces, the matrix $U_{ij}(k) = \langle \psi_i(k) | \hat{U}(k, k_0) | \psi_j(k_0) \rangle$ satisfies the parallel transport equation

$$\frac{d}{dk} \hat{U}(k) = i \hat{A}(k) \hat{U}(k), \quad (79)$$

where $\hat{A}(k)$ is the full non-Abelian adiabatic connection discussed by Wilczek and Zee in Ref. 39. For a more detailed discussion one can consult Ref. 40.

There is a direct relation between the determinant of the monodromy and the line integral of the Abelian connection (the trace of the full connection):

$$\det[\hat{U}(k_f, k_i)] = \exp \left(i \int_{k_i}^{k_f} \text{Tr}[\hat{A}(k)] dk \right). \quad (80)$$

Indeed, working with predefined basis sets for $\hat{P}_k \mathcal{C}^K$ and breaking the interval k_f, k_i in small subintervals k_f, k_n, \dots, k_i , we have, up to second-order corrections,

$$\begin{aligned} \hat{U}(k_f, k_i) &= \hat{U}(k_f, k_n) \hat{U}(k_n, k_{n-1}) \cdots \hat{U}(k_1, k_i) \\ &= [I + i(k_f - k_n) \hat{A}(k_n)] \cdots [I + i(k_1 - k_i) \hat{A}(k_i)]. \end{aligned} \quad (81)$$

Taking the determinant on both sides and using some elementary identities, we obtain

$$\begin{aligned} \det[\hat{U}(k_f, k_i)] &= (1 + i(k_f - k_n) \text{Tr}[\hat{A}(k_n)]) \cdots (1 + i(k_1 - k_i) \text{Tr}[\hat{A}(k_i)]) \\ &= e^{i(k_f - k_n) \text{Tr}[\hat{A}(k_n)]} \cdots e^{i(k_1 - k_i) \text{Tr}[\hat{A}(k_i)]}, \end{aligned} \quad (82)$$

from which the identity of Eq. (80) follows. The identity is valid in higher dimensions too.

Assuming $k_0 = -\pi$, a conjugation of Eq. (78) with the inversion operator \mathcal{P} gives

$$\partial_k \{ \mathcal{P} \hat{U}(k, -\pi) \mathcal{P}^{-1} \} = i [\hat{P}_{-k}, \partial_k \hat{P}_{-k}] \mathcal{P} \hat{U}(k, -\pi) \mathcal{P}^{-1},$$

with the initial condition $\mathcal{P} \hat{U}(-\pi, -\pi) \mathcal{P}^{-1} = \hat{P}(\pi)$. This is just the equation for $\hat{U}(-k, \pi)$, which shows that $\mathcal{P} \hat{U}(k, -\pi) \mathcal{P}^{-1}$ coincides with $\hat{U}(-k, \pi)$. Equivalently we can think that \mathcal{P} sends γ into γ' in Fig. 3. Now obviously $\hat{U}_\gamma \hat{U}_{\gamma'}$ equals the identity, therefore

$$\det[\hat{U}_\gamma \mathcal{P} \hat{U}_{\gamma'} \mathcal{P}^{-1}] = 1. \quad (83)$$

Using the elementary properties of the determinant, we conclude that $\det[\hat{U}_\gamma]^2 = 1$, hence $\det[\hat{U}_\gamma]$ can take only two values:

$$\det[\hat{U}_\gamma] = \pm 1. \quad (84)$$

The following calculation will show that the cases $\det[\hat{U}_\gamma] = \pm 1$ correspond to $P_1 = 0$ and $P_1 = \frac{\epsilon}{2} \pmod{Z}$, respectively. Indeed,

$$\begin{aligned} \det[\hat{U}_\gamma] &= \det[\hat{U}(\pi, 0)\hat{U}(0, -\pi)] = \det[\hat{U}(\pi, 0)\mathcal{P}\hat{U}(0, \pi)\mathcal{P}^{-1}] \\ &= \det[\hat{U}(\pi, 0)\hat{P}_0\mathcal{P}\hat{P}_0\hat{U}(0, \pi)\hat{P}_\pi\mathcal{P}^{-1}\hat{P}_\pi]. \end{aligned} \quad (85)$$

In the last line we have inserted the projectors $\hat{P}_{0,\pi}$ to see explicitly the spaces on which \mathcal{P} is acting. Using again the elementary properties of the determinant and the fact that $\hat{U}(\pi, 0)\hat{U}(0, \pi) = 1$, we obtain

$$\det[\hat{U}_\gamma] = \det[\hat{P}_0\mathcal{P}\hat{P}_0] \det[\hat{P}_\pi\mathcal{P}^{-1}\hat{P}_\pi] \quad (86)$$

or

$$\det[\hat{U}_\gamma] = \prod_{i=1}^N \zeta_i(0)\zeta_i(\pi) \quad (87)$$

and thus

$$P_1 = \frac{e}{2\pi i} \ln \det[\hat{U}_\gamma] \quad (88)$$

[cf. Eq. (80)].

For a topological insulator, no matter what definition one uses, it is always the case that, when the hopping terms between the neighbors are adiabatically turned off, that is, when one takes the atomic limit, the insulating gap of the system closes at some point in the process. One can investigate this issue using the inversion eigenvalues directly, as we have focused on, but here we see how the physical response enters into the picture. Note that the inversion eigenvalues can be easily computed for simple models, but may not always be available, especially for complex materials. P_1 or U_γ are physically measurable, so they can provide physical signatures of the nontrivial state. In the atomic limit, the bands have no dispersion, so in this limit \hat{U}_γ is just the identity matrix. If $\text{Det}[\hat{U}_\gamma] = -1$, it is obvious that U_γ cannot be smoothly connected to the identity and the insulator is topological. However, we also must note that if $\det[\hat{U}_\gamma] = 1$, it is *not* necessary that the insulator is trivial.

We can refine the investigation by asking when can \hat{U}_γ be smoothly connected to the identity? For this, let us look again at Eq. (85):

$$\hat{U}_\gamma = \hat{U}(\pi, 0)\hat{P}_0\mathcal{P}\hat{P}_0\hat{U}(0, \pi)\hat{P}_\pi\mathcal{P}\hat{P}_\pi. \quad (89)$$

The first term, $\hat{U}(\pi, 0)\hat{P}_0\mathcal{P}\hat{P}_0\hat{U}(0, \pi)$, is just $\hat{P}_0\mathcal{P}\hat{P}_0$ parallel transported from $k = 0$ to $k = \pi$. The parallel transport does not alter the eigenvalues of $\hat{P}(0)\mathcal{P}\hat{P}(0)$, which are pinned at ± 1 (recall that $\mathcal{P}^2 = 1$). The eigenvalues of $\hat{P}(\pi)\mathcal{P}\hat{P}(\pi)$ are also pinned at ± 1 . So what we have in Eq. (89) is a product of two operators with eigenvalues pinned at ± 1 and because of that the eigenvalues cannot change under any smooth deformation of the Hamiltonian that keeps the insulating gap open and preserves inversion symmetry. Now, if \hat{U}_γ can be deformed into the identity, then $\hat{U}(\pi, 0)\hat{P}_0\mathcal{P}\hat{P}_0\hat{U}(0, \pi)$ can be turned into the inverse of $\hat{P}_\pi\mathcal{P}\hat{P}_\pi$ and this requires that $\hat{P}_0\mathcal{P}\hat{P}_0$ and $\hat{P}_\pi\mathcal{P}\hat{P}_\pi$ have identical eigenvalues, counting the degeneracy too. The conclusion is this: if the set of inversion eigenvalues of

$$\hat{P}_0\mathcal{P}\hat{P}_0 \quad \text{and} \quad \hat{P}_\pi\mathcal{P}\hat{P}_\pi \quad (90)$$

are not identical, then \hat{U}_γ cannot be connected to the identity. Since the eigenvalues are restricted to just ± 1 values, then the following integer:

$$\mathcal{N} = \frac{1}{2} |\text{Tr}\{\hat{P}_0\mathcal{P}\hat{P}_0 - \hat{P}_\pi\mathcal{P}\hat{P}_\pi\}|, \quad (91)$$

tells how many eigenvalues are different for the two matrices in Eq. (90). To reach the atomic limit, we need to flip \mathcal{N} inversion eigenvalues, and that will require a minimum of \mathcal{N} gap closings. This definition of \mathcal{N} exactly matches the definition in Eq. (12). Unfortunately, we were not able to find an expression of the topological invariant \mathcal{N} solely in terms of the monodromy \hat{U}_γ , but we know there are precisely \mathcal{N} topological obstructions when trying to connect the monodromy to the identity. The topological invariant \mathcal{N} also gives the number of robust edge modes seen in the entanglement spectrum on a single cut as shown in Sec. III C 5.

B. 2D inversion symmetric insulators

The physical response of 2D inversion symmetric insulators is much richer than those in one dimension. Based solely on the inversion eigenvalues, one can define several invariants, the first of which is the isotropic extension of χ_P to two dimensions, i.e.,

$$\chi_P = \prod_{k_{\text{inv}; i \in \text{occ}}} \zeta_i(k_{\text{inv}}), \quad (92)$$

where k_{inv} runs over all four inversion invariant k points. We show that

$$\chi_P = (-1)^{C_1}, \quad (93)$$

where C_1 is the first Chern number of the ground state. Thus if χ_P is negative the system *must* be in a quantum Hall state, and if it is positive it is in a state with an even Chern number, which can be zero. Thus only if it is negative are we sure it is in a topological insulator state.

We will prove the statement of Eq. (93) in two ways, first using a band crossing argument and then a monodromy argument. Let us begin by assuming we are in a trivial insulator state in an atomic limit with N occupied bands and that we have inversion symmetry. We can reach any nontrivial topological insulator state from this limit through a series of Hamiltonian deformations that will lead us through band crossings. Our assumption of an atomic limit implies that $\chi_P = +1$ initially. If we want to generate $\chi_P = -1$ we need to have an odd number of band crossings between bands with *opposite* inversion eigenvalues. Assume we have an odd number of such crossings. This implies that there must be an odd number of crossings at the inversion invariant points. This is true since crossings occurring at noninvariant k are accompanied by a crossing at $-k$ always giving an even number of eigenvalue switches, which will not affect the value of χ_P . Thus we only need to consider the odd number of crossings occurring at the invariant momenta. The generic Hamiltonian of each crossing between opposite inversion eigenvalue states near an inversion invariant momentum is $H = p_1\sigma^1 + p_2\sigma^2 + m_{\text{eff}}\sigma^3$ where (p_1, p_2) is the momentum away from the inversion invariant point, m_{eff} is a term parametrizing the distance to the band crossing, and σ^3 is the inversion operator projected onto the two crossing bands. Exactly at the inversion invariant

momentum the Hamiltonian reduces to $m_{\text{eff}}\sigma^3$ as it must in order to commute with \mathcal{P} there. As the crossing occurs m_{eff} switches sign and an inversion eigenvalue of the occupied band is changed. We note that this Hamiltonian is a 2D massive Dirac Hamiltonian, which is switching the sign of the mass. At such a crossing, the Chern number changes by ± 1 and thus we see that going through an odd number of crossings changes the parity of the Chern number. Thus if $\chi_{\mathcal{P}} = -1$ the parity of the Chern number is odd since the parity is even in the initial atomic limit, i.e., $C_1 = 0$. The inversion eigenvalues thus give us a rough way to characterize the quantum Hall effect in an insulator.

The corresponding monodromy argument proceeds as follows. We consider the monodromy corresponding to the path 012345610 in Fig. 4, starting from the middle of the Brillouin zone and continuing on its rim. This path can be also be viewed as the composition $\gamma + \gamma'$ of the paths $\gamma = 012340$ and $\gamma' = 045610$, and the monodromy corresponding to $\gamma + \gamma'$ can be written as a product of partial monodromies:

$$\hat{U}_{\gamma+\gamma'} = \hat{U}_{01}\hat{U}_{16}\hat{U}_{65}\hat{U}_{54}\hat{U}_{43}\hat{U}_{32}\hat{U}_{21}\hat{U}_{10}. \quad (94)$$

Since the products $\hat{U}_{10}\hat{U}_{01}$, $\hat{U}_{16}\hat{U}_{54}$, $\hat{U}_{65}\hat{U}_{32}$, and $\hat{U}_{43}\hat{U}_{21}$ are all equal to the identity, taking the determinant of Eq. (94) leads us to conclude that $\det[\hat{U}_{\gamma+\gamma'}] = 1$. This is not surprising and is related to the fact that $\det[\hat{U}_{\gamma+\gamma'}] = e^{2i\pi C_1}$ [see Eq. (80)] and the first Chern number is an integer.

The next observation is that inversion sends γ into γ' and consequently

$$\det[\hat{U}_{\gamma+\gamma'}] = \det[\hat{U}_{\gamma}\mathcal{P}\hat{U}_{\gamma'}\mathcal{P}] = \det[\hat{U}_{\gamma}]^2. \quad (95)$$

The conclusion is that the determinant of \hat{U}_{γ} can only take the values ± 1 . Since the path γ encircles half of the Brillouin zone, and the adiabatic curvature is symmetric when $k \rightarrow -k$, it is also true that $\det[\hat{U}_{\gamma}] = e^{i\pi C_1}$ [see Eq. (80)].

We now take a closer look at \hat{U}_{γ} . Since inversion sends 10 into 40 and 20' into 30', we have

$$\begin{aligned} \hat{U}_{\gamma} &= \hat{U}_{04}\hat{U}_{43}\hat{U}_{30'}\hat{U}_{02}\hat{U}_{21}\hat{U}_{10} \\ &= \mathcal{P}\hat{U}_{01}\mathcal{P}\hat{U}_{12}\mathcal{P}\hat{U}_{20'}\mathcal{P}\hat{U}_{02}\hat{U}_{21}\hat{U}_{10}. \end{aligned} \quad (96)$$

Inserting the appropriate projectors to specify explicitly on which spaces are the \mathcal{P} operators acting, taking the determinant, and using its elementary properties together with the fact that $\hat{U}_{ij}\hat{U}_{ji}$ equals the identity, we obtain

$$\begin{aligned} (-1)^{C_1} &= \det[\hat{U}_{\gamma}] = \det[\hat{P}_{0,0}\mathcal{P}\hat{P}_{0,0}] \det[\hat{P}_{0,\pi}\mathcal{P}\hat{P}_{0,\pi}] \\ &\quad \times [\det \hat{P}_{\pi,\pi}\mathcal{P}\hat{P}_{\pi,\pi}] \det[\hat{P}_{\pi,0}\mathcal{P}\hat{P}_{\pi,0}], \end{aligned} \quad (97)$$

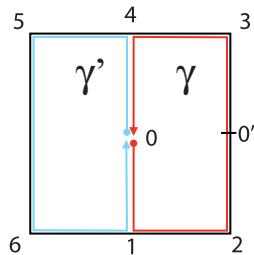


FIG. 4. (Color online) The two paths γ and γ' used in the monodromy argument in two dimensions.

which completes monodromy argument for Eq. (93).

We will briefly mention two other interesting inversion invariants one can define in two dimensions. The first is an anisotropic invariant defined by taking the product of the inversion eigenvalues at only two invariant momenta in the 2D Brillouin zone. We provide an example in Sec. V with $\chi_{\mathcal{P}} = +1$ but where this anisotropic invariant is nontrivial. This invariant has interesting implications for the charge polarization, but there are some subtleties that we will illustrate. To begin, assume we have an inversion invariant, insulator Hamiltonian $\hat{H}(k_x, k_y)$ with N occupied bands such that $\prod_{i=1}^N \zeta_i(0,0)\zeta_i(0,\pi) = -1$. This implies that the 1D Hamiltonian $\hat{H}(0, k_y)$ has a charge polarization $P_1 = e/2$ since this restricted Hamiltonian is inversion invariant. Now we want to know if this nontrivial anisotropic invariant is enough to specify the full polarization of the entire 2D system. The answer is no. To see why, we slightly deform $\hat{H}(0, k_y)$ away from the k_y axis. The 1D Hamiltonian $\hat{H}(\delta k_x, k_y)$ is *not* generically invariant under inversion symmetry because it gets mapped onto the Hamiltonian $\hat{H}(-\delta k_x, k_y)$ and thus the polarization does not have to remain quantized with value $e/2$.³⁶ In fact, by the time we have deformed all the way to the Hamiltonian $\hat{H}(\pi, k_y)$ the polarization, which must again be quantized since this Hamiltonian does have inversion, can be completely different. So while we can think of $\hat{H}(k_x, k_y)$ as a gapped interpolation between $\hat{H}(0, k_y)$ and $\hat{H}(\pi, k_y)$, inversion symmetry, and thus the value of the polarization, is not preserved along the interpolation. Intuitively this makes sense because it is exactly when the polarization changes its quantized value that the system has an odd Chern number. An odd Chern number is allowed because a quantum Hall effect is not forbidden by the requirement of inversion symmetry. Thus if we have 2D inversion symmetry the anisotropic invariant *does not* determine the 2D charge polarization.

As an aside, since we clearly know why inversion symmetry fails, we immediately know how to fix the problem. We fix it by requiring a *reflection* symmetry (i.e., parity symmetry) about an axis, instead of inversion. Without loss of generality we can have a reflection symmetry \mathcal{M} such that $\mathcal{M}\hat{H}(k_x, k_y)\mathcal{M}^{-1} = \hat{H}(k_x, -k_y)$. We will see that the reflection eigenvalues will specify the polarization in the y direction (for this choice of reflection symmetry). First, we see that the inversion invariant momenta are also reflection invariant momenta. Thus $[\hat{H}(k_{\text{inv}}), \mathcal{M}] = 0$, and we can label the states at these points by their reflection eigenvalues which we will also call $\zeta_i(k_{\text{inv}})$. Now let us assume the same setup as the previous paragraph with $\prod_{i=1}^N \zeta_i(0,0)\zeta_i(0,\pi) = -1$. The point is that now when we adiabatically deform away from the k_y axis the 1D Hamiltonian $\hat{H}(\delta k_x, k_y)$ is invariant under reflection. Additionally, the y component of the polarization is quantized as long as reflection is a good symmetry. Thus $\hat{H}(k_x, k_y)$ is a gapped interpolation along which reflection symmetry is preserved and thus the y component of the polarization is fixed and quantized to $e/2$ for each 1D Hamiltonian. This argument immediately implies that $\prod_{i=1}^N \zeta_i(\pi,0)\zeta_i(\pi,\pi) = -1$. Thus the parity of the Chern number is always *even* when reflection symmetry is required. In fact, it always vanishes because the quantum Hall effect is incompatible with reflection symmetry. Notice that the reflection eigenvalues do not uniquely specify

the polarization in the x direction since the two eigenvalue conditions can be satisfied by choosing $\prod_{i=1}^N \zeta_i(0,0)\zeta_i(\pi,0) = \prod_{i=1}^N \zeta_i(0,\pi)\zeta_i(\pi,\pi) = \pm 1$. Thus the anisotropic invariants in the x direction can take either value.

The other invariant one can define is the isotropic extension of $\chi_{\mathcal{P}}^{(2)}$ to two dimensions. If $\chi_{\mathcal{P}} = +1$ and the product over the inversion eigenvalues at *every* invariant momentum is separately trivial then $\chi_{\mathcal{P}}^{(2)}$ is well defined because there are an even number of negative inversion eigenvalues at each invariant momentum and by definition $\chi_{\mathcal{P}}^{(2)}$ is the product over half of those negative eigenvalues. This is the Z_2 topological invariant, which indicates a quantum spin Hall effect⁷ when an insulator has both inversion and time-reversal symmetry. Unfortunately this topological invariant does not yield a unique topological response. We can understand this in several ways. By explicit construction take two decoupled copies of the quantum anomalous Hall effect (QAHE) state each with $C_1 = 1$ to give an IQHE with $C_1 = 2$ or take two decoupled copies of QAHE, one with $C_1 = 1$ and the other with $C_1 = -1$. The first system breaks time reversal and still gives an IQHE while the second preserves time reversal and will not give a quantum Hall effect. These systems both have $\chi_{\mathcal{P}} = +1$ but $\chi_{\mathcal{P}}^{(2)} = -1$. We can immediately see why this invariant does yield a unique response in the presence of an additional time-reversal symmetry because this requires the total Chern number to vanish which only leaves the possibility of a quantum spin Hall state. Thus it is time-reversal symmetry which restricts the allowed physical response. We can understand this by a simple symmetry argument as well. The quantum spin Hall effect is even under both inversion symmetry $(x,y) \rightarrow (-x,-y)$ and parity $(x,y) \rightarrow (x,-y)$. We see that in even space dimensions inversion symmetry acting on the coordinates is a rotation. The quantum Hall effect is even under inversion but odd under parity. Thus having a quantum Hall effect is compatible with inversion symmetry but not parity (and not time reversal). This is why the *inversion* classification does not distinguish between the doubled quantum Hall state and a quantum spin Hall state. This type of ambiguity exists in every dimension where one can define a Chern number invariant. However, as we saw with the polarization, if we consider the eigenvalues of a reflection symmetric Hamiltonian we can eliminate the possibility of a nonzero Chern number thus leaving a quantum spin Hall state as the alternative.

C. 3D inversion symmetric insulators

We show that the isotropic extension of $\chi_{\mathcal{P}}$ in three dimensions,

$$\chi_{\mathcal{P}} = \prod_{k_{\text{inv}}; i \in \text{occ.}} \zeta_i(k_{\text{inv}}), \quad (98)$$

where the product runs over all eight inversion symmetric k points, is *always* trivial. We can first see this by using a band crossing argument. Start from the atomic limit in which bands have identical inversion eigenvalues at all inversion symmetric points. For $\chi_{\mathcal{P}}$ to be nontrivial (equal to -1) there has to be an odd number of band crossings between bands of opposite inversion eigenvalues at the inversion invariant momenta when beginning from this trivial limit. Without loss of generality let

us consider one crossing between two bands with opposite inversion eigenvalues everywhere in the Brillouin zone. The crossing can happen at either an inversion symmetric point (by tuning one parameter) or at a noninversion symmetric point k in the Brillouin zone. In the latter case, there are actually two crossings at k and $-k$ because of inversion symmetry. To initially close the gap between the two bands one needs a *quadratic* touching in at least one of the directions, otherwise we would be creating a nonzero Chern number Fermi surface (after gap closing) out of a zero Chern number surface (before the closing, in the trivial limit). If the crossing starts at an inversion symmetric point, the quadratic touching and the gap reopening at the inversion symmetric point will switch the inversion eigenvalues of the bands at that point and make $\chi_{\mathcal{P}} = -1$. However, the system will no longer be an insulator: it will have two crossings somewhere else in the Brillouin zone. That is, although the gap has opened at the inversion symmetric point, the gapless points have been moved away. The quadratic touching effectively splits into multiple 3D Dirac points. In the generic situation, there are two gapless points in the Brillouin zone (BZ), with relative position fixed by inversion, and in order to gap the system, we need to annihilate the two Dirac points. Note that a 3D Dirac point is locally stable even if inversion is not preserved. On a 2D surface surrounding a 3D Dirac point [$\hat{H}_{\text{local}}(k) = k_i A_{ij} \sigma_j$, ($i, j = 1, 2, 3$)], the Chern number is $C = \text{sgn}[\det(A_{ij})]$. The degeneracy points are stable unless two Dirac points of opposite Chern numbers annihilate. Inversion symmetry forces the points at k , $-k$ to have opposite Chern numbers. So, by inversion, annihilation can only happen at another inversion symmetric point, in which case inversion eigenvalues are switched again to give $\chi_{\mathcal{P}} = 1$ for an insulator. If the gap first closes at a nonsymmetric point k , we find the same end result: Generically two Dirac points are created close to k and two close to $-k$. They can annihilate in pairs, always switching an *even* (possibly zero in this case, since the four dirac points can annihilate two by two at noninversion symmetric points in the BZ) number of inversion eigenvalues.

Another similar way of understanding the 3D band crossings is the following: Since we are considering a two-band crossing in three dimensions there are three varying parameters and we cannot find a gapped phase with $\chi_{\mathcal{P}} = -1$, though it is possible to find a gapless phase. If we have an even number of band crossings then we can open a gap but this means that two inversion eigenvalues are switched leaving $\chi_{\mathcal{P}} = +1$. There is also a deeper reason why this cannot be done. Let us look at the simplest case of a single two-band crossing at the Γ point. The effective Hamiltonian can be put in the form $H_{\text{eff}} = p_1 \sigma^1 + p_2 \sigma^2 + p_3 \sigma^3$ which is a (chiral) Weyl-fermion Hamiltonian. From the Nielsen-Ninomiya no-go theorem this type of Hamiltonian cannot arise without a partner fermion with the opposite chirality.⁴¹ Thus all two-band crossings must generically occur in pairs and there cannot be an odd number of negative parity eigenvalues in an insulating system. Conversely, if no states at the inversion invariant momenta cross the Fermi level and $\chi_{\mathcal{P}} = -1$ we immediately know that the system contains a gapless point(s) somewhere in the Brillouin zone.

We now provide an alternate proof that the product of all the inversion eigenvalues of all the occupied bands must be positive in three dimensions. This will prove useful when

considering possible 3D QHE states. Assume a gapped insulator Hamiltonian $\hat{H}(k_x, k_y, k_z)$ which has N occupied bands and is invariant under inversion symmetry. We can take the plane $k_z = 0$, and think of $\hat{H}(k_x, k_y, 0)$ as a 2D inversion symmetric Hamiltonian. We have already proved that the inversion eigenvalues of a 2D inversion symmetric Hamiltonian are related to the Chern number, i.e.,

$$\prod_{i=1}^N \zeta_i(0,0,0)\zeta_i(\pi,0,0)\zeta_i(0,\pi,0)\zeta_i(\pi,\pi,0) = (-1)^{C_1[\hat{H}(k_x, k_y, 0)]}. \quad (99)$$

The same thing is true for the inversion symmetric 2D Hamiltonian $\hat{H}(k_x, k_y, \pi)$:

$$\begin{aligned} \prod_{i=1}^N \zeta_i(0,0,\pi)\zeta_i(\pi,0,\pi)\zeta_i(0,\pi,\pi)\zeta_i(\pi,\pi,\pi) \\ = (-1)^{C_1[\hat{H}(k_x, k_y, \pi)]}. \end{aligned} \quad (100)$$

Hence

$$\begin{aligned} \prod_{i=1}^N \zeta_i(0,0,0)\zeta_i(\pi,0,0)\zeta_i(0,\pi,0)\zeta_i(\pi,\pi,0) \\ \times \zeta_i(0,0,\pi)\zeta_i(\pi,0,\pi)\zeta_i(0,\pi,\pi)\zeta_i(\pi,\pi,\pi) \\ = (-1)^{C_1[\hat{H}(k_x, k_y, 0)] + C_1[\hat{H}(k_x, k_y, \pi)]}. \end{aligned} \quad (101)$$

Since $\hat{H}(k_x, k_y, k_z)$ is gapped due to our assumption of an insulator, we can think of it as an adiabatic interpolation between $\hat{H}(k_x, k_y, 0)$ and $\hat{H}(k_x, k_y, \pi)$ by varying the parameter k_z . Since this interpolation preserves the $U(1)$ charge *conservation* symmetry, i.e., there is no superconductivity, it means that the Chern number cannot change from $k_z = 0$ to $k_z = \pi$. Thus

$$C_1[\hat{H}(k_x, k_y, 0)] = C_1[\hat{H}(k_x, k_y, \pi)] = C_1. \quad (102)$$

Hence

$$\prod_{k_{\text{inv}}; i \in \text{occ.}} \zeta_i(k_{\text{inv}}) = (-1)^{2C_1} = 1. \quad (103)$$

1. Anisotropic invariants and the 3D quantum Hall effect

We have seen that the isotropic invariant in three dimensions, which is constructed by multiplying the inversion eigenvalues at all invariant momenta, is always trivial for an insulator. However, we can form anisotropic invariants by considering the products of inversion eigenvalues over planes or lines of the Brillouin zone that are mapped onto themselves under inversion.

First consider a plane in the 3D Brillouin zone that is mapped onto itself under inversion. To be explicit, take the plane $k_z = \pi$. If the product of inversion eigenvalues of all the occupied bands in that plane is

$$\prod_{i=1}^N \zeta_i(0,0,\pi)\zeta_i(\pi,0,\pi)\zeta_i(0,\pi,\pi)\zeta_i(\pi,\pi,\pi) = -1, \quad (104)$$

we have a 3D QHE,⁴² with 3D Hall conductance

$$\sigma_{xy} = \text{odd integer} \times \frac{2\pi}{c}, \quad (105)$$

where c is lattice constant in the z direction. From our above proof in Sec. IV B we know that the product of eigenvalues in the $k_z = 0$ plane must also be -1 . The proof of the 3D QHE is simple: $\hat{H}(k_x, k_y, k_z)$ can be thought of as an adiabatic continuation of $\hat{H}(k_x, k_y, \pi)$ (since we assumed it to be an insulator). As such, each k_z plane $\hat{H}(k_x, k_y, k_z = \text{const})$ has an odd integer QHE. Multiplying by the momentum, we get the above 3D Hall conductance. It is important to note that this argument depends crucially on the fact that the Chern number remains unchanged when performing adiabatic deformations as long as charge *conservation* symmetry is preserved (i.e., we do not allow superconducting perturbations).

In general, the 3D quantum Hall effect directions can be inferred from the eigenvalue formulas. The general formula for the 3D Hall conductance in terms of the inversion eigenvalues is

$$\sigma_{\alpha\beta\perp\gamma} = \mathbf{G}_\gamma \left(2n + 1/2 - \frac{1}{2} \prod_{i \in \text{occ.}} \prod_{k_{\text{inv}} \in \text{plane} \perp G_\gamma} \zeta_i(k_{\text{inv}}) \right). \quad (106)$$

This expression above gives the 3D Hall conductance as a product of the inversion eigenvalues in a plane $\alpha\beta$ perpendicular to the $\gamma (= x, y, z)$ direction. \mathbf{G}_γ is the reciprocal-lattice vector in the γ direction and we have left out the units of e^2/h . If the product over all the bands of the inversion symmetric eigenvalues in the $\alpha\beta$ plane is -1 we can see that the Hall conductance is an odd integer in that plane and hence cannot be zero. If the product is $+1$ then the 3D Hall conductance is even and can be zero.

Just as in two dimensions we can consider the product of inversion eigenvalues along a single inversion invariant line in the 3D Brillouin zone. Again inversion symmetry does not allow us to determine the polarization but a reflection symmetry about a *plane* allows us to specify the polarization perpendicular to that reflection plane. The argument is basically the same as in two dimensions so we do not include it here. The result, however, is explicitly illustrated with the 3D dimer model shown in Sec. V.

2. Topological metal state

As a corollary to the above proof of the 3D QHE, when the product over the inversion eigenvalues of several bands at all points in the Brillouin zone is negative,

$$\chi_{\mathcal{P}} = \prod_{k_{\text{inv}}; i \in \text{occ.}} \zeta_i(k_{\text{inv}}) = -1,$$

the system is a metal protected from opening a gap from infinitesimal perturbations. We can gain some intuition about why this metal state exists by looking at the effective Hamiltonian near a band crossing between states with opposite inversion eigenvalues at an inversion invariant momentum. In the most generic case, in which we do not have any

extra point-group symmetries, the effective Bloch Hamiltonian expanded for small k near k_{inv} is

$$\hat{H}(k) = (M + A_{ij}k_i k_j)\sigma_z + k_i B_{i\alpha}\sigma_\alpha, \quad (107)$$

where $i, j = 1, 2, 3$ while $\alpha = 1, 2$. Notice that since the bands have opposite parity, the mixing elements between them have to be odd in k . The Hamiltonian reduces to $M\sigma_z$ at k_{inv} and thus the sign of M dictates the occupied inversion eigenvalue. When M is tuned through zero, we have a phase transition with an eigenvalue switch between $+$ and $-$. For a given A_{ij} matrix, notice that on at least one side of the switch, we must have a gapless phase: if $M > 0$ and $\text{Det}(A_{ij}) < 0$ we have a metallic phase, or if $M < 0$ and $\text{Det}(A_{ij}) > 0$ we have gapless Dirac points away from k_{inv} . There are of course two Dirac points, which can then annihilate at another k_{inv} point with \pm eigenvalues and can reopen the gap and give $\chi_P = +1$. Because of the different eigenvalues under inversion, we only need to tune one parameter to get a band crossing in this case.

3. Magnetoelectric polarization and inversion symmetry

Although the first 3D isotropic invariant we mentioned is always trivial, Ref. 29 argues that inversion invariant insulators in three dimensions, which come from strong topological insulators with softly broken time-reversal invariance, can support an isotropic topological magnetoelectric response (i.e., a $\theta = \pi$ vacuum). Their argument uses the transformation properties of the effective response action, which we recount here. The topological response action in three dimensions for an insulator coupled to an electromagnetic field is

$$S_{\text{eff}}[A_\mu] = \frac{e^2}{2\pi h} \int d^4x \theta \mathbf{E} \cdot \mathbf{B}, \quad (108)$$

where \mathbf{E}, \mathbf{B} are external applied electric and magnetic fields, and θ is an intrinsic quantity proportional to the magnetoelectric polarizability.⁹ For translationally invariant systems the magnetoelectric polarizability for time-reversal invariant insulators is

$$P_3 = \frac{\theta}{2\pi} = \frac{1}{32\pi^3} \int d^3k \epsilon^{ijk} \text{Tr} \left[\hat{A}_i \hat{F}_{ij} - \frac{2i}{3} \hat{A}_i \hat{A}_j \hat{A}_k \right], \quad (109)$$

where $\hat{A}_i(k)$ is the non-Abelian adiabatic connection, and $\hat{F}_{ij}(k)$ is the non-Abelian adiabatic curvature. Under time-reversal symmetry $P_3 \rightarrow -P_3$ and thus for time-reversal invariant insulators $P_3 = 0, 1/2$ (in units of 2π). P_3 is not a gauge invariant quantity and only defined modulo an integer.⁹ Note that under time reversal \mathbf{B} does not change in the effective action since it is an externally applied field. Only intrinsic quantities such as P_3 get acted upon with time reversal. Using these two values of P_3 we can physically define a time-reversal invariant topological insulator as one with $P_3 = 1/2$. It has been shown that this definition is equivalent to the band-structure definition of strong topological insulators.^{7,9,13,14,43,44} In the presence of time-reversal and inversion symmetries there is an elegant topological invariant one can define,

$$(-1)^{2P_3} = \prod_{i \in \text{occ.}/2} \prod_{k_\alpha \in \{k_{\text{inv}}\}} \zeta_i(k_\alpha), \quad (110)$$

which is the product of the inversion eigenvalues at every invariant momenta in the 3D Brillouin zone for half the occupied bands. Since we have time reversal, half the bands just means one band out of each Kramers pair. We provide a physical proof of this equation in Appendix G.

The additional insight of Ref. 29 is that P_3 is also odd under inversion symmetry. This means that the values of P_3 are still quantized to be $0, 1/2$ even when the system does not have time-reversal symmetry but only inversion. We find that this argument holds for topological responses in all even space-time dimensions (see Appendix J). Thus there are inversion symmetric topological insulators in three dimensions where $P_3 = 1/2$, analogous to the case in one dimension where $P_1 = e/2$. This argument is an indicator that inversion symmetric insulators can support nontrivial topological states with interesting response properties. Now we can ask the question, is Eq. (110) still valid when only inversion symmetry is preserved? If we only have inversion symmetry and no time-reversal symmetry, then this formula continues to apply if we can adiabatically connect the system to the T and \mathcal{P} invariant limit without breaking inversion symmetry. However, this is not the only case, and we will prove exactly when the inversion eigenvalues in three dimensions indicate a nontrivial magnetoelectric polarizability protected by inversion symmetry in the following section. Our arguments use many of the results discovered in the previous sections.

4. Magnetoelectric polarizability for inversion invariant insulators

We begin by reintroducing the unitary matrix

$$B_{ij}(k) = \langle u_{i,-k} | P | u_{j,k} \rangle, \quad (111)$$

where $u_{i,k}$ is a Bloch function with i, j labeling which occupied band and k is the Bloch momentum. An important property of the matrix B is

$$B(-k) = B^\dagger(k), \quad (112)$$

which is true because \mathcal{P} is unitary and squares to the identity matrix. This means that at the inversion symmetric points, the matrix is real and symmetric. For inversion symmetric insulators, we prove in Appendix F that the non-Abelian adiabatic connection satisfies

$$\hat{A}_i(-k) = -B \hat{A}_i(k) B^\dagger + i B(k) \nabla_i B^\dagger(k), \quad (113)$$

which implies that the adiabatic curvature is gauge covariant via

$$\hat{F}_{ij}(-k) = B(k) \hat{F}_{ij}(k) B^\dagger(k). \quad (114)$$

From this the magnetoelectric polarizability is easy, but tedious (see Appendix F), to obtain

$$2P_3 = -\frac{1}{24\pi^2} \int d^3k \epsilon^{ijk} \text{Tr} \{ [B(k) \partial_i B^\dagger \times(k)] \cdot [B(k) \partial_j B^\dagger(k)] [(B(k) \partial_k B^\dagger(k))] \}. \quad (115)$$

This proves that P_3 is either integer or half integer depending on whether the right-hand side (which is an integer winding number) is even or odd. Since P_3 is itself defined mod 1 it means that P_3 defines a Z_2 classification that indicates a nontrivial topological response.

With time-reversal symmetry, states pair up in Kramers doublets and are degenerate at time-reversal invariant points (the same as inversion symmetric points). If we break all accidental degeneracies, in a time-reversal invariant system, we are still left with an *even* number of occupied bands—they are degenerate in pairs at time-reversal symmetric points. The B matrix then is a $U(2)$ matrix, and the $B(k)$ matrix function maps the 3D torus into the unitary group of two by two matrices. These maps can be nontrivial, and $\pi_3[U(2)] = Z$ (the mod 2 appears because P_3 is defined as a winding number mod 2, but the winding number itself can be integer. Once we lose time-reversal symmetry we do not have required degeneracies at the time-reversal (inversion) symmetric points. In fact, once time reversal is softly broken, the bands at inversion symmetric points experience eigenvalue repulsion: before TR was broken, the inversion eigenvalues of the Kramers' doublets had to be identical. Once Kramers' degeneracy is not required, these points exhibit strong eigenvalue repulsion. As such, it would naively seem that once TR is broken we can completely separate the occupied bands and isolate them from each other at all points in the Brillouin zone. We could then treat the system of N occupied bands as N systems of one band, which would imply that the matrix B could be reduced to an $N \times N$ diagonal matrix with $U(1)$ phases on the diagonal. We can view the matrix $B(k)$ as matrix mapping from 3D momentum space into $U(1)^{\otimes N}$. Since $\pi_3[U(1)^{\otimes N}] = 0$ this implies that the winding number in Eq. (115) always vanishes (note that by making this statement we are implicitly assuming that all of the mappings are smooth, which we will come back to later). This trivial reasoning would seem to imply that we cannot get a topological insulator with inversion symmetry. Fortunately, this line of reasoning fails because of the nontrivial global constraint that the product of all the inversion eigenvalues must be positive. Before we deal with the effects of the constraint we draw several conclusions about a Hamiltonian with only one occupied band. The non-Abelian form of the winding number implies that with only one occupied band $P_3 \equiv 0$. Thus no matter what the inversion eigenvalue content, there is no contribution to P_3 from a system with a single occupied band. This also holds for a band that can be completely separated and untangled from all other bands at all points in the Brillouin zone. Such isolated bands do not contribute to a nontrivial P_3 . This is in contrast to the statement at the end of Ref. 45 which seems to state that a nontrivial P_3 only requires an odd number of pairs of inversion eigenvalues. As a counterexample, a single occupied band can have a single pair of negative parity eigenvalues (which occur at different k_{inv}) and it has vanishing P_3 . We give such a Hamiltonian in Eq. (141). We will see that the important thing to consider is pairs of negative parity eigenvalues at the *same* k_{inv} .

The global constraint on the inversion eigenvalues is crucial for our discussion. We first give an explicit example to gain intuition about its importance. Let us assume that $N = 2$ and that the occupied bands have $\zeta_1(0,0,0) = \zeta_2(0,0,0) = -1$ and all other inversion eigenvalues at all other inversion symmetric momenta positive. The naive reasoning from above implies that by perturbing this Hamiltonian while preserving inversion symmetry we should be able to separate these bands so that they are isolated with no intermingling degeneracies. However, if we could make the two bands nondegenerate everywhere

we would contradict the constraint $\chi_P = +1$. This is easy to see because if we could separate the two bands we could consider a different insulating ground state with only one of the previous two bands occupied and then the product of the inversion eigenvalues of the single occupied band would be negative. We have proved this is not possible, so we cannot make the bands fully nondegenerate over the entire Brillouin zone. Alternatively, if we could separate the bands, we would have a single band that has eigenvalues $- + + +$ in the $k_z = 0$ plane and $+ + + +$ on the $k_z = \pi$ plane. If we consider the 3D Hamiltonian as a gapped interpolation between these two planes then we have adiabatically connected 2D Hamiltonians with odd and even Chern number, respectively. This cannot happen and is thus another contradiction. Hence we know that the two occupied bands are degenerate at at least two points in the Brillouin zone (by inversion symmetry). These two points are exactly enough to transfer an even Chern number from one plane to the other, which fixes the Chern number issue. Due to this required degeneracy between the two bands, $B(k)$ restricted to these two bands does not reduce to a $U(1) \otimes U(1)$ matrix, but instead the restricted $B(k) \in U(2)$. Since $\pi_3[U(2)] = Z$ this shows that a 3D inversion symmetric insulator can have a nontrivial contribution to P_3 . Any other degeneracies that bands might have that are not required by the constraint can be removed. As such, for the case with many occupied bands, $B(k)$ can be put into the form, by removing all the accidental degeneracies, of a matrix of decoupled $U(2)$ and $U(1)$ blocks. The winding comes from the $U(2)$ parts of the matrix, and is additive in the block diagonal terms due to the trace in the winding number.

We first discuss the winding number in the continuum (sphere) and then focus on the lattice (torus). We know from Ref. 11 that when considering the isotropic topological invariants such as P_3 it is sufficient to think of momentum space as a sphere S^3 instead of the Brillouin zone torus T^3 . Allowing for the full torus structure gives a rich set of anisotropic states which we will consider later, but for now we assume that the momentum space topology is spherical. This effectively reduces the number of invariant momenta we need to consider to just two: the origin and the “point at infinity.” Equivalently we could think of the torus with unrestricted inversion eigenvalues at $k_{\text{inv}} = (0,0,0)$ but with the inversion eigenvalues at all the other k_{inv} constrained to be equal band by band. Now consider a Hamiltonian with N occupied bands (again N does not have to be even, a crucial difference with the time-reversal case). Since we are in three dimensions we know that the product of all the inversion eigenvalues must be $+1$. This means that there can only be an even number of inversion eigenvalues that are different between $k = 0$ and $k = \infty$. For example, the number of negative eigenvalues at $k = \infty$ must have the same parity (i.e., even or odd) as the number of negative eigenvalues at $k = 0$. It is clear that, by exchanging parity eigenvalues between bands, either at $k = 0, \infty$, we can split the bands into two classes: (i) bands with $\chi_P = +1$ and (ii) pairs of bands with $\chi_P = -1$ for each band. We see case (i) when the eigenvalues match at $k = 0$ and ∞ and case (ii) when they are opposite. For case (i) the bands can be isolated from each other, but in case (ii) they must generically be in tangled pairs where the $\chi_P = +1$ for the pair. Thus we can understand both cases by considering just two occupied bands.

For example, a trivial case is that of two bands with no negative inversion eigenvalues. This is a realization of case (i) where the inversion eigenvalues of each band separately multiply to +1. The global constraint does not prevent us from isolating all the occupied bands and thus, with all eigenvalues positive, $P_3 = 0$. All realizations of case (i) are trivial for the same reason.

The first interesting case is that of two bands with a single pair of negative inversion eigenvalues at the same point (say $k = 0$) but positive inversion eigenvalues at the other point. We consider that case now. The important consequence of the global constraint, as we just saw, is that the two bands with the negative eigenvalues can never be completely separated from each other—the (generically) two degeneracy points between them cannot be lifted or annihilated. $B(k)$ restricted to these two bands is a $U(2)$ matrix and generically takes the form

$$B(k) = e^{i\phi(k)}[f(k)I + i g_a(k)\sigma_a] \quad (116)$$

where

$$[f(k)]^2 + g_a(k)g_a(k) = 1. \quad (117)$$

There is a global \pm sign ambiguity in the choice of $f(k)$ but once the sign is chosen at one point, smoothness assures the signs at the other points. This ambiguity does not have implications for the final result. If we substitute this form into Eq. (115) all of the dependence on $\phi(k)$ [i.e., the $U(1)$ part] drops out as long as $e^{i\phi(k)}$ is smooth. Since all loops in S^3 are contractible we can gauge transform $B(k)$ to remove the k -dependent phase so the assumption of smoothness is not an issue. What remains is the winding of the $SU(2)$ part, which must be an integer. Now, with only the $SU(2)$ part we know that, due to $B(k) = B^\dagger(-k)$,

$$f(k) = f(-k), \quad g_a(k) = -g_a(-k). \quad (118)$$

If we think of $S^3 = R^3 \cup \{\infty\}$ then it is easy to consider the general form of B . The function $f(k) : S^3 \rightarrow R$ and its derivative vanishes at $k = 0$ (and $k = \infty$). This is a Morse function for the sphere are we can expand it around the origin to find

$$f(k) = N(k)(M + k_a C_{ab} k_b + \dots), \quad (119)$$

where C_{ab} is a 3×3 constant matrix with three nonzero eigenvalues of the same sign,⁴⁶ and $N(k)$ is a normalization factor, which is even in k and constrains the matrix B to have unit determinant.

Without loss of generality we choose the case when the eigenvalues of C_{ab} are all positive (another reason the eigenvalues have to have the same sign is to fix the boundary condition at $k = \infty$ so that it is independent of the path taken to get there). This choice determines which sign of M will lead to the nontrivial phase. Similarly we can expand the function

$$g_a(k) = N(k)(D_{ab} k_b + \dots) \quad (120)$$

for a 3×3 constant matrix D_{ab} with no restriction on the eigenvalues. Generically, D_{ab} will have nonzero determinant (i.e., it will have rank 3). In cases where the determinant of D_{ab} is tuned to zero, we have to look use a higher-order Taylor expansion in *both* $f(k)$ and $g_a(k)$ —maintaining even terms in $f(k)$ and odd terms in $g_a(k)$. As long as the boundary

conditions are fixed, which requires us to keep terms in $f(k)$ with higher order than $g_a(k)$, this will not change the result. Without loss of generality we take the case $\det D \neq 0$, and by rescaling and rotating we transform to the momentum space basis (k_1, k_2, k_3) with $C_{ab} = D_{ab} = \delta_{ab}$. For this choice we have

$$N(k) = \frac{1}{\sqrt{(M + k^2)^2 + k^2}} \quad (121)$$

with $k^2 = k_1^2 + k_2^2 + k_3^2$. For this $B(k)$ we have

$$B(0) = \text{sgn}(M)I_{2 \times 2}, \quad B(\infty) = I_{2 \times 2}. \quad (122)$$

By explicit calculation, we find that

$$P_3 = \frac{1}{\pi} \int_0^\infty \frac{(M - k^2)}{[(M + k^2)^2 + k^2]^2} k^2 dk = \frac{\text{sgn}(M) - 1}{4}. \quad (123)$$

We notice that when there is an eigenvalue switch when passing from zero to infinity, we have $P_3 = 1/2$, whereas when there is no eigenvalue switch, we have $P_3 = 0$. Although more terms can be kept in the expansion around the origin this does not influence the result of the winding number, as long as the eigenvalues of $B(0)$ and $B(\infty)$ are not changed.

We have seen from this simple argument that for two bands which cannot be separated, the contribution to P_3 depends only on the change in inversion eigenvalues. If there is only a single pair of bands, which is in case (ii), i.e., cannot be untangled from its partner, then the other $N - 2$ occupied bands are not constrained and may each be isolated away from all other bands. Each of these isolated bands does not contribute to P_3 and thus the nontrivial value of P_3 only comes from the two tangled bands. To finish the proof we must consider the case when there is more than one set of tangled occupied bands. If, for example, there are four bands that have negative eigenvalues at $k = 0$ (for simplicity we fix all the eigenvalues at $k = \infty$ to be positive) we can generically isolate the four bands into two pairs. The two pairs can be separated from each other and all other bands, but the bands making up a single pair must share degeneracies from the arguments above. Once we have decoupled the inversion eigenvalues of the two pairs, we can remove all the accidental degeneracies and isolate the pairs from each other because a combined pair of bands with negative inversion eigenvalues by itself does not contradict the global constraint. Since the pairs can be isolated, they contribute independently to P_3 . Each pair will contribute a half integer giving $P_3 = n = 0 \pmod{Z}$. We see there is an even-odd effect so that an odd number of pairs of bands with negative inversion eigenvalues is nontrivial while an even number of pairs is trivial.

To complete the picture we will discuss how these arguments carry over to the lattice case when momentum space is a torus T^3 . We now have eight invariant momenta to consider, which can lead to many more different combinations of inversion eigenvalues. We will not enumerate all the possible phases but instead construct the necessary general principles to classify such states. We again consider a set of N occupied bands, which does not have to be an even number. In general the only restriction is that the product of all the inversion eigenvalues of all the occupied bands is equal to 1. We can

generically perform band crossings only between the occupied bands to split the bands into three possible classes: (i) a set of n_+ bands with positive inversion eigenvalues at all k_{inv} , (ii) a set of n_-^e bands with an even number of negative eigenvalues on each band, and a set of n_-^o bands where the product of eigenvalues on each band is -1 and the product *cannot* be made equal to $+1$ via band crossings among the other bands in n_-^o . From the arguments above, the sets of n_+ and n_-^e bands contribute nothing to P_3 , because they can be isolated one by one from all of the occupied bands. Note that the n_-^e can contribute to nontrivial 3D QHE states in the same manner shown above. The number of bands in the third class n_-^o must be an even number to satisfy the global constraint. We will now show that the value of $P_3 = (1/2)n_-^o \bmod Z$. We call this process the band decoupling process and we give explicit examples of this band decoupling picture for lattice models shown in Appendix I.

We know that the only bands which can contribute to P_3 are those in n_-^o . We can consider these bands as a set of $n_-^o/2$ decoupled pairs. Each one of them contributes a $U(2)$ block to the $B(k)$ matrix. We show in Appendix H that once the band decoupling process is finished then the $U(1)$ phase in each of the $n_-^o/2$ $U(2)$ blocks is smooth and can thus be completely eliminated from consideration. Thus each $U(2)$ block can be contracted to $SU(2)$. Since this implies that we are really considering maps from $T^3 \rightarrow SU(2)$, which have the same dimension, we can connect the winding number of each $SU(2)$ block of $B(k)$ to the degree of the map. This argument follows along the same lines shown in Ref. 44 so we will not include all the details. To calculate the degree of the map from T^3 to an $SU(2)$ block of $B(k)$ we can choose any point in $SU(2)$. For example, we could choose $-I_{2 \times 2}$. Since $B(k) = B^\dagger(-k)$, any k that is not inversion symmetric contributes to the degree of the map twice, i.e., if $-I_{2 \times 2}$ occurs at k it will occur at $-k$, thereby leaving the P_3 invariant. The only contributions therefore come from the inversion symmetric points, and hence the winding number counts the number of inversion symmetric points that have $-I_{2 \times 2}$ as their inversion eigenvalues. This implies that we can simply apply the Kane-Fu formula⁷ to the bands in n_-^o to determine the value of P_3 .

V. SIMPLE EXAMPLE MODELS

In this section we provide a set of explicit models that illustrate the majority of the technical details discussed in the previous sections. For each model we list the interesting phases, inversion eigenvalue structure, and describe what the entanglement spectra should look like. Additionally we provide figures showing the entanglement spectra for each model, which confirms our analytic formulas. The models we choose are similar to ones used in many contexts especially in the field of topological insulators. Combined with the models introduced in Sec. II these examples provide valuable intuition about inversion invariant topological insulators and the similarities and differences between the states protected by inversion symmetry and those protected by other discrete symmetries, e.g., charge-conjugation, or time reversal.

A. 1D models

We have already introduced two illustrative 1D models for which we will analyze the entanglement spectrum. Additionally we will introduce a 1D model of a dimerized chain.⁴⁷

1. Simple two-band model

Here we focus on the Hamiltonian given in Eq. (2) and reproduced it here,

$$\hat{H}_2(k) = \alpha \cos k + \sin(k)\hat{\sigma}_1 + (1 + m - \cos k)\hat{\sigma}_3.$$

This model has one occupied band, and in one dimension there are two inversion symmetric momenta $k = 0, \pi$. There is a phase transition in this model between two insulating phases as a function of the parameter m and we have previously characterized the two phases of this model by examining the inversion eigenvalues of the occupied band. For $m > 0$ the occupied band has two negative inversion eigenvalues. This implies that this system can be adiabatically continued to an atomic limit where the occupied atomic orbital has a negative inversion eigenvalue. In the atomic limit the entanglement entropy is identically zero and so we expect on physical grounds that there should be no stable entanglement eigenvalues at $1/2$. Using our inversion criterion we see that this is the case since the inversion eigenvalues do not change between 0 and π . This same characterization applies for $m < -2$ where the two occupied bands have positive inversion eigenvalues. The final case is for $-2 < m < 0$ where $\zeta(0) = -\zeta(\pi) = +$. This cannot be adiabatically connected to an atomic limit. Here the inversion criterion implies that we should see a pair of entanglement modes at $1/2$ (cf. Sec. III C 5), which is shown in Fig. 1(c). Thus the entanglement spectrum is a good indicator for a nontrivial topological insulator. The trivial case is shown in Fig. 1(d), which has no $1/2$ mode. We can compare these results to the values of the topological invariant \mathcal{N} [see Eq. (12)], which takes on values $\mathcal{N} = 0$ when $m < -2$ or $m > 0$ and $\mathcal{N} = 1$ when $-2 < m < 0$. The number of required $1/2$ modes in the entanglement spectrum is $0, 0$, and 2 , respectively, which is exactly what we found numerically.

To illustrate the protection due to inversion symmetry we also consider H_2 with an on-site disorder term added,

$$H = H_2 + \sum_i W_i c_i^\dagger c_i, \quad (124)$$

where the W_i are randomly chosen from a uniform distribution $[-W/2, W/2]$. If it is purely random, uncorrelated disorder the midgap entanglement modes are no longer protected, as shown in Fig. 5(a). Next we mirror the disorder around the center of the chain to make a system with inversion symmetric disorder. Although unphysical, this helps illustrate the fact that only inversion symmetry is required for the protected midgap entanglement states, as we show in Fig. 5(b) where the cut is along the remaining inversion center.

2. Simple four-band model

The Hamiltonian for the simple four-band model was given in Eq. (5) and the set of inversion eigenvalues for the different

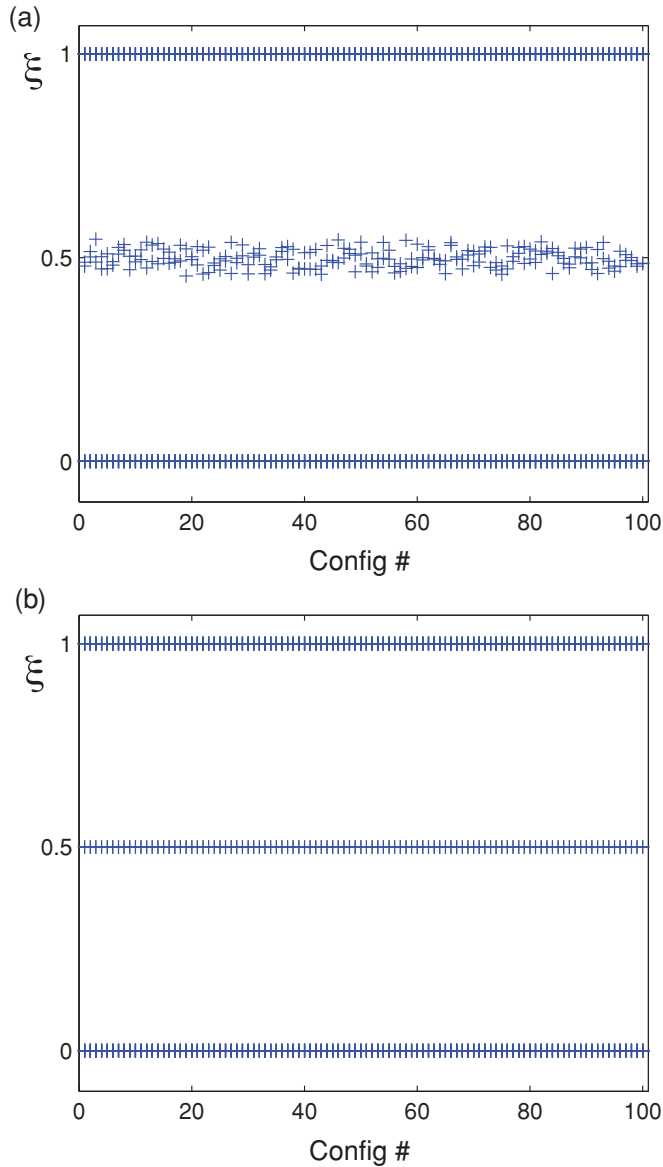


FIG. 5. (Color online) Entanglement spectrum for the two-band 1D model with (a) random site disorder, (b) random site disorder that is inversion symmetric around the center of the 1D chain. We show the entanglement spectra for many different random disorder configurations.

phases were listed in Eqs. (5). For convenience we reproduce the Hamiltonian here,

$$\hat{H}_4(k) = \sin(k)\hat{\Gamma}_1 + \sin(k)\hat{\Gamma}_2 + (1 - m - \cos k)\hat{\Gamma}_0 + \delta\hat{\Gamma}_{24} + \epsilon \cos(k)(1 + \hat{\Gamma}_0). \quad (125)$$

From the inversion criterion we see that case 2 and case 3 should have entanglement modes at $1/2$. In fact, case 2 should have a pair of modes localized on each cut, one for each occupied band that flips the sign of the inversion eigenvalue. The entanglement spectra for the five cases are shown in Figs. 2(f)–2(h) and they agree with the analytic prediction. For cases 1–5 the invariant $\mathcal{N} = 0, 2, 1, 0, 0$ yielding

0, 4, 2, 0, 0 entanglement modes at $1/2$, which is what we found numerically.

3. Dimerized chain

As a final 1D test case we will look at spinless fermions hopping on a dimerized chain. This model is the familiar Su-Schrieffer-Heeger model for electrons in a polyacetylene chain.⁴⁷ Later we will extend this model into two and three dimensions to illustrate anisotropic systems with nontrivial entanglement spectra. The layout of the chain is shown in Fig. 6(a) along with the choice of two-atom unit cell. The Hamiltonian is given by

$$H = \sum_m \Delta (c_{mA}^\dagger c_{mA} - c_{mB}^\dagger c_{mB}) + [(-t - \delta)c_{mA}^\dagger c_{mB} + (-t + \delta)c_{mB}^\dagger c_{m+1A} \text{H.c.}], \quad (126)$$

where A, B indicate sublattice A or B and $t > 0$. For our purposes we will set the on-site energy $\Delta = 0$. With this choice the Hamiltonian has an inversion symmetry with respect to the middle of a bond with $\mathcal{P} = \sigma^x$, i.e., \mathcal{P} exchanges sublattices A and B .

The Hamiltonian can be Fourier transformed and becomes

$$H = \sum_k \Psi_k^\dagger ([-(t + \delta) - (t - \delta) \cos k] \sigma^x + (t - \delta) \sin k \sigma^y) \Psi_k \quad (127)$$

$$\Psi_k = (c_{kA} \ c_{kB})^T.$$

This model has two insulating phases: (i) $\delta < 0$; (ii) $\delta > 0$. At the two inversion invariant points we have the Bloch Hamiltonians $\hat{H}(0) = -2t\sigma^x$ and $\hat{H}(\pi) = -2\delta\sigma^x$. As expected they both commute with \mathcal{P} . For fixed $t = 1$ we see that the inversion eigenvalue of the occupied band at $k = 0$ is fixed to be $+$. For $k = \pi$ the eigenvalue depends on the sign of δ . So for $\delta < 0$ (> 0) we have $\zeta(\pi) = -1$ ($+1$). We see that the nontrivial phase occurs when $\delta < 0$. In this case the Wannier center of the electrons is shifted to the midbond center *between* unit cells. Thus if we cut the system between unit cells there will be a charge polarization. If $\delta > 0$ the Wannier center is on the midbond center *within* a unit cell. Thus our definition

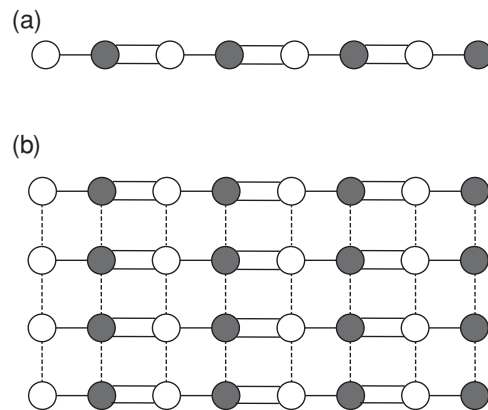


FIG. 6. (a) 1D dimerized chain; (b) 2D dimerized square lattice model. Solid and dotted lines represent different hopping amplitudes.

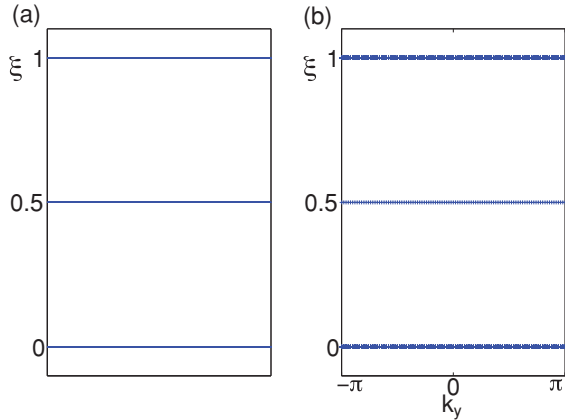


FIG. 7. (Color online) Entanglement spectra for (a) dimerized chain; (b) dimerized square lattice.

of unit cells is important and simply reflects the fact that the polarization is not well defined absolutely but is gauge variant.

The entanglement spectra for this model for $\delta < 0$ is shown in Fig. 7(a). We expect that because the inversion eigenvalues change from positive to negative between $k = 0$ and π that there should be $1/2$ modes in the spectrum and this is confirmed numerically, as seen in the figure. The topological invariant $\mathcal{N} = 0, 1$ for $\delta > 0$ and $\delta < 0$, respectively. The number of the entanglement modes in the spectrum matches the value of $2\mathcal{N}$ as expected for a system with periodic boundary conditions and thus two entanglement cuts.

There is a subtlety in the entanglement characterization of this model, which we will now discuss. The real-space Hamiltonian as written in Eq. (126) has broken translational symmetry. As stated earlier, our classification method only applies to translationally invariant Hamiltonians since we need to evaluate inversion eigenvalues in momentum space. However, by construction, the Hamiltonian for the dimerized chain only has a very mild breaking of translational symmetry. In fact, as implicitly assumed in the analysis, we can just define a unit cell encapsulating two sites, and in terms of the larger unit cell the Hamiltonian is translationally invariant and our method applies. Our choice for a unit cell has already been implicitly assumed by the time we write the Bloch Hamiltonian in Eq. (127). The choice made here is that sites connected by the hopping term $-(t + \delta)$ form a single unit cell and the hopping between unit cells is $(-t + \delta)$. After making this choice we are free to carry out the entanglement analysis by cutting the system *between* unit cells. Cutting the system *within* a unit cell is not a position-space cut of a translationally invariant Hamiltonian.

Now, the important outstanding question is, is the analysis invariant under the choice of unit cell? It is, and we explicitly show it for this model. Suppose that we take the unit cell to be sites connected by the hopping $(-t + \delta)$. Then the Bloch Hamiltonian becomes

$$\begin{aligned} \bar{H} &= \sum_k \Psi_k^\dagger \{[-(t - \delta) - (t + \delta) \cos k] \sigma^x + (t + \delta) \sin k \sigma^y\} \Psi_k, \\ \bar{H}(0) &= -2t \sigma^x \quad \bar{H}(\pi) = 2\delta \sigma^x. \end{aligned} \quad (128)$$

If we fix $t > 0$ then the inversion eigenvalue for the occupied band at $k = 0$ is always positive. Thus we see that for $\delta > 0$

the system is in a nontrivial phase with opposite inversion eigenvalues at 0 and π , and for $\delta < 0$ the system is trivial. The sign of δ that exhibits the nontrivial phase has changed when compared with the choice of the other unit cell. The physics, however, remains identical. Now when $\delta > 0$ the Wannier centers are shifted to the bonds *between* the new unit cells. This would lie *within* the unit cell for our previous choice and explains why the sign of δ has changed. For the choice of unit cell in \bar{H} the entanglement spectrum will have midgap modes when $\delta > 0$, i.e., when the inversion eigenvalues are opposite at the two invariant momenta. Thus we see that for the new choice of unit cell the physics and entanglement analysis yields the same results.

B. 2D models

1. Dimerized square lattice model

The first 2D model we consider is a trivial extension of the dimerized chain, as illustrated in Fig. 6(b). This extension has a Hamiltonian that is simply constructed from Eq. (127):

$$\begin{aligned} H &= \sum_k \Psi_k^\dagger \{[-(t + \delta) - (t - \delta) \cos k_x] \sigma^x \\ &\quad + (t - \delta) \sin k_x \sigma^y - 2t_y \cos k_y\} \Psi_k. \end{aligned} \quad (129)$$

This model has an inversion symmetry with $\mathcal{P} = \sigma^x$. At the inversion invariant points we have

$$\begin{aligned} \hat{H}(0,0) &= -2t_y - 2t \sigma^x, & \hat{H}(\pi,0) &= -2t_y - 2\delta \sigma^x, \\ \hat{H}(0,\pi) &= 2t_y - 2t \sigma^x, & \hat{H}(\pi,\pi) &= 2t_y - 2\delta \sigma^x. \end{aligned}$$

We see that although this is more complicated than the 1D case everything still commutes with \mathcal{P} . For simplicity we pick $t = 2t_y = 1$ and focus on the two gapped phases $\delta < 0$ and $\delta > 0$. In these two phases we have the following set of eigenvalues:

$$\delta > 0 : \begin{cases} \zeta(00) = + \\ \zeta(\pi 0) = + \\ \zeta(0\pi) = + \\ \zeta(\pi\pi) = + \end{cases}, \quad \delta < 0 : \begin{cases} \zeta(00) = + \\ \zeta(\pi 0) = - \\ \zeta(0\pi) = + \\ \zeta(\pi\pi) = - \end{cases}.$$

The product of all the eigenvalues in each case is $+1$ so the parity of the first Chern number for these two cases is even. In fact, it is exactly zero for this model. Just as in the 1D case we see that the $\delta < 0$ phase is interesting. Here the Wannier center for each electron is moved along the x axis to the midbond center *between* each unit cell. If we cut an edge that is perpendicular to the x direction there will be a finite charge density on the boundary. Although the inversion symmetry is not enough to determine the polarization, we see that this Hamiltonian also has a reflection symmetry, $\mathcal{M} \hat{H}(k_x, k_y) \mathcal{M}^{-1} = \hat{H}(-k_x, k_y)$ with $\mathcal{M} = \sigma^x = \mathcal{P}$. Thus the charge polarization in the x direction is quantized and equal to $P_1 = e/2a$ where a is the lattice constant in the y direction.

Finally we can consider the entanglement spectra of these two phases. We outlined this procedure for higher dimensional systems in Sec. III C 6. For $\delta > 0$ the phase is adiabatically connected to the atomic limit and thus will not require the existence of $1/2$ modes. For $\delta < 0$ we must first specify a cut direction to locate the $1/2$ modes. Let us first pick the cut to be parallel to the x direction. Thus k_x remains a good quantum number and we can ask whether or not there are $1/2$ modes at

$k_x = 0$ or $k_x = \pi$. For $k_x = 0$ we look at $\zeta(0,0)\zeta(0,\pi) = +1$ and for $k_x = \pi$ we consider $\zeta(\pi,0)\zeta(\pi,\pi) = +1$. Thus for this cut there are no $1/2$ modes. Next we look at a cut parallel to the y direction such that k_y is a conserved quantum number. For $k_y = 0$ we have $\zeta(0,0)\zeta(\pi,0) = -1$ and for $k_y = \pi$ we have $\zeta(0,\pi)\zeta(\pi,\pi) = -1$ which implies there will be $1/2$ modes at both $k_x = 0$ and π . The entanglement spectrum for a cut parallel to the y direction is shown in Fig. 7(b). In this figure there are clear $1/2$ modes at $k_y = 0, \pi$. In fact, for this simple model there are $1/2$ modes for all values of k_y though our criterion only constrains the modes at the inversion invariant points.

2. Chern insulator

Next we move on to study the well-known 2D topological insulators beginning with the Chern insulator (quantum anomalous Hall effect).¹ This is a 2D topological insulator which exhibits a quantum Hall effect and is classified by an integer invariant, the Chern number.⁴⁸ Instead of studying the initially proposed honeycomb lattice model we will use the square lattice version, which is Dirac fermions on a lattice with a Wilson mass term. The Hamiltonian is

$$H = \sum_{m,n} \left\{ \frac{1}{2} [\Psi_{m+1,n}^\dagger (i\sigma^x - \sigma^z) \Psi_{m,n} + \Psi_{m,n+1}^\dagger (i\sigma^y - \sigma^z) \Psi_{m,n} + \text{H.c.}] + (2-m) \Psi_{m,n}^\dagger \sigma^z \Psi_{m,n} \right\}. \quad (130)$$

We can Fourier transform to get the Bloch Hamiltonian,

$$\hat{H}(k) = \sin k_x \sigma^x + \sin k_y \sigma^y + M(k) \sigma^z, \quad (131)$$

$$M(k) = -m - \cos k_x - \cos k_y. \quad (132)$$

This model exhibits several different phases as a function of m . For $m < 0, m > 4$ the system is in a trivial insulator phase and for $0 < m < 2, 2 < m < 4$ the system is in Chern insulator (quantum Hall) phases with Chern number -1 and $+1$, respectively. This Hamiltonian has an inversion symmetry with $\mathcal{P} = \sigma^z$ and at the four inversion invariant momenta we have

$$\begin{aligned} \hat{H}(0,0) &= -m\sigma^z, & \hat{H}(\pi,0) &= 2 - m\sigma^z, \\ \hat{H}(0,\pi) &= 2 - m\sigma^z, & \hat{H}(\pi,\pi) &= 4 - m\sigma^z. \end{aligned}$$

For $m < 0, m > 4$ the inversion eigenvalues are all positive/negative, respectively. For $0 < m < 2$ $\zeta(0,0) = -1$ and $\zeta(\pi,0) = \zeta(0,\pi) = \zeta(\pi,\pi) = +1$ and the system must have a Chern number with odd parity. It does since $C_1 = -1$. For $2 < m < 4$ all the eigenvalues except $\zeta(\pi,\pi)$ are negative and again the Chern number must have odd parity ($C_1 = +1$).

The location of the $1/2$ modes in the entanglement spectrum is also clear. If we choose to cut along the x or y directions the picture remains the same. This indicates that we are not dealing with an (weak) anisotropic insulator as in the dimerized case but a fully 2D topological insulator state. This is similar to saying that for the quantum Hall effect, no matter what edge we cut in the system, there will be edge states. For definiteness assume that we cut parallel to y so that k_y is a good quantum number. For $0 < m < 2$ there will be a $1/2$ entanglement mode at $k_y = 0$ and for $2 < m < 4$ there will

be a $1/2$ mode at $k_y = \pi$. In addition to these modes there is actually a dispersing set of modes that are localized on the cut. To clearly see the dispersing modes we look at the entanglement ‘‘energies’’ which are defined to be

$$\epsilon_m = \frac{1}{2} \ln \left[\frac{1}{\xi_m} - 1 \right], \quad (133)$$

where ξ_m are the eigenvalues of the reduced correlation matrix C_L . The entanglement energies show the full structure of the entanglement spectrum because they clearly separate the eigenvalues of C_L , which are clustered near 0 and 1. The energy, entanglement eigenvalues, and entanglement energies for the Chern insulator in the $m < 0, 0 < m < 2$, and $2 < m < 4$ phases are shown in Fig. 8. In the two nontrivial phases the location of the $1/2$ mode is different. For $0 < m < 2$ it is at $k_y = 0$ and for $2 < m < 4$ it is at $k_y = \pi$. For the entanglement energies these become *zero* modes. These entanglement spectra were cut from a torus geometry so that there are two entanglement cuts. This is the reason why there are entanglement modes dispersing in both directions in the $C_1 \neq 0$ phases.

3. Quantum spin Hall insulator

The quantum spin Hall insulator (QSH) is a time-reversal invariant topological insulator,^{2,4,5} which is most easily thought of as two copies of the Chern insulator, one for each spin, with opposite chiralities. The realistic material in which this state is realized, HgTe/CdTe quantum wells, is best modeled by exactly this type of Hamiltonian. The effective HgTe Hamiltonian is a four-band model on the square lattice with a Hamiltonian given by

$$\hat{H}(k) = \sin k_x \hat{\Gamma}_1 + \sin k_y \hat{\Gamma}_2 + M(k) \hat{\Gamma}_0, \quad (134)$$

$$M(k) = 2 - m - \cos k_x - \cos k_y, \quad (135)$$

where $\hat{\Gamma}_1 = \sigma^z \otimes \tau^x$, $\hat{\Gamma}_2 = 1 \otimes \tau^y$, $\hat{\Gamma}_0 = 1 \otimes \tau^z$ where σ^a is spin and τ^a is the orbital degree of freedom. For this system the time-reversal operator is $T = (i\sigma^y \otimes 1)K$ and the inversion operator is $\mathcal{P} = \hat{\Gamma}_0$. This Hamiltonian is invariant under both symmetries. It exhibits phases directly analogous to the Chern insulator, i.e., it is a trivial insulator for $m < 0, m > 4$ and a topological quantum spin Hall insulator for $0 < m < 2$ and $2 < m < 4$. The only difference with the Chern insulator is that now there are two occupied bands that are related by time-reversal symmetry. The total Chern number of the ground state vanishes but there is a Z_2 invariant given (in the presence of time reversal and inversion⁷) by

$$\chi_{Z_2} = \prod_{n \in \text{occ.}/2} \zeta_n(0,0) \zeta_n(\pi,0) \zeta_n(0,\pi) \zeta_n(\pi,\pi), \quad (136)$$

where the product runs over half the occupied bands. This invariant has the same formula as $\chi_{\mathcal{P}}^{(2)}$ defined in Eq. (11), but we distinguish it here to prevent confusion since this invariant only implies a nontrivial physical response when time reversal is preserved. To specify which *half* of the occupied bands you just take one from every Kramers pair of bands. If we focus on the transition when $m \sim 0$ we see that for $m < 0$ the inversion eigenvalues of both occupied bands are all positive.

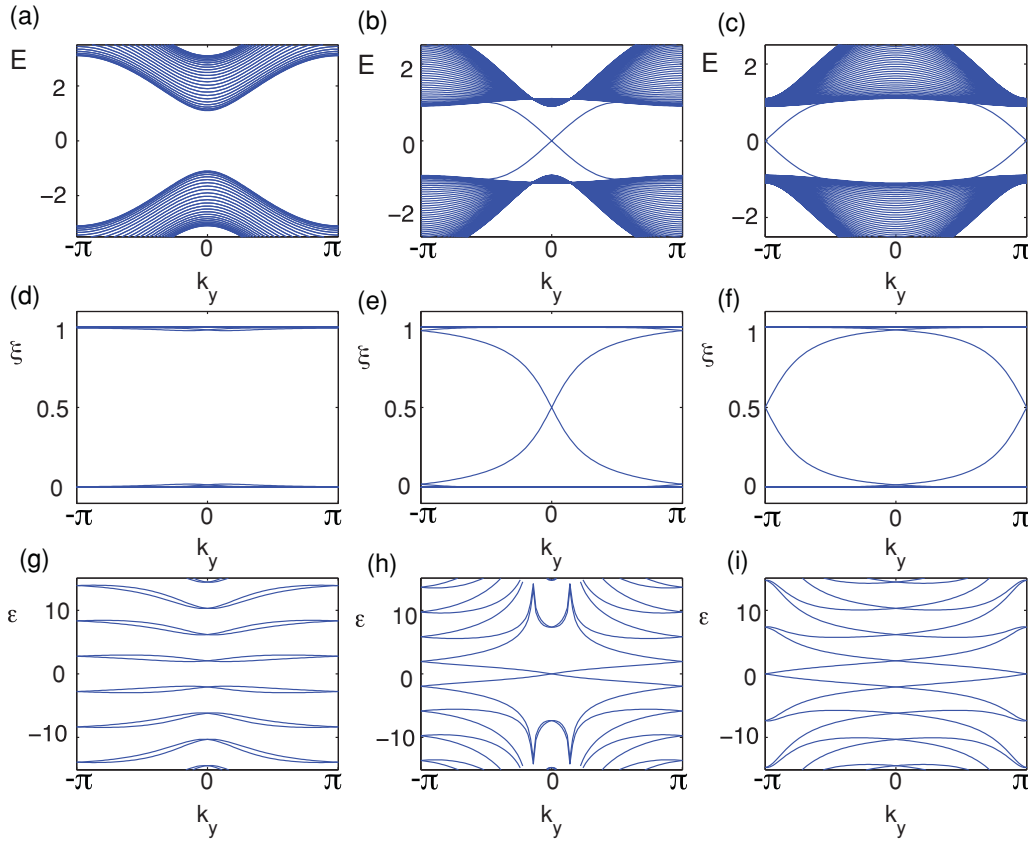


FIG. 8. (Color online) Energy spectrum with an open boundary, entanglement spectrum with a cut parallel to the y direction, and entanglement energies for [left panel, (a),(d),(g)] a trivial insulator; [middle panel, (b),(e),(h)] nontrivial Chern insulator with negative inversion eigenvalue at $(k_x, k_y) = (0, 0)$ implying entanglement midgap modes at $k_y = 0$ [right panel, (c),(f),(i)]. Chern insulator with negative inversion eigenvalues at $(k_x, k_y) = (0, 0), (\pi, 0)$, and $(0, \pi)$. This implies entanglement midgap modes at $k_y = \pi$.

For $2 > m > 0$ the inversion eigenvalues at $(k_x, k_y) = (0, 0)$ for *both* occupied bands are negative while all others are positive. The product over inversion eigenvalues of *all* the occupied bands is trivial, but if we only multiply over half the Kramers pairs we find that $\chi_{Z_2} = -1$ and is nontrivial. Since the product over all the bands is trivial this means that the parity of the first Chern number is even, in fact it is zero for this case. The energies, entanglement eigenvalues, and entanglement energies for these two phases are shown in the left and middle panels of Fig. 9. Without time-reversal symmetry this type of inversion invariant (product over half the occupied states) does not uniquely specify a topological response in two dimensions since a $C_1 = 2$ quantum anomalous Hall state could have the same inversion eigenvalue structure.

4. Quantum spin Hall insulator without time-reversal symmetry

So far the studies of the Chern insulator and QSH insulator have just been reconfirmed by recognizing the importance of inversion eigenvalues when there is an inversion symmetry. The most interesting prospect is when we take the QSH effect and *break* time reversal but keep inversion. The importance of inversion symmetry for this type of case in three dimensions was emphasized in Ref. 29. To break time-reversal symmetry we will consider an additional Zeeman term in the QSH

Hamiltonian:⁴⁹

$$\hat{H}(k) = \sin k_x \hat{\Gamma}_1 + \sin k_y \hat{\Gamma}_2 + M(k) \hat{\Gamma}_0 + B_x \hat{\Gamma}_B$$

$$\hat{\Gamma}_B = \begin{pmatrix} 0 & 0 & 1 & 0 \\ 0 & 0 & 0 & 0 \\ 1 & 0 & 0 & 0 \\ 0 & 0 & 0 & 0 \end{pmatrix}. \quad (137)$$

For small values of B_x this term lifts the Kramers' degeneracy of the occupied bands but does not cause any crossings at the Fermi level. Although time reversal is broken, inversion is still preserved and we can still see that $\chi_{Z_2} = -1$. This is still well defined because the product of all inversion eigenvalues at a particular k_{inv} is still trivial for all k_{inv} . Thus this system is an *inversion invariant* topological insulator. It was first noted that such states could exist in Ref. 29 where it was suggested that as long as inversion symmetry was not broken the entanglement spectra for the time-reversal preserved and broken cases were the same. However, there is an important difference between the two. For the time-reversal broken QSH state we show the entanglement eigenvalues and entanglement energies in the right panel of Fig. 9. Comparing with the middle panel we see that the entanglement eigenvalues seemingly show very little difference due to the fact that most are exponentially close to

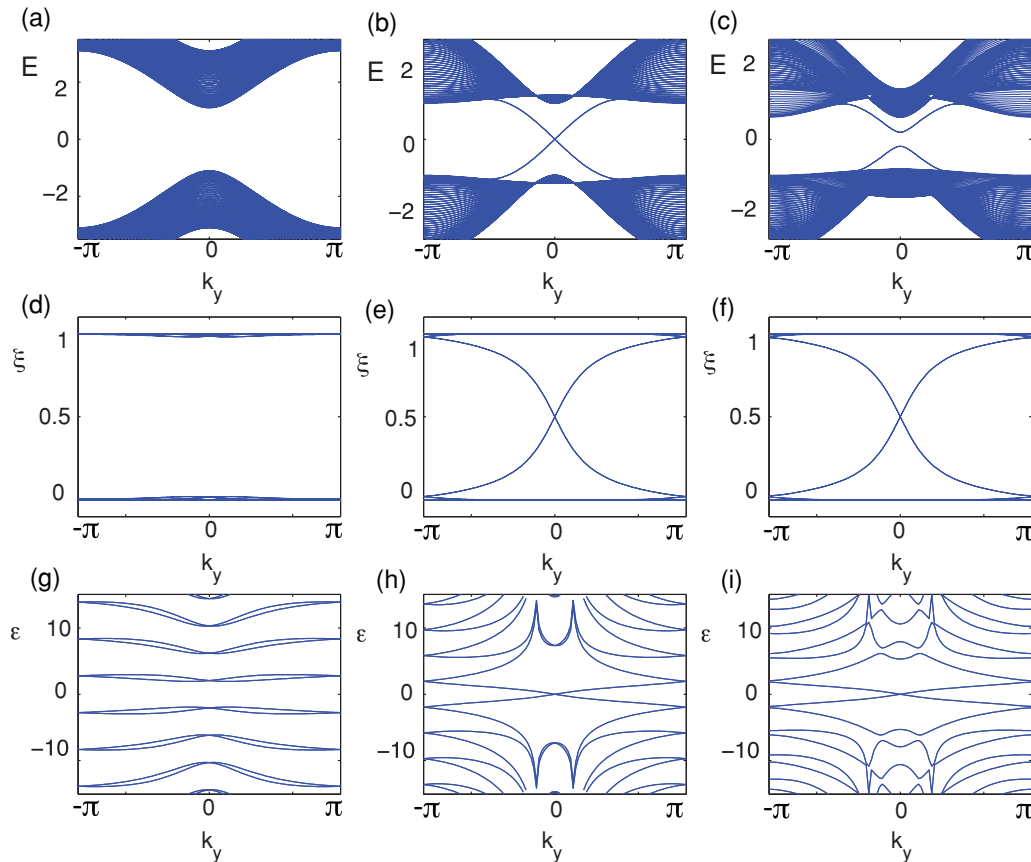


FIG. 9. (Color online) Energy spectrum with an open boundary, entanglement spectrum with a cut parallel to the y direction, and entanglement energies for [left panel, (a),(d),(g)] a trivial insulator, [middle panel, (b),(e),(h)] nontrivial quantum spin Hall insulator with time-reversal symmetry, [right panel, (c),(f),(i)] quantum spin Hall insulator with mildly broken time-reversal symmetry. Comparing (h) and (i) one can see that all Kramers degeneracies are lifted when time reversal is broken except the ones at $\epsilon = 0$. By just looking at (e) and (f) it is difficult to tell the difference in the two cases, i.e., that spectral flow is broken.

0 or 1, but the entanglement energies are quite different. The mode at $1/2$ is protected by inversion symmetry but all of the other “Kramers” degeneracies are lifted, e.g., all the crossings at $k_y = -\pi$ and $k_y = \pi$ are lifted. This occurs because the spectral flow between the bulk valence and conduction bands is cut off when time reversal is broken. The edge states no longer tie together both bands and there is no “anomaly”-type structure. Thus states on the left and right half of the system are no longer tied together through the bulk in a topological way.

We ask now if there is anything interesting in this system once time reversal is broken. As long as inversion is preserved we cannot connect this state to a trivial atomic limit while preserving inversion symmetry and there must always be a finite entanglement entropy. The finite entanglement entropy is due to the fact that the mode at $1/2$ is protected and cannot be removed. Thus the system is not trivial in the sense that it cannot ever be continuously deformed to a trivial atomic insulator; the entanglement spectrum clearly shows this. Now we can also ask if there is any nontrivial physical response. The robust electromagnetic response discussed in Refs. 9,50 and 51 comes from coupling the quantum spin Hall state to varying adiabatic parameters. For example, applying a magnetic domain wall to the edge of a QSH system induces a midgap state and fractional charge localized on the

domain wall. This response requires time-reversal symmetry to be broken and thus could still exist in the presence of a Zeeman term. The Zeeman term is an external time-reversal breaking field and it opens a gap in the edge states. If we are able to create a magnetic domain wall on the edge, i.e., a field strong enough to reverse the direction of the Zeeman field in some region of the edge, then there will be trapped domain-wall states. Thus the state is a topological insulator in a very physical sense as well. Unfortunately the inversion invariant ($\chi_p^{(2)}$) in two dimensions does not imply that this *must* be the physical response. As mentioned above, a $C_1 = 2$ quantum anomalous Hall effect can have the same value of the Z_2 invariant. However, for this model Hamiltonian we are saved because there is an additional mirror symmetry $\mathcal{M}\hat{H}(k_x, k_y)\mathcal{M}^{-1} = \hat{H}(k_x, -k_y)$ with $\mathcal{M} = \sigma^x \otimes \tau^z$. Note that $[\mathcal{M}, \mathcal{P}] = [\mathcal{M}, \hat{\Gamma}_B] = 0$. Thus the inversion eigenvalues are still valid labels and the Zeeman term does not break the mirror symmetry. This symmetry forbids a nonzero C_1 and thus the QSH response is the unique result.

5. 2D eight-band model

Here we consider a more complicated case of a model with eight bands total and four occupied bands. The model we

choose is simply two copies of the QSH model. The Bloch Hamiltonian is given by

$$\hat{H}(k) = \sin k_x \gamma^x + \sin k_y \gamma^y + M(k) \gamma^z \quad (138)$$

with $M(k)$ given in Eq. (135) and $\gamma^a = 1_{2 \times 2} \otimes \Gamma^a$. This model preserves time-reversal symmetry with $T = (1 \otimes i\sigma^y \otimes 1)K$ and inversion symmetry with $\mathcal{P} = \gamma^z$. In the presence of time-reversal symmetry this model does not yield any nontrivial topological insulators since you always get an even number of pairs of edge states. If one adds perturbations which break time-reversal symmetry then it is possible to generate nontrivial states such as Chern insulator states. At half filling this model will have four occupied bands, and will exhibit edge states for the same range of parameters as the quantum spin Hall model above in Eq. (134). These edge states are not protected generically, i.e., one can add a time reversal and inversion *preserving* perturbation to the model, which will open a gap in the edge states. We use this model to illustrate three points: (i) Even though there is no topological invariant in the system associated with time-reversal symmetry, the presence of inversion symmetry predicts that there will be nontrivial midgap states in the entanglement spectrum. (ii) These midgap states are completely stable as long as you do not break inversion symmetry. (iii) The number of midgap states is proportional to the difference in negative parity eigenvalues at the invariant momenta.

In Fig. 10 we show the energy and entanglement spectra for two different cases. In Figs. 10(a) and 10(c) we simply diagonalize Eq. (138) with $m = 1.0$ on an open boundary. One can clearly see the (unstable) edge states lying in the

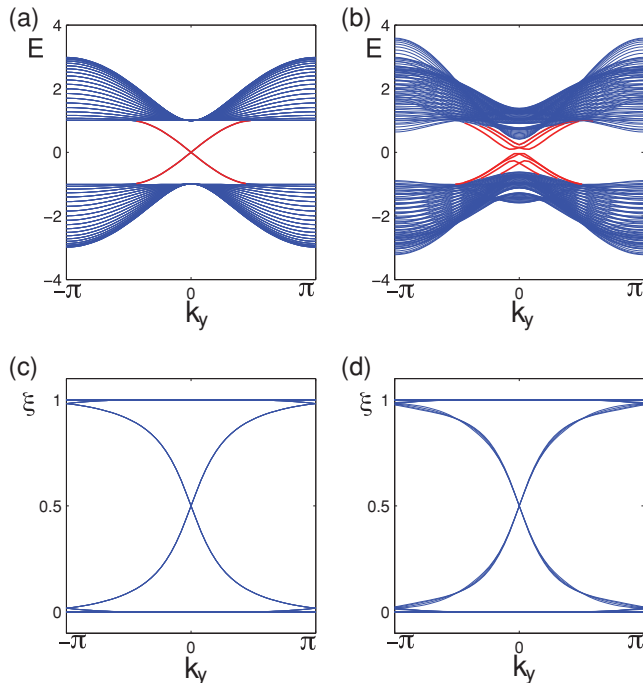


FIG. 10. (Color online) Energy spectrum with open boundary conditions for (a) eight-band model with T symmetry, (b) eight-band model with random inversion preserving perturbation. Entanglement spectrum for (c) eight-band model with T , (d) eight-band model with random inversion preserving perturbation.

midgap region. The entanglement spectrum is shown for a system with periodic boundary conditions cut parallel to the y axis. The difference between the number of negative inversion eigenvalues at $(k_x, k_y) = (0, 0)$ and $(\pi, 0)$ is 4 giving a total number of $2 \times 4 = 8$ modes at $1/2$. If we leave out the identity matrix, and \mathcal{P} itself, there are 30 matrices which commute with \mathcal{P} . To illustrate the stability of the $1/2$ modes in the entanglement spectrum we add a perturbation, which includes all 30 matrices with random couplings chosen from a uniform distribution $[-\delta/2, \delta/2]$ where $\delta > 0$ is chosen small enough not to close the bulk gap. This perturbation will break all of the “accidental” symmetries in the problem but preserves inversion symmetry. We see in Fig. 10 where $\delta = 0.20$ that the energy spectrum still has states in the gap but the crossing points have been lifted. The entanglement spectrum, however, still has eight exact $1/2$ modes.

Finally we take a very small anisotropic sized system with $L_x = 20$ and $L_y = 2$. We cut the system in the middle between $x = 10$ and $x = 11$ and plot the entanglement spectrum vs k_y . There are only two allowed values for $k_y = 0, \pi$. The energy spectrum for such a system (with the random perturbation included but chosen from a uniform distribution $[0, \delta]$, which is no longer symmetric about zero) is gapped and has an entanglement spectrum with six midgap $1/2$ modes when $\delta = 0.19$. Counting the occupied states we find numerically that there is a difference of three negative inversion eigenvalues, which agrees with the entanglement spectrum. The energy and entanglement spectra are shown in Fig. 11.

C. 3D models

1. Dimerized Cubic Lattice

The 3D dimerized model on a cubic lattice is a trivial extension of the 2D dimerized case into three dimensions. The Hamiltonian is given by

$$H = \left\{ \begin{array}{l} \sum_k \Psi_k^\dagger \\ [-(t + \delta) - (t - \delta) \cos k_x] \sigma^x \\ + (t - \delta) \sin k_x \sigma^y - 2t_y \cos k_y - 2t_z \cos k_z \end{array} \right\} \Psi_k. \quad (139)$$

For $t = 2t_y = 2t_z = 1$ there are two different phases $\delta < 0$ and $\delta > 0$. As before, for $\delta > 0$ the Wannier center of the electron is located within a unit cell and all inversion eigenvalues are $+1$. For $\delta < 0$ the Wannier center is shifted along the x axis to the midbond site between unit cells. The inversion eigenvalues are $\zeta(000) = \zeta(00\pi) = \zeta(0\pi 0) = \zeta(0\pi\pi) = +1$ and $\zeta(\pi 00) = \zeta(\pi 0\pi) = \zeta(\pi\pi 0) = \zeta(\pi\pi\pi) = -1$. Again this system has a nontrivial charge polarization on a surface with \hat{x} as a normal vector. However, this is protected by the reflection symmetry about the yz plane, i.e., $\mathcal{M}\hat{H}(k_x, k_y, k_z)\mathcal{M}^{-1} = \hat{H}(-k_x, k_y, k_z)$ with $\mathcal{M} = \sigma^x = \mathcal{P}$. Thus since the product of the reflection eigenvalues is -1 for each reflection invariant line in the Brillouin zone, the polarization on a surface perpendicular to the x axis is $P_1 = e/2a^2$ where a^2 is the area of a plaquette in the yz plane. The product of all the parity eigenvalues is trivial as it must be in three dimensions, and additionally the product of the eigenvalues in every plane is trivial. For an entanglement cut such that k_y and k_z are good quantum numbers it is clear that there will be $1/2$ modes at $(k_y, k_z) = (0, 0), (\pi, 0), (0, \pi)$,

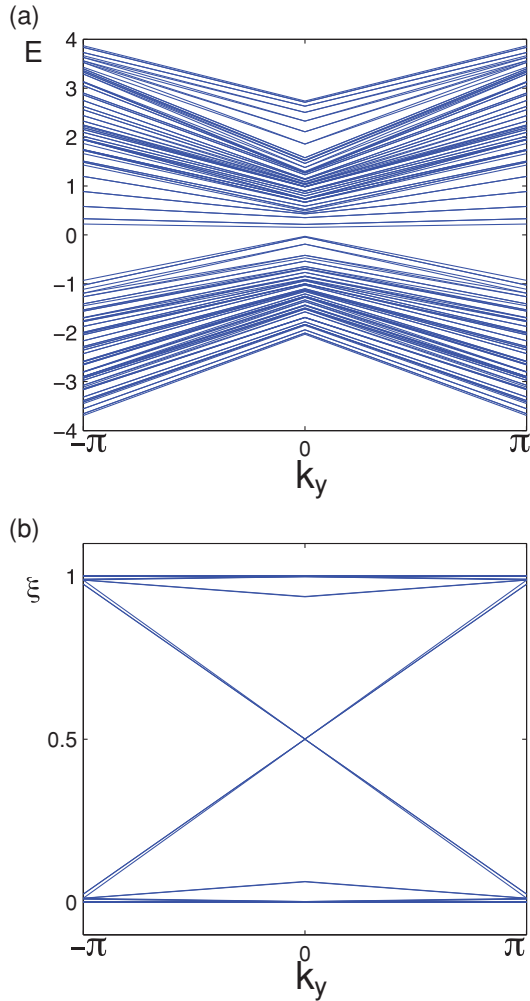


FIG. 11. (Color online) (a) Energy spectrum for the small anisotropic eight-band Hamiltonian with periodic boundary conditions. The difference in negative parity eigenvalues at $k_y = 0, \pi$ is 3. (b) Entanglement spectrum for the same. At $k_y = 0$ there are six modes at $\xi = 1/2$. The lines are only filled in as guides to the eye. The only allowed k values are $k_y = 0$ and $k_y = \pi$. This is why the spectra appear to have kinks.

and (π, π) . On the other translationally invariant cuts parallel to the xz or xy planes there will be no $1/2$ modes.

2. 3D Quantum Hall Effect

The 3D quantum Hall effect state can be thought of as stacks of 2D quantum Hall states that are connected together. We will use a very simple model for the 3D quantum (anomalous) Hall effect, which is a trivial extension of the 2D Chern insulator. The Hamiltonian is

$$\hat{H}(k) = \sin k_x \sigma^x + \sin k_y \sigma^y + M(k) \sigma^z, \quad (140)$$

$$M(k) = 2 - m - \cos k_x - \cos k_y - t_\perp \cos k_z. \quad (141)$$

This system has an inversion symmetry with $\mathcal{P} = \sigma^z$. This model exhibits several different phase transitions but we will only focus on one, namely the phase transition that occurs with a gapless point at $(k_x, k_y, k_z) = (0, 0, 0)$. For $m < -t_\perp$ the system is in a trivial insulating phase with all inversion eigenvalues positive. At $m = -t_\perp$ the system becomes gapless

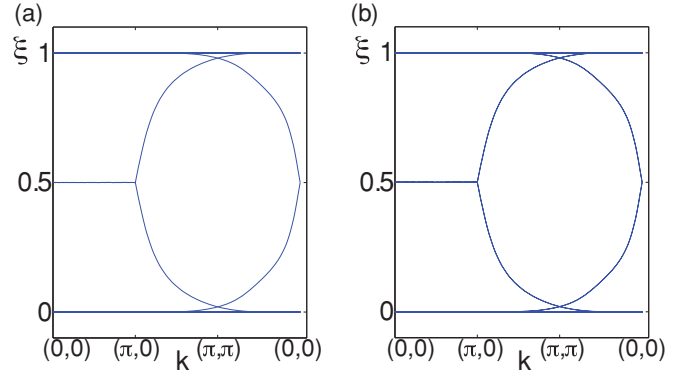


FIG. 12. (Color online) Entanglement spectra for (a) 3D QHE, (b) 3D weak topological insulator (WTI) with a cut parallel to the z - x plane plotted along a line in the Brillouin zone. The states in (b) are all doubly degenerate compared to (a). The coordinates are in the form $\mathbf{k} = (k_z, k_x)$.

and stays gapless until $m > t_\perp$. For $m > t_\perp$ the system is in a 3D quantum Hall effect phase⁴² with effectively 2D quantum Hall states stacked up in the z direction. The Bloch Hamiltonians at the inversion invariant points which switch eigenvalues are

$$\hat{H}(0, 0, 0) = -(m + t_\perp) \sigma^z, \quad \hat{H}(0, 0, \pi) = (-m + t_\perp) \sigma^z.$$

At $m = -t_\perp$ the eigenvalue around the Γ point switches from positive to negative but the system is still gapless. Then at $m = +t_\perp$ the eigenvalue at $(0, 0, \pi)$ switches and the system becomes a gapped insulator. The product over all the eigenvalues is trivial as expected but if we restrict the product to the $k_z = 0$ or $k_z = \pi$ planes the product is negative. We proved earlier that this indicates a nontrivial 3D QHE response.

For this arrangement of eigenvalues we can calculate the location of the $1/2$ modes in the entanglement spectrum. For a cut parallel to the xy plane there will be no $1/2$ modes at the inversion invariant points. If we take the cut, e.g., parallel to the zx plane then there will be $1/2$ modes at $(k_z, k_x) = (0, 0)$ and $(\pi, 0)$. These nodes are shown in Fig. 12(a). The figure shows, in addition to the $1/2$ modes at the two invariant momenta, a line of $1/2$ modes between $(k_z, k_x) = (0, 0)$ and $(\pi, 0)$.

3. 3D Weak Topological Insulator

There are several different classes of the recently proposed 3D time-reversal invariant topological insulators. The anisotropic classes, the so-called weak topological insulators, are effectively 2D quantum spin Hall states stacked into three dimensions. This is similar to the 3D quantum Hall effect and is essentially just two copies of that system, one for each spin. We use the following model:

$$\hat{H}(k) = \sin k_x \hat{\Gamma}_1 + \sin k_y \hat{\Gamma}_2 + M(k) \hat{\Gamma}_0, \quad (142)$$

$$M(k) = 2 - m - \cos k_x - \cos k_y - t_\perp \cos k_z, \quad (143)$$

where the $\hat{\Gamma}_a$ matrices are the same as in the quantum spin Hall state. This system is time reversal and inversion invariant with an inversion operator $\mathcal{P} = \hat{\Gamma}_0$. It exhibits phase transitions at the same values of m as the 3D quantum Hall effect and the only difference is that there are two occupied bands instead of one. For $2 - t_\perp > m > t_\perp$. The system has two pairs of negative

inversion eigenvalues, one pair at $(0,0,0)$ and one at $(0,0,\pi)$. The rest of the eigenvalues are all positive. The total product of inversion eigenvalues is trivial, and unlike the 3D quantum Hall case the product of the eigenvalues when restricted to the $k_z = 0, \pi$ planes is also trivial. However, there is something nontrivial here that arises from taking the eigenvalues from only one of the Kramers pairs at each invariant momentum. We see that this product is nontrivial and indicates an anisotropic inversion invariant topological insulator. In this case, since time-reversal symmetry is preserved, it is a weak topological insulator state.⁷ However, without time-reversal symmetry the inversion invariant being nontrivial does not require that it is a weak topological insulator. As a counterexample it could be a 3D quantum Hall effect with a Chern number “per layer” that is an odd multiple of 2 (unless there is a reflection symmetry that requires the Chern number to vanish in each plane). The interesting thing about this model is that even when time reversal is softly broken (i.e., broken without causing a phase transition) the system still is not in a trivial topological state and even though the surface states are no longer protected it can exhibit nontrivial behavior in the entanglement. The entanglement spectrum for the T -invariant case is shown in Fig. 12(b) and exhibits the same 1/2 mode structure as the 3D quantum Hall effect model but with twice as many modes.

4. 3D Strong Topological Insulator

The last class of models we will consider is the 3D lattice Dirac model, which is the minimal model for time-reversal invariant strong topological insulators in three dimensions. The Bloch Hamiltonian is given by

$$\hat{H}(k) = \sin k_x \hat{\Gamma}_1 + \sin k_y \hat{\Gamma}_2 + \sin k_z \hat{\Gamma}_3 + M(k) \hat{\Gamma}_0, \quad (144)$$

$$M(k) = 3 - m - \cos k_x - \cos k_y - \cos k_z,$$

where $\hat{\Gamma}_3 = \sigma^y \otimes \tau^x$. As a function of m this model exhibits many phase transitions. We will focus on the range $m < 0$ and $0 < m < 3$. There is a phase transition at $m = 0$ with a band crossing at the Γ point in k space. Four bands meet at this point and a pair of inversion eigenvalues is exchanged. For $m < 0$ the inversion eigenvalues are positive for both occupied bands at all the invariant momenta. The Bloch Hamiltonian at $k = 0$ is $\hat{H}(0) = -m \hat{\Gamma}_0$ and thus when m switches sign the inversion eigenvalues at $k = 0$ are exchanged. For $0 < m < 3$ both inversion eigenvalues at $k = 0$ are negative. In this phase the product over all inversion eigenvalues is trivial, but if we only keep one of the Kramers pairs, then the product of all the eigenvalues of half the occupied bands is nontrivial. In the presence of inversion and time reversal, which is the case here, this invariant is the strong topological Z_2 index.⁷ Physically this index has two implications: (1) the presence of an odd number of massless Dirac cones on *any* surface, (2) a topological magnetoelectric effect. To see the topological response one must apply a time-reversal breaking field on the surface to open a gap in the gapless Dirac fermions. This induces a quantum Hall effect confined to the surface which leads to the magnetoelectric response. For the topological phase we picked ($0 < m < 3$), the surface states are located around the surface Γ point and the (pair of) entanglement modes will be located at the Γ point of the conserved momenta

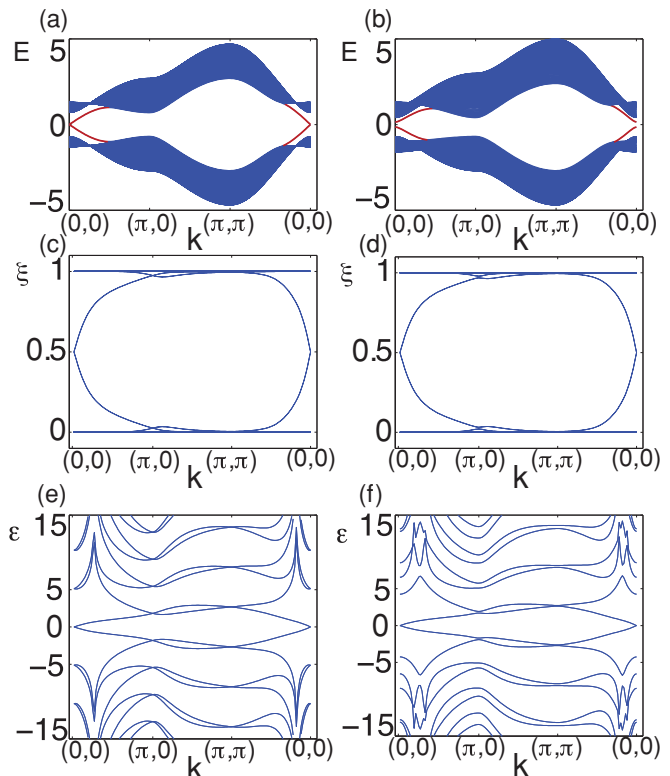


FIG. 13. (Color online) Left column: Strong topological insulator. (a) Energy spectrum plotted along a line in the Brillouin zone for open boundary conditions along the z direction; (c) entanglement spectrum with a cut parallel to the x - y plane with periodic boundary conditions; (e) entanglement energies. Right column: Strong topological insulator with time-reversal symmetry breaking (b) energy spectrum, (d) entanglement spectrum, (f) entanglement energies. In (a) and (b) the midgap states are localized on the surfaces. In (b) there is a gap in the surface states due to time-reversal symmetry breaking. In (f) all Kramers degeneracies are lifted except the one at $\epsilon = 0$.

parallel to the entanglement cut. The energy spectrum, entanglement eigenvalues, and entanglement energies are shown in Figs. 13(a), 13(c), and 13(e), respectively. The energy spectrum is shown with periodic boundary conditions along x and y and open boundary conditions along z . The surface states are shown in red and the spectrum is plotted along a 1D path in the Brillouin zone.

5. 3D strong topological insulator without time-reversal symmetry

Now we can consider the more interesting question of the properties of the system when we break time reversal but keep inversion. We add the same Zeeman term shown in Eq. (138) to the bulk of the insulator. We only break time reversal softly which opens a gap in the surface states but does not close the bulk gap. Thus while we can no longer consider the Z_2 invariant protected by time reversal, this system will still exhibit a magnetoelectric effect since the Zeeman field simply establishes a quantum Hall effect on the surface. This distinction was first considered in Ref. 29. Additionally, although we can add surface potentials to push the surface states into the bulk bands we still cannot adiabatically connect this insulator with an atomic limit. This is clearly shown in the

entanglement spectrum where there are still modes protected at $1/2$, which cannot be removed without breaking inversion or passing through a phase transition. Thus, it is impossible to continuously connect this to a system with vanishing entanglement entropy. Figures 13(b), 13(d), and 13(f) show the energy, entanglement eigenvalues, and entanglement energies, respectively. For the energies the red surface states are now clearly gapped, but the entanglement eigenvalues are hard to distinguish between the time-reversal invariant and breaking cases. The distinction, we see, comes when we look at the entanglement energies, which show that while there is still a pair of zero modes, all of the other degeneracies at the inversion invariant momenta (which arose from Kramers degeneracies) are lifted generically. This shows that the spectral flow between the valence and conduction bands of the entanglement spectrum has been cut off.

Now we will prove that $P_3 \neq 0$ for this model. To be explicit we take

$$\hat{H}(k) = \sin k_1 \hat{\Gamma}_1 + \sin k_2 \hat{\Gamma}_2 + \sin k_3 \hat{\Gamma}_3 + (5/2 - \cos k_1 - \cos k_2 - \cos k_3) \hat{\Gamma}_0 + \frac{1}{4} \hat{\Gamma}_B. \quad (145)$$

This Hamiltonian can be connected through a gapped interpolation with the trivial Hamiltonian:

$$\hat{H}_0(k) = \sin k_1 \hat{\Gamma}_1 + \sin k_2 \hat{\Gamma}_2 + \sin k_3 \hat{\Gamma}_3 + 5/2 \hat{\Gamma}_0 \quad (146)$$

using the inversion symmetric homotopy

$$\hat{H}(k, \theta) = \frac{1}{2}(1 + \cos \theta) \hat{H}(k) + \frac{1}{2}(1 - \cos \theta) \hat{H}_0(k) + \sin \theta \hat{\Gamma}_5, \quad (147)$$

where $\hat{\Gamma}_5 = \hat{\Gamma}_0 \hat{\Gamma}_1 \hat{\Gamma}_2 \hat{\Gamma}_3$. The second Chern number generated by $\hat{H}(k, \theta)$ is $C_2 = 1$ (odd) and consequently $P_3 = \frac{1}{2} \pmod{Z}$ for $\hat{H}(k)$ since we specifically chose the form of $\hat{H}_0(k)$ to be trivial. Note that as with the cases shown in Appendix I we calculated C_2 numerically using the standard gauge invariant formula in terms of ground-state projection operators.

D. Continuum models

So far we have exclusively used tight-binding models but the discussion can be carried out for continuum models as well. Let us consider a periodic crystal described by a Hamiltonian

$$H = -\nabla^2 + \hat{V}(\mathbf{r}) \quad (148)$$

acting on two-component spinors. The 2×2 matrix potential $\hat{V}(\mathbf{r})$ is assumed periodic in \mathbf{r} : $\hat{V}(\mathbf{r} + \mathbf{R}) = \hat{V}(\mathbf{r})$, where \mathbf{R} is a lattice vector of the crystal. We also assume that $\hat{V}(\mathbf{r})$ has an inversion symmetry \mathcal{P} , where \mathcal{P} is a unitary operation implementing the transformation $\mathbf{r} \rightarrow -\mathbf{r}$ on the space of spinors. The unitary \mathcal{P} can be more complicated than just $(\mathcal{P}\Psi)(\mathbf{r}) = \Psi(-\mathbf{r})$.

We now consider the Bloch decomposition, given by the isometry:

$$U : \mathcal{H} \rightarrow \oplus_k \mathcal{H}_k, \quad U\Psi = \oplus_k \Psi_k, \quad \Psi_k(\mathbf{r}) = \sum_{\mathbf{R}} e^{-i\mathbf{k}\cdot\mathbf{R}} \Psi(\mathbf{r} + \mathbf{R}), \quad (149)$$

where \mathcal{H} is the original Hilbert space and \mathcal{H}_k represents the space of square integrable spinors defined over only one unit cell, and satisfying the Bloch boundary conditions (the prime indicates the derivative):

$$\Psi_k(\mathbf{r} + \mathbf{R}) = e^{i\mathbf{k}\cdot\mathbf{R}} \Psi_k(\mathbf{r}), \quad \Psi'_k(\mathbf{r} + \mathbf{R}) = e^{i\mathbf{k}\cdot\mathbf{R}} \Psi'_k(\mathbf{r}) \quad (150)$$

whenever \mathbf{r} and $\mathbf{r} + \mathbf{R}$ are on the boundaries of the unit cell. Under this isometry, we have

$$UHU^{-1} = \oplus_k H_k, \quad (151)$$

where H_k is given by $-\nabla^2 + \hat{V}(\mathbf{r})$ but this time defined only over one unit cell and with the Bloch boundary conditions. The inversion operation \mathcal{P} becomes $U\mathcal{P}U^{-1}$, an operator from $\oplus_k H_k$ into itself, taking each \mathcal{H}_k into its counterpart \mathcal{H}_{-k} . We will denote this operation by the same symbol $\mathcal{P} : \mathcal{H}_k \rightarrow \mathcal{H}_{-k}$. At this point, the situation is very similar to that presented for the tight-binding models; the only difference is that the Bloch Hamiltonians H_k and the inversion operation act on more complex Hilbert spaces. Therefore one will be able to apply the conclusions of the last sections once we show how to compute the inversion eigenvalues $\zeta_i(k_{\text{inv}})$ at the TRI points.

The following discussion is independent of how one represents the continuum Hilbert space. Both H_k and \mathcal{P} can be explicitly computed with existing electronic structure codes. Now, at the TRI points \mathbf{k}_{inv} , \mathcal{P} becomes a unitary matrix sending $\mathcal{H}_{\mathbf{k}_{\text{inv}}}$ into itself. One can diagonalize the explicit Bloch Hamiltonian $H_{\mathbf{k}_{\text{inv}}}$ and form the projector $\hat{P}_{\mathbf{k}_{\text{inv}}}$ onto the spectrum below the given Fermi level E_F . At last, one can compute the inversion eigenvalues $\zeta_i(k_{\text{inv}})$ at each \mathbf{k}_{inv} by diagonalizing $\hat{P}_{\mathbf{k}_{\text{inv}}} \mathcal{P} \hat{P}_{\mathbf{k}_{\text{inv}}}$. With this machinery one can apply our formulas presented in Secs. III and IV to classify continuum models.

VI. CONCLUSIONS

The question of what makes an insulator ‘‘topological’’ has many answers. In this paper we presented an answer which encompasses all of the known topological insulators. The fundamental distinction between an ordinary band insulator and a topological insulator is the inability to adiabatically connect a topological insulator to the atomic limit. This distinction can have many manifestations including nontrivial topological responses to external fields and robust boundary states, however, these properties are not necessary conditions for a topological insulator. In fact, we have seen examples in this paper without protected boundary states, and examples with no topological response. At first sight these insulators seem to have no characteristics that distinguish them from trivial band insulators. Admittedly these are not the most interesting systems to consider experimentally, but they still show a striking signature in the entanglement spectrum. In fact, all known topological insulators show a signature in the entanglement spectrum when the bipartition is a position-space cut. Instead of taking the whole spectrum, one can calculate just the entanglement entropy, which for all topological insulators cannot be adiabatically deformed to zero. This fact is what serves as the basis for our definition and unifies the inversion symmetric insulators with the ones that are invariant

under other discrete symmetries. Our procedure for analyzing inversion symmetric crystals stems from the calculation and application of the set of discrete inversion eigenvalues for the occupied bands. Given a set of eigenvalues one can determine the topological nature of the insulating state by comparison with atomic band insulators, and in certain special cases predict the existence of nontrivial topological responses to electromagnetic fields.

The experimental relevance of inversion symmetric topological insulators is unclear, but not out of the question.⁴⁵ Although in principle disorder immediately destroys any stability of the topological state (unlike the typical topological insulators¹⁰), the robustness of the insulator state is ultimately a question to be answered in practice. Many of the well-known topological insulators simplify when inversion symmetry is required along with the discrete symmetry that stabilizes the topological state. Thus it seems like the most interesting inversion symmetric insulators are ones which are derived from parent topological insulator states with weakly broken T or C symmetries. These types of materials would be the first place to search for signatures of topological protection due to inversion symmetry. Recently, we became aware of a paper by Turner, Zhang, Mong, and Vishwanath dealing with similar issues.⁵²

ACKNOWLEDGMENTS

We acknowledge useful conversations with C.-K. Chiu, E. Fradkin, and F. D. M. Haldane. T.L.H. was supported in part by the NSF Grant No. DMR 0758462 at the University of Illinois, and by the ICM. E.P. acknowledges support from the Research Corporation for Science Advancement. B.A.B. was supported by Princeton Startup Funds, Alfred P. Sloan Foundation, NSF Grant No. DMR-095242, and NSF China Grant No. 11050110420. T.L.H. and B.A.B. thank the Institute of Physics in Beijing, China for generous hosting. B.A.B. thanks the Princeton Center for Complex Materials, Ecole Normale Supérieure, and Microsoft Station Q for generous hosting.

APPENDIX A: PROOF THAT THE ONE-BODY CORRELATION FUNCTION IS A PROJECTION OPERATOR

Here we prove that the one-body correlation function over the full system (not only over part of the system) is a projector. This can easily be proved: C_{ij} (which is a matrix at each i, j , i.e., $C_{ij}^{\alpha\beta}$) has the property

$$\begin{aligned} \sum_j C_{ij}(k_y) C_{jk}(k_y) &= \sum_j \frac{1}{N} \sum_{k_x} e^{ik_x(i-j)} \hat{P}^*(k_x, k_y) \frac{1}{N} \sum_{k'_x} e^{ik'_x(j-k)} \hat{P}^*(k'_x, k_y) \\ &= \sum_{k_x, k'_x} \sum_j \frac{1}{N^2} e^{i(k'_x - k_x)j} e^{ik_x i} \hat{P}^*(k_x, k_y) e^{-ik'_x k} \hat{P}^*(k'_x, k_y) = \sum_{k_x, k'_x} \frac{1}{N} \delta_{k'_x - k_x} e^{ik_x i} \hat{P}^*(k_x, k_y) e^{-ik'_x k} \hat{P}^*(k'_x, k_y) \\ &= \frac{1}{N} \sum_{k_x} e^{ik_x(i-k)} \hat{P}^*(k_x, k_y) \hat{P}^*(k_x, k_y) = \frac{1}{N} \sum_{k_x} e^{ik_x(i-k)} \hat{P}^*(k_x, k_y) = C_{ik}(k_y). \end{aligned} \quad (\text{A1})$$

Note that we have used the notation $\hat{P}(k_x, k_y)$ to represent the k -dependent projector onto the occupied states instead of \hat{P}_k to make the momentum dependence easier to see.

APPENDIX B: ENTANGLEMENT EIGENVALUES FOR TWO OCCUPIED BANDS AND FOUR SITES

We will analyze only one case of inversion eigenvalues, i.e., when both inversion eigenvalues at $k = 0$ differ from the inversion eigenvalues at $k = \pi$. For simplicity and without loss of generality, we particularize to $\zeta_1(0) = \zeta_2(0) = 1$, $\zeta_1(\pi) = \zeta_2(\pi) = -1$, where the orthogonality relations between the wave functions at the same k and at different inversion symmetric k 's hold due to the opposite inversion eigenvalues. Let the wave functions of the two occupied bands be $\psi_1(k)$ and $\psi_2(k)$. Similar to the above the arguments in Sec. III C 3, the entanglement wave functions take the form $(\psi_A, m\mathcal{P}\psi_A)$ where ψ_A diagonalizes the operator $\hat{C}_0 + m\hat{C}_1\mathcal{P} = \frac{1}{4}[(1+m)(\hat{P}_0^* + \hat{P}_\pi^*) + \hat{P}_{\pi/2}^*\mathcal{P}(\mathcal{P} + im) + \mathcal{P}\hat{P}_{\pi/2}^*(\mathcal{P} - im)]$. We expand the wave function ψ_A :

$$\psi_A = a_1\psi_1(0) + a_2\psi_2(0) + b_1\psi_1(\pi) + b_2\psi_2(\pi). \quad (\text{B1})$$

With this expansion, we have to look at the solutions ψ_A which are in the null space of $\hat{P}_{\pi/2}^*\mathcal{P}(\mathcal{P} + im) + \mathcal{P}\hat{P}_{\pi/2}^*(\mathcal{P} - im)$. Once we have found such solutions, we know they have $1/2$ eigenvalues for $m = 1$ since $(\hat{C}_0 + \hat{C}_1\mathcal{P})\psi_A = \frac{1}{2}(\hat{P}_0^* + \hat{P}_\pi^*)\psi_A = \frac{1}{2}\psi_A$ due to the fact that wave functions at different inversion symmetric momenta are orthogonal if their inversion eigenvalues are different. We denote the overlaps:

$$\begin{aligned} \left\langle \psi_1\left(\frac{\pi}{2}\right) \middle| \psi_1(0) \right\rangle &= \alpha_1, & \left\langle \psi_1\left(\frac{\pi}{2}\right) \middle| \psi_2(0) \right\rangle &= \alpha_2, \\ \left\langle \psi_1\left(\frac{\pi}{2}\right) \middle| \psi_1(\pi) \right\rangle &= \alpha_3, & \left\langle \psi_1\left(\frac{\pi}{2}\right) \middle| \psi_2(\pi) \right\rangle &= \alpha_4, \\ \left\langle \psi_2\left(\frac{\pi}{2}\right) \middle| \psi_1(0) \right\rangle &= \beta_1, & \left\langle \psi_2\left(\frac{\pi}{2}\right) \middle| \psi_2(0) \right\rangle &= \beta_2, \\ \left\langle \psi_2\left(\frac{\pi}{2}\right) \middle| \psi_1(\pi) \right\rangle &= \beta_3, & \left\langle \psi_2\left(\frac{\pi}{2}\right) \middle| \psi_2(\pi) \right\rangle &= \beta_4. \end{aligned} \quad (\text{B2})$$

These are the only unknown overlaps, as the wave function at $3\pi/2$ is related to the one at $\pi/2$ by inversion symmetry. Thus its overlaps with eigenstates of \mathcal{P} are, up to a sign, identical to the ones above. We find the following two exact half modes of

the entanglement spectrum:

$$\begin{aligned} & (a_1, a_2, a_3, a_4) \\ &= (i(\beta_3\alpha_4 - \beta_4\alpha_3), 0, \beta_4\alpha_1 - \beta_1\alpha_4, \beta_3\alpha_1 - \beta_1\alpha_3); \\ & (\beta_2\alpha_3 - \beta_3\alpha_2, \beta_3\alpha_1 - \beta_1\alpha_3, I(\beta_2\alpha_1 - \beta_1\alpha_2), 0). \end{aligned} \quad (\text{B3})$$

The other two midgap entanglement eigenvalues are obtained when $m = -1$, in which case we have to diagonalize the operator $\frac{1}{4}[\hat{P}_{\pi/2}^* \mathcal{P}(\mathcal{P} - i) + \mathcal{P} \hat{P}_{\pi/2}^* (\mathcal{P} + i)]$. In this case, we expand the eigenstate:

$$|\psi_A\rangle = (c_1 + c_3 \mathcal{P}) \left| \psi_1 \left(\frac{\pi}{2} \right) \right\rangle + (c_2 + c_4 \mathcal{P}) \left| \psi_2 \left(\frac{\pi}{2} \right) \right\rangle; \quad (\text{B4})$$

we find $1/2$ modes if, just like in the previous section,

$$(c_1, c_2, c_3, c_4) = (0, 1, 0, i), \quad (1, 0, i, 0). \quad (\text{B5})$$

We then see that we have four robust modes at exactly $1/2$ in the entanglement spectrum, or exactly twice the difference of negative inversion eigenvalues at the two inversion symmetric momenta.

APPENDIX C: EXPLICIT PROOF FOR THE GENERIC TWO-SITE PROBLEM WITH N OCCUPIED BANDS

We now show that the two-site problem with n_1 negative inversion eigenvalues at $k = 0$ and n_2 negative inversion eigenvalues at $k = \pi$ out of a number N of occupied bands contains $2|n_1 - n_2|$ zero modes in the entanglement spectrum. Without loss of generality denote the eigenstates of the original Hamiltonian $|\psi_1(0)\rangle \cdots |\psi_{n_1}(0)\rangle$ as the ones with negative inversion eigenvalue at $k = 0$, $|\psi_{n_1+1}(0)\rangle \cdots |\psi_N(0)\rangle$ as the ones with positive inversion eigenvalue at $k = 0$, $|\psi_1(\pi)\rangle \cdots |\psi_{n_2}(\pi)\rangle$ as the ones with negative inversion eigenvalue at $k = \pi$, $|\psi_{n_2+1}(\pi)\rangle \cdots |\psi_N(\pi)\rangle$ as the ones with positive inversion eigenvalue at $k = \pi$. Bands at the same momentum are *all* orthogonal, while bands at different momenta are orthogonal if they have opposite inversion eigenvalues. The simplest case of the above, which should be obvious from our previous examples, is that of all the N inversion eigenvalues at $k = 0$ are identical and negative of the N eigenvalues at $k = \pi$. In this case, the projector at one of the inversion symmetric k 's annihilates all the eigenstates at the other inversion symmetric k , and the $2N$ occupied eigenstates of the original two-site Hamiltonian are also the eigenstates of the entanglement spectrum at fixed eigenvalue $1/2$. Due to their orthogonality, they are linearly independent. From here it is clear that our formula is physically correct: adding the same eigenvalues to both $k = 0, \pi$ cannot change the result.

We again expand the eigenstates $|\psi_A\rangle$ of the correlation function $C_L = (\hat{P}_0^* + \hat{P}_\pi^*)/2$ as a sum over all the occupied eigenstates, even though these might not be (and in general are not) orthogonal,

$$\begin{aligned} \psi_A &= \sum_{m=1}^{n_1} a_m \psi_m(0) + \sum_{m=n_1+1}^N a_m \psi_m(0) \\ &+ \sum_{m=1}^{n_2} b_m \psi_m(\psi) + \sum_{m=n_2+1}^N b_m \psi_m(\pi). \end{aligned} \quad (\text{C1})$$

In the generic case, we assume that the norms that are not fixed to vanish by symmetry (such as different inversion eigenvalues) are all nonzero. In general, it might be the case that not all the eigenstates in the expansion above are linearly independent, i.e., $\psi_m(0)$ might not be linearly independent from a sum of the eigenvalues $\psi_m(\pi)$, which have identical inversion eigenvalues. In building the matrix to be diagonalized, we take this into consideration, but when writing the eigenvalue equation, we *assume* they are linearly independent—generically, they will be, because there are $2N$ wave vectors of $2N$ components. The vector $(a_1, \dots, a_{n_1}, a_{n_1+1}, \dots, a_N, b_1, \dots, b_{n_2}, b_{n_2+1}, \dots, b_N)$ has to diagonalize the matrix:

$$\begin{pmatrix} \frac{1}{2} n_1 \times n_1 & 0 & B_{n_1 \times n_2} & 0 \\ 0 & \frac{1}{2} N - n_1 \times N - n_1 & 0 & A_{N - n_1 \times N - n_2} \\ B_{n_2 \times n_1}^\dagger & 0 & \frac{1}{2} n_2 \times n_2 & 0 \\ 0 & A_{N - n_2 \times N - n_1}^\dagger & 0 & \frac{1}{2} N - n_2 \times N - n_2 \end{pmatrix}, \quad (\text{C2})$$

where $B_{ij} = \langle \psi_i(0) | \psi_j(\pi) \rangle$ with $i = 1, \dots, n_1, j = 1, \dots, n_2$ and $A_{ij} = \langle \psi_i(0) | \psi_j(\pi) \rangle$ with $i = n_1 + 1, \dots, N, j = n_2 + 1, \dots, N$. It is easy to see that this matrix has $2|n_1 - n_2|$ eigenvalues at exactly $\frac{1}{2}$ irrespective of the A, B matrices. We show it for $n_2 = 0$, the generalization to $n_2 \neq 0$ being straightforward. For $n_2 = 0$, the matrix reads

$$\begin{pmatrix} \frac{1}{2} n_1 \times n_1 & 0 & 0 \\ 0 & \frac{1}{2} N - n_1 \times N - n_1 & A_{N - n_1 \times N} \\ 0 & A_{N \times N - n_1}^\dagger & \frac{1}{2} N \times N \end{pmatrix}. \quad (\text{C3})$$

Half of the entanglement eigenvalues at $1/2$ are obvious—they are the eigenvalues of the $\psi_i(0), i = 1, \dots, n_1$ eigenstates. The remaining eigenvalues must then be part of the eigenvalues of the matrix:

$$R_N^{N - n_1} = \begin{pmatrix} \frac{1}{2} N - n_1 \times N - n_1 & A_{N - n_1 \times N} \\ A_{N \times N - n_1}^\dagger & \frac{1}{2} N \times N \end{pmatrix}, \quad (\text{C4})$$

where we have indexed the matrix by the dimension $N - n_1$ of the upper block-diagonal square matrix and by the dimension N of the lower block diagonal square matrix. We need to compute the determinant of

$$R_N^{N - n_1} = \begin{pmatrix} (\frac{1}{2} - \lambda)_{N - n_1 \times N - n_1} & A_{N - n_1 \times N} \\ A_{N \times N - n_1}^\dagger & (\frac{1}{2} - \lambda)_{N \times N} \end{pmatrix}. \quad (\text{C5})$$

We can prove that this matrix has n_1 eigenvalues at $1/2$, independent of what the matrices A are; as such, we denote by M_β^α a matrix of the form above, but with any random numbers instead of the matrix made out of norms matrix $A_{ij} = \langle \psi_i(0) | \psi_j(\pi) \rangle$. We want to compute the determinant of $M_N^{N - n_1}$. By expanding first on the last column of the matrix, then immediately after, expanding on the last row of all the matrices obtained, we find the recurrence relation:

$$\det(M_N^{N - n_1}) = (\frac{1}{2} - \lambda) \det M_{N-1}^{N - n_1} + x \cdot \det(M_{N-1}^{N - n_1 - 1}), \quad (\text{C6})$$

which, applied successively, leads to

$$\begin{aligned} \det(M_N^{N-n_1}) &= \left(\frac{1}{2} - \lambda\right)^r \det M_{N-r}^{N-n_1} \\ &+ \sum_{i=1}^r x_i \cdot \left(\frac{1}{2} - \lambda\right)^{i-1} \det(M_{N-i}^{N-n_1-1}), \end{aligned} \quad (\text{C7})$$

where $r \leq N - 1$ and x_r are numbers. We choose $r = N - 1$. Notice we have so far applied the recursion relation only to the lower index of the matrix. We now apply it to the $\det(M_{N-i}^{N-n_1-1})$ to obtain

$$\begin{aligned} \det(M_{N-i}^{N-n_1-1}) &= \left(\frac{1}{2} - \lambda\right)^{p-i} \det M_{N-p}^{N-n_1-1} \\ &+ \sum_{q=1}^{p-i} x_q \cdot \left(\frac{1}{2} - \lambda\right)^{q-1} \det(M_{N-i-q}^{N-n_1-2}), \end{aligned} \quad (\text{C8})$$

where $p > i$ is an integer and the x_q are complex numbers not necessarily equal to the x_i 's in the previous recursion. We again choose $p = N - 1$, which means $i \leq N - 2$ in the above formula. By plugging in $\det(M_{N-i}^{N-n_1-1})$ into Eq. (C7), and separating the sum to take into account the restriction $i \leq N - 2$ for which Eq. (C8) is valid, we find

$$\begin{aligned} \det(M_N^{N-n_1}) &= O\left[\left(\frac{1}{2} - \lambda\right)^{N-2}\right] + \sum_{q_0=1}^{N-1} \sum_{q_1=1}^{N-1-q_0} x_{q_0} x_{q_1} \\ &\times (1 - \delta_{q_0, N-1}) \left(\frac{1}{2} - \lambda\right)^{q_0+q_1-2} \det(M_{N-(q_0+q_1)}^{N-n_1-2}), \end{aligned}$$

where $O[(\frac{1}{2} - \lambda)]$ means terms proportional to at least the $(\frac{1}{2} - \lambda)^{N-2}$. By applying the recursion relation successively, we obtain

$$\begin{aligned} \det(M_N^{N-n_1}) &= O\left[\left(\frac{1}{2} - \lambda\right)^{N-(l+1)}\right] \\ &+ \sum_{q_0=1}^{N-1} \sum_{q_1=1}^{N-1-q_0} \sum_{q_2=1}^{N-1-(q_0+q_1)} \cdots \sum_{q_l=1}^{N-1-(q_0+\cdots+q_{l-1})} \\ &\times (1 - \delta_{q_0, N-1})(1 - \delta_{q_0+q_1, N-1}) \cdots (1 - \delta_{q_0+\cdots+q_{l-1}, N-1}) \\ &\times \left(\frac{1}{2} - \lambda\right)^{(q_0+\cdots+q_l-(l+1))} \det(M_{N-(q_0+\cdots+q_l)}^{N-n_1-(l+1)}) \end{aligned} \quad (\text{C9})$$

when $N - n_1 - (l + 1) = 0$, the matrix $M_{N-(q_0+\cdots+q_l)}^{N-n_1-(l+1)}$ is fully diagonal and has determinant $(\frac{1}{2} - \lambda)^{N-(q_0+\cdots+q_l)}$. Hence the term in the sum is

$$\left(\frac{1}{2} - \lambda\right)^{q_0+\cdots+q_l-l-1} \left(\frac{1}{2} - \lambda\right)^{N-q_0-\cdots-q_l} = \left(\frac{1}{2} - \lambda\right)^{n_1} \quad (\text{C10})$$

while the lowest-order term in $O[(\frac{1}{2} - \lambda)^{N-(l+1)}]$ is again $(\frac{1}{2} - \lambda)^{n_1}$. We hence see that the determinant of $\det(M_N^{N-n_1}) \sim (\frac{1}{2} - \lambda)^{n_1}$, and these are the remaining n_1 eigenvalues. Combined

with the first n_1 eigenvalues, we see we have a total of $2n_1$ eigenvalues in the entanglement spectrum at $1/2$, just as the formula predicts.

APPENDIX D: PROPERTIES OF THE 1D ADIABATIC CONNECTION UNDER INVERSION SYMMETRY

We begin by recalling some basic facts of inversion symmetric Hamiltonians. Assume that $|u_i(k)\rangle$ is an eigenstate of the Hamiltonian at energy

$$\hat{H}(k) |u_i(k)\rangle = E_i(k) |u_i(k)\rangle. \quad (\text{D1})$$

Then $\mathcal{P} |u_i(k)\rangle$ is necessarily an eigenstate at $-k$ of the same energy:

$$\begin{aligned} \hat{H}(-k) \mathcal{P} |u_i(k)\rangle \mathcal{P} &= \hat{H}(k) \mathcal{P}^{-1} \mathcal{P} |u_i(k)\rangle = \mathcal{P} \hat{H}(k) |u_i(k)\rangle \\ &= \mathcal{P} E_i(k) |u_i(k)\rangle = E_i(k) \mathcal{P} |u_i(k)\rangle. \end{aligned}$$

We assumed no degeneracies in the spectrum, which means

$$|u_i(-k)\rangle = e^{i\alpha_k} \mathcal{P} |u_i(k)\rangle. \quad (\text{D2})$$

Thus we have

$$|u_i(k)\rangle = e^{-i\alpha_k} \mathcal{P} |u_m(-k)\rangle \quad (\text{D3})$$

with $E_i(k) = E_i(-k)$.

We assume that we are in an insulating state where the charge polarization is

$$P_1 = -ie \int_{-\pi}^{\pi} \frac{dk}{2\pi} \sum_{E_i(k)<0} \langle u_{k,i} | \partial_k | u_{k,i} \rangle. \quad (\text{D4})$$

Using Eq. (D3) we get

$$\begin{aligned} P_1 &= -ie \int_{-\pi}^{\pi} \frac{dk}{2\pi} \sum_{i \in \text{occ.}} \langle \mathcal{P} u_i(-k) | e^{i\alpha_k} \partial_k e^{-i\alpha_k} \mathcal{P} | u_i(-k) \rangle \\ &= -ie \int_{-\pi}^{\pi} \frac{dk}{2\pi} \sum_{i \in \text{occ.}} \langle \mathcal{P} u_i(-k) | \partial_k \mathcal{P} | u_i(-k) \rangle \\ &\quad -ie \int_{-\pi}^{\pi} \frac{dk}{2\pi} \sum_{i \in \text{occ.}} (-i) \partial_k \alpha_k. \end{aligned} \quad (\text{D5})$$

The last term is an integer because it depends only on $\alpha_\pi - \alpha_{-\pi}$, which can at most be $2\pi j$, so we will drop it and be left with

$$\begin{aligned} P_1 &= -ie \int_{-\pi}^{\pi} \frac{dk}{2\pi} \sum_{i \in \text{occ.}} \langle u_i(-k) | \partial_k | u_i(-k) \rangle \\ &= ie \int_{\pi}^{-\pi} \frac{dk}{2\pi} \sum_{i \in \text{occ.}} \langle u_i(k) | \partial_{-k} | u_i(k) \rangle \\ &= -ie \int_{-\pi}^{\pi} \frac{dk}{2\pi} \sum_{i \in \text{occ.}} \langle u_i(k) | \partial_k | u_i(k) \rangle \\ &= ie \int_{-\pi}^{\pi} \frac{dk}{2\pi} \sum_{i \in \text{occ.}} \langle u_i(k) | \partial_k | u_i(k) \rangle = -P_1. \end{aligned} \quad (\text{D6})$$

Since P_1 is defined only mod m the two values consistent with inversion symmetry are

$$P_1 = 0, \quad \frac{e}{2}. \quad (\text{D7})$$

We define the trivial insulator as $P_1 = 0$, while the topological one is $P_1 = \frac{\epsilon}{2}$. The $e/2$ value means that when the system is cut in two, there exists *half* a charge on each end.

APPENDIX E: RELATION BETWEEN ADIABATIC CONNECTION AND $B(k)$ IN ONE DIMENSION

We now prove that the matrix

$$B_{ij} = \langle u_{i,-k} | \mathcal{P} | u_{j,k} \rangle$$

is unitary and that

$$\hat{A}(-k) = -\hat{A}(k) + i \text{Tr}[B(k) \nabla_k B^\dagger(k)].$$

We define the matrix B_{ij} as the matrix connecting the bands at k with the ones at $-k$:

$$|u_i(-k)\rangle = B_{ij}^*(k) \mathcal{P} |u_j(k)\rangle, \quad (\text{E1})$$

where i, j run over the occupied bands $1, \dots, N$.

That B_{ij} has to be unitary can be easily seen by extending the matrix to belong to *all* bands, occupied *and* unoccupied. Since we have a full gap in the system none of the occupied bands at k can transform to unoccupied bands at $-k$ and vice versa (otherwise we would not have an insulator). This means that the full matrix $B^{\text{full}} = \text{diag}(B^{\text{occupied}}, B^{\text{unoccupied}})$ is block diagonal. One can prove the full B is unitary by using completeness:

$$\sum_{i \in \text{all bands}} |u_i(k)\rangle \langle u_i(k)| = I; \quad (\text{E2})$$

we have (double index means summation)

$$\begin{aligned} (B^\dagger B)_{ij} &= (B^\dagger)_{im} B_{mj} = \langle u_{i,k} | \mathcal{P}^\dagger | u_{m,-k} \rangle \langle u_{m,-k} | \mathcal{P} | u_{j,k} \rangle \\ &= \langle u_{i,k} | \mathcal{P}^\dagger \mathcal{P} | u_{j,k} \rangle = \langle u_{i,k} | u_{j,k} \rangle = \delta_{ij}. \end{aligned}$$

Hence since the full matrix B is unitary, so are the $B^{\text{(un)occupied}}$.

We now want to express a connection between $A(-k)$ and $A(k)$. We have

$$\begin{aligned} \hat{A}(-k) &= -i \langle u_{i,-k} | \nabla_{-k} | u_{i,-k} \rangle = i [u_i(-k)] *_{\alpha} \nabla_k [u_i(-k)]_{\alpha} = i B_{il}(k) \mathcal{P}_{\alpha\beta}^* (u_{l,k})_{\beta}^* \nabla_k [B_{ij}^*(k) \mathcal{P}_{\alpha\theta} (u_{j,k})_{\theta}] \\ &= i B_{il}(k) [\nabla_k B_{ij}^*(k)] \mathcal{P}_{\alpha\beta}^* (u_{l,k})_{\beta}^* \mathcal{P}_{\alpha\theta} (u_{j,k})_{\theta} + i B_{il}(k) B_{ij}^*(k) \mathcal{P}_{\alpha\beta}^* (u_{l,k})_{\beta}^* \nabla_k \mathcal{P}_{\alpha\theta} (u_{j,k})_{\theta} \\ &= i B_{il}(k) [\nabla_k B_{ij}^*(k)] (u_{l,k})_{\beta}^* \delta_{\beta\theta} (u_{j,k})_{\theta} + i B_{il}(k) B_{ij}^*(k) \delta_{\beta\theta} (u_{l,k})_{\beta}^* \nabla_k (u_{j,k})_{\theta} \\ &= i B_{il}(k) [\nabla_k B_{ij}^*(k)] \delta_{jl} + i B_{il}(k) B_{ij}^*(k) (u_{l,k})_{\beta}^* \nabla_k (u_{j,k})_{\beta} = i B_{il}(k) [\nabla_k B_{il}^*(k)] + i \delta_{jl} (u_{l,k})_{\beta}^* \nabla_k (u_{j,k})_{\beta} \\ &= i B_{il}(k) [\nabla_k B_{il}^*(k)] + i (u_{j,k})_{\beta}^* \nabla_k (u_{j,k})_{\beta} = i \text{Tr}[B(k) \nabla_k B^\dagger(k)] - \hat{A}(k), \end{aligned} \quad (\text{E3})$$

where repeated indices are summed over.

APPENDIX F: MAGNETOELECTRIC POLARIZATION AS WINDING NUMBER OF THE $B(k)$ MATRIX

The Abelian $\hat{A}(k)$ in the previous section obeys a special case of the more general non-Abelian transformation,

$$\hat{A}(-k) = -B \hat{A}(k) B^\dagger + i B(k) \vec{\nabla} B^\dagger(k), \quad (\text{F1})$$

where the non-Abelian adiabatic connection is $\hat{A}_i^{\alpha\beta}(k) = -i \langle u_{\alpha,k} | \nabla_{k_i} | u_{\beta,k} \rangle$. The above implies that the Berry gauge fields at k and $-k$ are non-Abelian gauge transformed of each other. The field strength gauge transformation is

$$\hat{F}_{ij}(-k) = B(k) \hat{F}_{ij}(k) B^\dagger(k). \quad (\text{F2})$$

From here the magnetoelectric polarizability is easy but tedious to obtain:

$$\begin{aligned} P_3 &= \frac{1}{16\pi^2} \int d^3k \epsilon_{ijk} \text{Tr} \left\{ \left[\hat{F}_{ij}(k) - \frac{2}{3} i \hat{A}_i(k) \hat{A}_j(k) \right] \hat{A}_k(k) \right\} = \frac{1}{16\pi^2} \int d^3k \epsilon_{ijk} \text{Tr} \left\{ \left[\hat{F}_{ij}(-k) - \frac{2}{3} i \hat{A}_i(-k) \hat{A}_j(-k) \right] \hat{A}_k(-k) \right\} \\ &= \frac{1}{16\pi^2} \int d^3k \epsilon_{ijk} \text{Tr} \left(\left\{ B(k) \hat{F}_{ij}(k) B^\dagger - \frac{2}{3} i [B(k) \hat{A}_i(k) \hat{A}_j(k) B^\dagger(k) - i B(k) \hat{A}_i(k) \partial_j B^\dagger(k)] \right. \right. \\ &\quad \left. \left. - i [\partial_i B(k)] \hat{A}_j(k) B^\dagger(k) + \partial_i B \partial_j B^\dagger \right\} [-B(k) \hat{A}_k(k) B^\dagger(k) + i B(k) \partial_k B^\dagger(k)] \right) \\ &= -\frac{1}{16\pi^2} \int d^3k \epsilon_{ijk} \text{Tr} \left\{ \left[\hat{F}_{ij}(k) - \frac{2}{3} i \hat{A}_i(k) \hat{A}_j(k) \right] \hat{A}_k(k) \right\} - \frac{1}{24\pi^2} \int d^3k \epsilon_{ijk} \text{Tr} \{ [B(k) \partial_i B^\dagger] [B(k) \partial_j B^\dagger] [B(k) \partial_k B^\dagger] \} \\ &\quad + \frac{i}{8\pi^2} \int d^3k \epsilon_{ijk} \partial_i [B(k) \hat{A}_j(k) \partial_k B^\dagger] = -P_3 - \frac{1}{24\pi^2} \int d^3k \epsilon_{ijk} \text{Tr} \{ [B(k) \partial_i B^\dagger] [B(k) \partial_j B^\dagger] [B(k) \partial_k B^\dagger] \}, \end{aligned} \quad (\text{F3})$$

which proves the formula in the text.

APPENDIX G: PROOF OF FU-KANE FORMULA

In this Appendix we provide an alternative proof for the Fu-Kane formula⁷ for the Z_2 invariant of 3D T and \mathcal{P} invariant insulators. Consider the Bloch Hamiltonian $\hat{H}(k)$ of an insulator with both inversion \mathcal{P} and time-reversal symmetry T . We have

$$\begin{aligned} \mathcal{P}^2 = 1, \quad T^2 = -1, \quad [\mathcal{P}, T] = 0, \quad T\hat{H}(k)T^{-1} = \hat{H}(-k), \\ \mathcal{P}\hat{H}(k)\mathcal{P}^{-1} = \hat{H}(-k) \end{aligned} \quad (\text{G1})$$

and hence

$$\mathcal{PT}\hat{H}(k)(\mathcal{PT})^{-1} = \hat{H}(k), \quad (\mathcal{PT})^2 = -1, \quad (\text{G2})$$

which proves that the insulator has doubly degenerate bands at each momentum k . This does not depend on the dimensionality of the space. The two ingredients we will use to prove Eq. (110) are (i) band crossing arguments between a 3D insulator in the trivial atomic limit and a topologically nontrivial insulator, and (ii) the fact that a $4 + 1 - d$ Dirac Hamiltonian changes its 4D ‘‘Hall conductance’’ by 1 if there is a band crossing of *four* bands—these are actually two doubly degenerate bands. Without loss of generality we consider a topological insulator with four bands—two occupied bands and two unoccupied. As we take a generic T and \mathcal{P} invariant insulator through a phase transition, four (i.e., two doubly degenerate) bands are generically needed.

Assume we have two T and \mathcal{P} symmetric Hamiltonians in 3D $\hat{h}_1(k)$ and $\hat{h}_2(k)$ with

$$T\hat{h}_{1,2}(k)T^{-1} = \hat{h}_{1,2}(-k), \quad \mathcal{P}\hat{h}_{1,2}(k)\mathcal{P}^{-1} = \hat{h}_{1,2}(-k).$$

We choose $\hat{h}_1(k)$ to be trivial (in the atomic limit with all hoppings taken to vanish). We now construct a time-reversal and inversion invariant interpolation between these two Hamiltonians. We first prove that such a gapped interpolation exists. To see this, it is easiest to remain with our reduced Hamiltonian with four bands, which represents the generic effective Hamiltonian of the two doubly degenerate bands immediately above and below the Fermi level, out of the total N bands in the insulator. In this basis, the 3D effective insulating Hamiltonian with inversion and time-reversal symmetry has co-dimension 2 (there are three momenta k_x, k_y, k_z and five Clifford generator Γ^a matrices in which a four-band insulating Hamiltonian with doubly degenerate bands can be expanded). In four dimensions, a topological insulator with inversion and time-reversal symmetry has co-dimension 1 (there are four momenta and five Γ^a matrices), so there is still always a way to make it gapped. This shows that generically, a 3D or 4D insulator with inversion and time reversal is always gapped. It can be made gapless by tuning two and one parameter(s), respectively. Now, let the gapped interpolation between $\hat{h}_1(k)$ and $\hat{h}_2(k)$ be $\hat{h}(k, \theta)$ which satisfies the properties

$$\begin{aligned} \hat{h}(k, 0) = \hat{h}_1(k); \quad \hat{h}(k, \pi) = \hat{h}_2(k), \\ T\hat{h}(k, \theta)T^{-1} = \hat{h}(-k, -\theta), \quad \mathcal{P}\hat{h}(k, \theta)\mathcal{P}^{-1} = \hat{h}(-k, -\theta). \end{aligned} \quad (\text{G3})$$

The interpolation between the 3D Hamiltonians is chosen this way so that if one interprets θ as a fourth momentum then the resulting 4D Hamiltonian would respect inversion and time reversal. It was shown in Ref. 9 that $2\{P_3[\hat{h}_2(k)] - P_3[\hat{h}_1(k)]\} =$

$C_2[\hat{h}(k, \theta)]$ where C_2 is the second Chern number of the 4D Hamiltonian $\hat{h}(k, \theta)$. Since we chose $\hat{h}_1(k)$ to be trivial,

$$P_3(\hat{h}_1) = 0 \pmod{n \in \mathbb{Z}}. \quad (\text{G4})$$

Hence if the second Chern number of the 4D $\hat{h}(k, \theta)$ is *odd*, we have

$$P_3(\hat{h}_2) = 1/2 \pmod{n \in \mathbb{Z}}, \quad (\text{G5})$$

giving rise to the result that if C_2 of the 4D Hamiltonian is odd, then either $\hat{h}_1(k)$ or $\hat{h}_2(k)$ is a nontrivial topological insulator. Since we pick $\hat{h}_1(k)$ to be our reference trivial Hamiltonian then this would imply that $\hat{h}_2(k)$ is nontrivial.

To understand how to classify the 3D insulators we first need to understand how to get a 4D insulator with an odd second Chern number. The 4D trivial Hamiltonian is simply a momentum-independent interpolation between $\hat{h}_1(k)$ and itself. This clearly has vanishing C_2 . Since C_2 is a topological invariant, we must have a gap-closing phase transition to change it. As the system is inversion and TR invariant, we have to analyze the crossings between two doubly degenerate bands. This is the generic case, even for insulators with an arbitrary number of bands N , because we can build an ‘‘effective’’ Hamiltonian close to the transition which will be a four-band model. With time reversal and inversion, the Bloch Hamiltonian has to be of the form $\hat{H}(k) = d_a(k)\Gamma^a$. We first consider transitions which occur away from the invariant momenta. Because of inversion (or time reversal) a gap closing at k must be matched by one at $-k$. Such transitions can be tuned by a single parameter. Since the gap closing and re-opening happens away from an invariant momentum, the inversion eigenvalues of the occupied bands remain unmodified. The non-Abelian adiabatic field strengths at the two k points are equal (up to a gauge transformation, and a minus sign in case of time reversal). Thus a gap closing at two points k and $-k$ makes the total change in second Chern number, which is *even*. Thus a 4D Chern insulator with inversion and time reversal has an even second Chern number if the inversion eigenvalues of the occupied bands are the same as in the atomic limit.

We now look at the case where the gap closing and reopening happens at an inversion symmetric point. In this case, the Hamiltonian is still 4×4 but the co-dimension of any two doubly degenerate bands is 5 because we have five Clifford matrices and no tunable momenta—the momenta are fixed at the inversion symmetric points. If the bands involved in the phase transition at the inversion symmetric points have the same inversion eigenvalues (e.g., all positive) then, up to a gauge choice, the inversion matrix is the identity operator. This means that $[\mathcal{P}, \hat{H}(0)]$ is trivially satisfied and does not provide an additional constraint and so the crossing is always avoided with such a large co-dimension. However, if the bands have different inversion eigenvalues (e.g., bonding and antibonding bands), so that the inversion matrix in a specific choice of basis is $\mathcal{P} = 1_{2 \times 2} \otimes \tau^z$, then we find that the effective Hamiltonian matrix at the inversion symmetric points $G_i/2$ is

$$\hat{H}(G_i/2) = M_i \mathcal{P}, \quad (\text{G6})$$

where M_i is the mass at the inversion symmetric point $G_i/2$.^{53–55} As such, a gap closing transition whereby the M_i

changes sign is accompanied by two effects: (i) the second Chern number will change by ± 1 if only one mass goes through zero, or more generally, it will change by the number of masses that go through zero (multiplied by a sign), and (ii) the inversion eigenvalues of a pair of occupied bands change sign as a result of every M_i that switches sign. This is the crucial difference between phase transitions which change the first and second Chern numbers. In two dimensions a change in the first Chern number is accompanied by a single inversion eigenvalue switch since the minimal crossing is between two bands. In four dimensions, changes in the second Chern number require a four-band crossing and thus two inversion eigenvalues are exchanged. This carries over to three dimensions where we are interested in the Z_2 valued parity of the second Chern number. A change of the parity is effected when a four-band crossing switches two inversion eigenvalues. We hence proved that a 4D Chern insulator with inversion and time-reversal symmetry has odd second Chern number if the product of half of the inversion eigenvalues (half meaning each Kramers pair is only counted once) at all TR invariant points is -1 . By keeping $\hat{h}_1(k)$ constant and changing only $\hat{h}_2(k)$ through a gap closing and reopening we can make $\hat{h}(k, \theta)$ a 4D insulator with an odd second Chern number. Thus $\hat{h}_2(k)$ is a nontrivial Z_2 insulator when Eq. (110) is negative and we have proved the Fu and Kane formula.

APPENDIX H: PROOF THAT PHASE IS SMOOTH FOR 3D LATTICE CASE

We show in this appendix that after band decoupling process the U(1) phases in all the decoupled U(2) blocks are all smooth. It is important to consider the generic form the inversion eigenvalues can take for a single pair of bands in n_-^o . The definition of bands in this set is that the product of inversion eigenvalues for a single band is negative, and cannot be made positive by performing band crossings with other occupied bands in the set n_-^o . We note that for a given pair, the eigenvalues for one member of the pair at a k_{inv} must be the same as the eigenvalues for the other member of the pair. If this is not true then we could perform a band crossing within this pair to make the product of inversion eigenvalues on the individual bands within the pair equal to $+1$, which contradicts the definition of bands in the set n_-^o . We will now prove that the U(1) phase for a U(2) block of $B(k)$ is only nonsmooth if there are k_{inv} where the eigenvalues are opposite. This result implies that for all pairs of bands that make up the set n_-^o the phase is smooth since we just showed that there can be no such k_{inv} points.

A simple example of a U(2) matrix with a nonsmooth phase to keep in mind for intuition is

$$B(k) = e^{(1/2)ik} \left(\cos \frac{k}{2} + i \sin \frac{k}{2} \sigma_z \right) \equiv e^{i\theta(k)} U(k), \quad (\text{H1})$$

where $U(k) \in \text{SU}(2)$. Note that this $B(k)$ satisfies all the required constraints and we can see that in Eq. (H1) everything is smooth as k is continuously varied, except when we are close to the end of the 2π cycle. If we start, for example, from $k = -\pi$, one can see that the phase and the SU(2) factor take different values when k approaches π , but as a whole $B(k)$ reaches the same value as the one we started with at $k = \pi$.

In the following we argue that such a discontinuity in the phase immediately implies the existence of a $(-+)$ pattern of inversion eigenvalues at some k_{inv} point. Let us start from a k_{inv}^1 and continuously vary k until it advances by 2π , along one of the k_i directions. At the k_{inv} points, θ can take only integer or half integer values (in units of π), and an important observation is that, if θ is half integer at a k_{inv} point, then $B(k_{\text{inv}})$ necessarily takes the form $\hat{n}\hat{\sigma}$ (\hat{n} = unit vector), which has ± 1 inversion eigenvalues. So let us assume that $\theta = 0$ at k_{inv}^1 . In general we can have

$$\theta_{k_{\text{inv}}^1+2\pi} = \theta_{k_{\text{inv}}^1} + \begin{cases} 2n\pi & (\text{a}) \\ (2n+1)\pi & (\text{b}) \end{cases}. \quad (\text{H2})$$

In case (a) the phase factor is smooth, in which case there is no problem removing it from the winding number calculation. In case (b), the phase factor changes sign. Now let us consider the inversion properties of $B(k)$ relative to the $k_{\text{inv}}^2 = k_{\text{inv}}^1 + \pi$ point. We have

$$e^{i\theta_{k_{\text{inv}}^2+k}} (f_{k_{\text{inv}}^2+k} + i\vec{g}_{k_{\text{inv}}^2+k}\vec{\sigma}) = e^{-i\theta_{k_{\text{inv}}^2-k}} (f_{k_{\text{inv}}^2-k} - i\vec{g}_{k_{\text{inv}}^2-k}\vec{\sigma}). \quad (\text{H3})$$

Since f_k and \vec{g}_k take only real values, we can see that if $\theta_{k_{\text{inv}}^2+k}$ is half integer then necessarily $\theta_{k_{\text{inv}}^2-k}$ is also half integer. In other words, the half integer values of θ_k come in pairs, unless k is the k_{inv}^2 invariant point itself. Since θ varies from 0 to $(2n+1)\pi$ as we vary k by 2π , there will be an odd number of times when θ_k assumes a half integer value. It is then evident that one such half integer value must occur at k_{inv}^2 and consequently the $(-+)$ inversion eigenvalue pattern will show up at k_{inv}^2 .

APPENDIX I: INVERSION EIGENVALUE PATTERNS AND THE CORRESPONDING MAGNETOELECTRIC POLARIZABILITY

In this Appendix we provide some explicit examples of our proof of the connection between inversion eigenvalues and the magnetoelectric polarization for inversion invariant insulators. We focus on four-band, gapped Hamiltonians $\hat{H}(k)$ in three dimensions displaying various patterns of inversion eigenvalues. Assuming two occupied bands, we will write these inversion eigenvalue patterns as

$$\begin{array}{cccccccc} + & + & + & + & + & + & + & + \\ - & - & - & - & + & + & + & + \end{array}, \quad (\text{I1})$$

for example, where one should understand that the two nonzero eigenvalues of $P_{k_{\text{inv}}}\mathcal{P}P_{k_{\text{inv}}}$ are $+1$ and -1 at four k_{inv} points and $+1$ and $+1$ at the remaining k_{inv} points. The order of the k_{inv} is not important for the magnetoelectric polarizability, but to be precise we will order them as

$$\begin{aligned} & \{(0,0,0), (\pi,0,0), (0,\pi,0), (0,0,\pi), (\pi,\pi,0), (\pi,0,\pi), \\ & (0,\pi,\pi), (\pi,\pi,\pi)\}. \end{aligned}$$

For each case, to compute the magnetoelectric polarizability P_3 , we will begin with a trivial reference Hamiltonian ($P_3 = 0$) and find a gapped and inversion symmetric interpolation $\hat{H}(k, \theta)$ between this and our example Hamiltonians. We can compute P_3 as half the second Chern number C_2 generated by the interpolation $\hat{H}(k, \theta)$, which is considered as a $4 + 1 - d$ inversion symmetric Hamiltonian. An odd C_2 corresponds

to a nontrivial insulator with half integer magnetoelectric polarizability, while an even C_2 indicates a trivial insulator. This method of calculation is convenient because C_2 can be computed using a gauge-invariant projector method, so we can bypass the task of finding a smooth gauge. All of our numerical observations are in agreement with our mathematical proofs above.

(1) The pattern

$$\begin{array}{cccccccc} + & + & + & + & + & + & + & + \\ - & - & + & + & + & + & + & + \end{array} \quad (12)$$

is seen with the following gapped Hamiltonian:

$$\begin{aligned} \hat{H}(k) = & \sin k_1 \hat{\Gamma}_1 + \sin k_2 \hat{\Gamma}_2 + \sin k_3 \hat{\Gamma}_3 \\ & + (-2.5 + \cos k_1 + \cos k_2 + \cos k_3) \hat{\Gamma}_0 \\ & + 0.75(\cos k_1 + \cos k_2)(\hat{\Gamma}_{15} + \hat{\Gamma}_{25} - \hat{\Gamma}_{35} - \hat{\Gamma}_{12}). \end{aligned} \quad (13)$$

This Hamiltonian can be connected through a gapped interpolation with the Hamiltonian:

$$\begin{aligned} \hat{H}_0(k) = & \sin k_1 \hat{\Gamma}_1 + \sin k_2 \hat{\Gamma}_2 + (-2.5 + \cos k_1 + \cos k_2) \hat{\Gamma}_0 \\ & + 0.75(\cos k_1 + \cos k_2)(\hat{\Gamma}_{15} + \hat{\Gamma}_{25} - \hat{\Gamma}_{35} - \hat{\Gamma}_{12}) \end{aligned} \quad (14)$$

using the inversion symmetric homotopy

$$\hat{H}(k, \theta) = \frac{1}{2}(1 + \cos \theta) \hat{H}(k) + \frac{1}{2}(1 - \cos \theta) \hat{H}_0(k). \quad (15)$$

The second Chern number generated by $\hat{H}(k, \theta)$ is $C_2 = 0$ (even) and the P_3 of $\hat{H}_0(k)$ is zero because it depends only on k_1 and k_2 . Consequently, the P_3 of $\hat{H}(k)$ is $0 \pmod{Z}$.

(2) The pattern

$$\begin{array}{cccccccc} + & + & + & + & + & + & + & + \\ - & - & - & - & + & + & + & + \end{array} \quad (16)$$

is seen using the following gapped Hamiltonian:

$$\begin{aligned} \hat{H}(k) = & \sin k_1 \hat{\Gamma}_1 + \sin k_2 \hat{\Gamma}_2 + \sin k_3 \hat{\Gamma}_3 \\ & + (-2.5 + \cos k_1 + \cos k_2 + \cos k_3) \hat{\Gamma}_0 \\ & - (2 - \cos k_3)(\cos k_1 + \cos k_2) \\ & \times (\hat{\Gamma}_{15} + \hat{\Gamma}_{25} - \hat{\Gamma}_{35} - \hat{\Gamma}_{12}). \end{aligned} \quad (17)$$

This Hamiltonian can be connected through a gapped interpolation with the Hamiltonian:

$$\begin{aligned} \hat{H}_0(k) = & \sin k_1 \hat{\Gamma}_1 + \sin k_2 \hat{\Gamma}_2 + (-2.5 + \cos k_1 + \cos k_2) \hat{\Gamma}_0 \\ & - 2(\cos k_1 + \cos k_2)(\hat{\Gamma}_{15} + \hat{\Gamma}_{25} - \hat{\Gamma}_{35} - \hat{\Gamma}_{12}) \end{aligned} \quad (18)$$

using the inversion symmetric homotopy

$$\hat{H}(k, \theta) = \frac{1}{2}(1 + \cos \theta) \hat{H}(k) + \frac{1}{2}(1 - \cos \theta) \hat{H}_0(k). \quad (19)$$

The second Chern number generated by $\hat{H}(k, \theta)$ is $C_2 = 0$ (even) and the P_3 of $\hat{H}_0(k)$ is zero because it depends only on k_1 and k_2 . Consequently, the P_3 of $\hat{H}(k)$ is $0 \pmod{Z}$.

(3) The pattern

$$\begin{array}{cccccccc} - & - & - & - & + & + & + & + \\ - & - & - & - & + & + & + & + \end{array} \quad (110)$$

is seen with the following gapped Hamiltonian:

$$\begin{aligned} \hat{H}(k) = & \sin k_1 \hat{\Gamma}_1 + \sin k_2 \hat{\Gamma}_2 + \sin k_3 \hat{\Gamma}_3 \\ & + \left(-\frac{1}{2} + \cos k_1 + \cos k_2 + \cos k_3\right) \hat{\Gamma}_0 + \frac{1}{2} \hat{\Gamma}_{25}. \end{aligned} \quad (111)$$

This Hamiltonian can be connected through a gapped interpolation with the trivial Hamiltonian:

$$\hat{H}_0(k) = \sin k_1 \hat{\Gamma}_1 + \sin k_2 \hat{\Gamma}_2 + \sin k_3 \hat{\Gamma}_3 - \frac{1}{2} \hat{\Gamma}_0, \quad (112)$$

using the inversion symmetric homotopy of Eq. (147). The second Chern number generated by $\hat{H}(k, \theta)$ is $C_2 = 2$ (even) and consequently $P_3 = 0 \pmod{Z}$.

(4) The pattern

$$\begin{array}{cccccccc} + & + & + & + & + & + & + & + \\ - & - & - & - & - & - & - & - \end{array} \quad (113)$$

is seen using the following gapped Hamiltonian:

$$\begin{aligned} \hat{H}(k) = & \sin k_1 \hat{\Gamma}_1 + \sin k_2 \hat{\Gamma}_2 + \sin k_3 \hat{\Gamma}_3 - \frac{1}{2} \hat{\Gamma}_0 \\ & + (2 + \cos k_1 + \cos k_2 + \cos k_3) \hat{\Gamma}_{15} \\ & + (-2 + \cos k_1 + \cos k_2 + \cos k_3) \hat{\Gamma}_{25}. \end{aligned} \quad (114)$$

This Hamiltonian can be connected through a gapped interpolation with the trivial Hamiltonian:

$$\hat{H}_0(k) = \sin k_1 \hat{\Gamma}_1 + \sin k_2 \hat{\Gamma}_2 + \sin k_3 \hat{\Gamma}_3 - \frac{1}{2} \hat{\Gamma}_0 \quad (115)$$

using the inversion symmetric homotopy

$$\begin{aligned} \hat{H}(k, \theta) = & \sin k_1 \hat{\Gamma}_1 + \sin k_2 \hat{\Gamma}_2 + \sin k_3 \hat{\Gamma}_3 - \frac{1}{2} \hat{\Gamma}_0 \\ & + \frac{1}{2}(1 + \cos \theta)(2 + \cos k_1 + \cos k_2 + \cos k_3) \hat{\Gamma}_{15} \\ & + \frac{1}{2}(1 + \cos \theta)(-2 + \cos k_1 + \cos k_2 + \cos k_3) \hat{\Gamma}_{25} \\ & + \sin \theta \hat{\Gamma}_5. \end{aligned} \quad (116)$$

The second Chern number generated by $\hat{H}(k, \theta)$ is $C_2 = 0$ (even) and consequently $P_3 = 0 \pmod{Z}$.

(5) The pattern

$$\begin{array}{cccccccc} - & - & + & + & + & + & + & + \\ - & - & + & + & + & + & + & + \end{array} \quad (117)$$

is seen using the following gapped Hamiltonian:

$$\begin{aligned} \hat{H}(k) = & \sin k_1 \hat{\Gamma}_1 + \sin k_2 \hat{\Gamma}_2 \\ & + \left(-\frac{3}{2} + \cos k_1 + \cos k_2\right) \hat{\Gamma}_0 \\ & + \left[-\frac{1}{4} + 0.1(\cos k_1 - \cos k_2)\right] \hat{\Gamma}_{25}. \end{aligned} \quad (118)$$

This Hamiltonian can be connected through a gapped interpolation with the trivial Hamiltonian:

$$\hat{H}_0(k) = \sin k_1 \hat{\Gamma}_1 + \sin k_2 \hat{\Gamma}_2 + \sin k_3 \hat{\Gamma}_3 - \frac{3}{2} \hat{\Gamma}_0 \quad (119)$$

using the inversion symmetric homotopy

$$\begin{aligned} \hat{H}(k) = & \sin k_1 \hat{\Gamma}_1 + \sin k_2 \hat{\Gamma}_2 + \frac{1}{2}(1 - \cos \theta) \sin k_3 \hat{\Gamma}_3 \\ & + \left[-\frac{3}{2} + \frac{1}{2}(1 + \cos \theta)(\cos k_1 + \cos k_2)\right] \hat{\Gamma}_0 \\ & + \frac{1}{2}(1 + \cos \theta) \left[-\frac{1}{4} + 0.1(\cos k_1 - \cos k_2)\right] \hat{\Gamma}_{25} \\ & + \sin \theta \hat{\Gamma}_5. \end{aligned} \quad (120)$$

The second Chern number generated by $\hat{H}(k, \theta)$ is $C_2 = 0$ (even) and consequently $P_3 = 0 \pmod{2}$.

APPENDIX J: RESPONSE THEORY ARGUMENT IN HIGHER DIMENSIONS

Although we do not rigorously prove anything in higher dimensions we note that the physical response arguments presented in this work and Refs. 9, 29 and 29 continue to apply in higher dimensions. This gives us a hint that there are interesting inversion symmetric topological insulators in higher dimensions. For *even* space-time dimensions the topological response actions all take a standard form

$$S_{\text{eff}}[A_\mu] = \int d^{2n}x P_n \epsilon^{a_1 a_2 \dots a_{2n-1} a_{2n}} F_{a_1 a_2} \dots F_{a_{2n-1} a_{2n}},$$

where P_n is a response coefficient and F_{ab} is the electromagnetic field-strength tensor. If these were all dynamical fields then the entire action must transform like a scalar, which means that the intrinsic response coefficients P_n must transform the same way as the product of the electromagnetic fields. Thus P_n must be odd under inversion symmetry for all n . Additionally for even (odd) n , P_n is odd under time-reversal T (charge conjugation C) symmetry. Since we are talking about external electromagnetic fields we do not transform them under the symmetry operation and hence only the P_n are changed. Thus in alternating even space-time dimensions topological insulators are protected by either T or C symmetry.

However, in *every* even space-time dimension there is a topological insulator protected by inversion symmetry, which has a topological response. In all of these cases P_n is not gauge invariant under transformations of the occupied wave functions and the oddness under the different symmetries quantizes P_n to take only two independent values. This yields a Z_2 classification for the *response coefficient* in line with the arguments presented in Ref. 9.

In *odd* space-time dimensions the generalized Chern-Simons terms describing the electromagnetic responses in topological insulators are *compatible* with inversion symmetry. The general action is

$$S_{\text{eff}}^{(\text{odd})}[A_\mu] = \frac{C_n}{(n+1)!(2\pi)^n} \times \int d^{2n+1}x \epsilon^{a_1 a_2 \dots a_{2n+1}} A_{a_1} F_{a_2 a_3} \dots F_{a_{2n} a_{2n+1}}.$$

The quantity C_n is the n th Chern number and is even under inversion symmetry and thus not restricted by the requirement of preserving inversion symmetry. If n is even (odd) then the action is also compatible with T (C) symmetry. We have not proven it, but our intuition suggests that the parity of C_n can be characterized by the inversion topological invariants given by the $\chi_{\mathcal{P}}^{(n)}$ defined in Eqs. (4) and (11) when calculated in $(2n+1) - d$, where by $\chi_{\mathcal{P}}^{(n)}$ we mean we only take the product of inversion eigenvalues over a set of $\frac{1}{2^{n-1}}$ of the occupied bands.

-
- ¹F. D. M. Haldane, *Phys. Rev. Lett.* **61**, 2015 (1988).
²C. L. Kane and E. J. Mele, *Phys. Rev. Lett.* **95**, 226801 (2005).
³C. L. Kane and E. J. Mele, *Phys. Rev. Lett.* **95**, 146802 (2005).
⁴B. A. Bernevig and S. C. Zhang, *Phys. Rev. Lett.* **96**, 106802 (2006).
⁵B. A. Bernevig, T. L. Hughes, and S. C. Zhang, *Science* **314**, 1757 (2006).
⁶M. König, S. Wiedmann, C. Brüne, A. Roth, H. Buhmann, L. Molenkamp, X.-L. Qi, and S.-C. Zhang, *Science* **318**, 766 (2007).
⁷L. Fu and C. L. Kane, *Phys. Rev. B* **76**, 045302 (2007).
⁸D. Hsieh, D. Qian, L. Wray, Y. Xia, Y. S. Hor, R. J. Cava, and M. Z. Hasan, *Nature (London)* **452**, 970 (2008).
⁹X.-L. Qi, T. L. Hughes, and S.-C. Zhang, *Phys. Rev. B* **78**, 195424 (2008).
¹⁰A. P. Schnyder, S. Ryu, A. Furusaki, and A. W. W. Ludwig, *Phys. Rev. B* **78**, 195125 (2008).
¹¹A. Kitaev, *AIP Conf. Proc.* **1134**, 22 (2009).
¹²L. Fu and C. L. Kane, *Phys. Rev. B* **74**, 195312 (2006).
¹³J. E. Moore and L. Balents, *Phys. Rev. B* **75**, 121306 (2007).
¹⁴R. Roy, *Phys. Rev. B* **79**, 195322 (2009).
¹⁵E. Prodan, *Phys. Rev. B* **80**, 125327 (2009).
¹⁶E. Prodan, *J. Phys. A* **42**, 082001 (2009).
¹⁷A. M. Essin, J. E. Moore, and D. Vanderbilt, *Phys. Rev. Lett.* **102**, 146805 (2009).
¹⁸M. Freedman, C. Nayak, K. Shtengel, and K. Walker, *Ann. Phys. (NY)* **310**, 428 (2004).
¹⁹A. Hamma, R. Ionicioiu, and P. Zanardi, *Phys. Lett. A* **337**, 22 (2004).
²⁰A. Kitaev and J. Preskill, *Phys. Rev. Lett.* **96**, 110404 (2006).
²¹M. Levin and X.-G. Wen, *Phys. Rev. Lett.* **96**, 110405 (2006).
²²H. Li and F. D. M. Haldane, *Phys. Rev. Lett.* **101**, 010504 (2008).
²³S. Ryu and Y. Hatsugai, *Phys. Rev. B* **73**, 245115 (2006).
²⁴N. Bray-Ali, L. Ding, and S. Haas, *Phys. Rev. B* **80**, 180504(R) (2009).
²⁵S. T. Flammia, A. Hamma, T. L. Hughes, and X.-G. Wen, *Phys. Rev. Lett.* **103**, 261601 (2009).
²⁶R. Thomale, A. Sterdyniak, N. Regnault, and B. A. Bernevig, *Phys. Rev. Lett.* **104**, 180502 (2010).
²⁷R. Thomale, D. P. Arovas, and B. A. Bernevig, *Phys. Rev. Lett.* **105**, 116805 (2010).
²⁸F. Pollman and J. E. Moore, *New J. Phys.* **12**, 025006 (2010).
²⁹A. M. Turner, Y. Zhang, and A. Vishwanath, *Phys. Rev. B* **82**, 241102(R) (2010).
³⁰L. Fidkowski, *Phys. Rev. Lett.* **104**, 130502 (2010).
³¹M. Kargarian and G. A. Fiete, *Phys. Rev. B* **82**, 085106 (2010).
³²E. Prodan, T. L. Hughes, and B. A. Bernevig, *Phys. Rev. Lett.* **105**, 115501 (2010).
³³A. Sterdyniak, N. Regnault, and B. A. Bernevig, e-print arXiv:1006.5435 (to be published).
³⁴F. D. M. Haldane, *APS 2009 March Meeting Proceedings* (unpublished).
³⁵I. Peschel, *J. Phys. A: Math. Gen.* **36**, L205 (2003).
³⁶J. Zak, *Phys. Rev. Lett.* **62**, 2747 (1989).

- ³⁷J. Goldstone and F. Wilczek, *Phys. Rev. Lett.* **47**, 986 (1981).
- ³⁸B. Simon, *Phys. Rev. Lett.* **51**, 2167 (1983).
- ³⁹F. Wilczek and A. Zee, *Phys. Rev. Lett.* **52**, 2111 (1984).
- ⁴⁰E. Prodan and F. D. M. Haldane, *Phys. Rev. B* **80**, 115121 (2009).
- ⁴¹H. B. Nielsen and M. Ninomiya, *Nucl. Phys. B* **185**, 20 (1981).
- ⁴²B. Halperin, *Jpn. J. Appl. Phys., Suppl.* **26**, 1913 (1987).
- ⁴³L. Fu, C. L. Kane, and E. J. Mele, *Phys. Rev. Lett.* **98**, 106803 (2007).
- ⁴⁴Z. Wang, X.-L. Qi, and S.-C. Zhang, *New J. Phys.* **12**, 065007 (2010).
- ⁴⁵X. Wan, A. Turner, A. Vishwanath, and S. Y. Savrasov, e-print arXiv:1007.0016 (to be published).
- ⁴⁶J. Milnor, *Morse Theory* (Princeton University Press, Princeton, NJ, 1963).
- ⁴⁷W. P. Su, J. R. Schrieffer, and A. J. Heeger, *Phys. Rev. Lett.* **42**, 1698 (1979).
- ⁴⁸D. J. Thouless, M. Kohmoto, M. P. Nightingale, and M. den Nijs, *Phys. Rev. Lett.* **49**, 405 (1982).
- ⁴⁹M. König, H. Buhmann, L. W. Molenkamp, T. Hughes, C.-X. Liu, X.-L. Qi, and S.-C. Zhang, *J. Phys. Soc. Jpn.* **77**, 031007 (2008).
- ⁵⁰X.-L. Qi, T. Hughes, and S.-C. Zhang, *Nat. Phys.* **4**, 273 (2008).
- ⁵¹X.-L. Qi and S.-C. Zhang, *Phys. Rev. Lett.* **101**, 086802 (2008).
- ⁵²A. M. Turner, Y. Zhang, R. S. K. Mong, and A. Vishwanath, e-print arXiv:1010.4335 (to be published).
- ⁵³S. Murakami, S. Iso, Y. Avishai, M. Onoda, and N. Nagaosa, *Phys. Rev. B* **76**, 205304 (2007).
- ⁵⁴S. Murakami, *New J. Phys.* **9**, 356 (2007).
- ⁵⁵S. Murakami and S.-I. Kuga, *Phys. Rev. B* **78**, 165313 (2008).